Sustainable irrigation reduces arsenic bioavailability in fluvio-alluvial soils promoting microbial responses, high rice productivity and economic profit

Arnab Majumdar[1,2]*, Munish Kumar Upadhyay[3], Biswajit Giri[2], Debojyoti Moulick[4], Sukamal Sarkar[5], Barun Kumar Thakur[6], Poonam Yadav[7], Kashinath Sahu[8], Ashish Kumar Srivastava[9], Martin Buck[10], Mark Tibbett[11], Manoj Kumar Jaiswal[2], Tarit Roychowdhury[1]

[1]School of Environmental Studies, Jadavpur University, Kolkata-700032, India
[2]Department of Earth Sciences, Indian Institute of Science Education and Research (IISER) Kolkata, Mohanpur, West Bengal 741246, India
[3]Centre for Environmental Science & Engineering, Department of Civil Engineering, Indian Institute of Technology Kanpur-208016, India
[4]Department of Environmental Science, University of Kalyani, Nadia, West Bengal, 741235, India
[5]School of Agriculture and Rural Development, Ramakrishna Mission Vivekananda Educational and Research Institute, Ramakrishna Mission Ashrama, Narendrapur, Kolkata – 700103, India
[6]Department of Economics, FLAME University, Pune, Maharashtra-412115, India
[7]Institute of Environment and Sustainable Development, Banaras Hindu University, Varanasi, Uttar Pradesh-221005, India
[8]Department of Chemical Sciences, Indian Institute of Science Education and Research (IISER) Kolkata, Mohanpur, West Bengal 741246, India
[9]Nuclear Agriculture and Biotechnology Division, Bhabha Atomic Research Centre, Mumbai, Maharashtra- 400085, India
[10]Department of Life Science, Faculty of Natural Sciences, Imperial College, London, SW7 2AZ, UK
[11]Department of Sustainable Land Management and Soil Research Centre, School of Agriculture Policy and Development, University of Reading, Reading, RG6 6AR, UK

*Corresponding author- Dr. Arnab Majumdar (arnabmajumdar891@gmail.com, geomicrobiology.arnab@gmail.com)

This manuscript is a non-peer-reviewed preprint submitted to EarthArXiv. At present, this manuscript is submitted to ACS Environmental Science & Technology.

Author details-

Arnab Majumdar*

School of Environmental Studies, Jadavpur University, Kolkata-700032, India
Department of Earth Sciences, Indian Institute of Science Education and Research (IISER) Kolkata, Mohanpur, West Bengal 741246, India
Email- arnabmajumdar891@gmail.com, geomicrobiology.arnab@gmail.com
Twitter handle- https://twitter.com/ArnabMa41557200

Munish Kumar Upadhyay

Centre for Environmental Science & Engineering, Department of Civil Engineering, Indian Institute of Technology Kanpur-208016, India

Email- munish007up@gmail.com

Biswajit Giri

Department of Earth Sciences, Indian Institute of Science Education and Research (IISER) Kolkata, Mohanpur, West Bengal 741246, India
Email- giri.biswajit605@gmail.com

Debojyoti Moulick

Department of Environmental Science, University of Kalyani, Nadia, West Bengal, 741235, India
Email- drubha31@gmail.com

Sukamal Sarkar

School of Agriculture and Rural Development, Ramakrishna Mission Vivekananda Educational and Research Institute, Ramakrishna Mission Ashrama, Narendrapur, Kolkata – 700103, India
Email- sukamalsarkarc@yahoo.com

Barun Kumar Thakur

Department of Economics, FLAME University, Pune, Maharashtra-412115, India
Email- barun.thakur@flame.edu.in

Poonam Yadav

Institute of Environment and Sustainable Development, Banaras Hindu University, Varanasi, Uttar Pradesh-221005, India
Email- poonamyadav.b.h.u@gmail.com

Kashinath Sahu

Department of Chemical Sciences, Indian Institute of Science Education and Research (IISER) Kolkata, Mohanpur, West Bengal 741246, India
Email- getkashi2011@gmail.com

Ashish Kumar Srivastava

Nuclear Agriculture and Biotechnology Division, Bhabha Atomic Research Centre, Mumbai, Maharashtra- 400085, India
Email- ashishbarc@gmail.com

Martin Buck

Department of Life Science, Faculty of Natural Sciences, Imperial College, London, SW7 2AZ, UK
Email- m.buck@imperial.ac.uk

Mark Tibbett

Department of Sustainable Land Management and Soil Research Centre, School of Agriculture Policy and Development, University of Reading, Reading, RG6 6AR, UK
Email- m.tibbett@reading.ac.uk

Manoj Kumar Jaiswal

Department of Earth Sciences, Indian Institute of Science Education and Research (IISER) Kolkata, Mohanpur, West Bengal 741246, India

Email- manoj@iiserkol.ac.in

Tarit Roychowdhury

School of Environmental Studies, Jadavpur University, Kolkata-700032, India
Email- rctarit@yahoo.com

Abstract

To minimize arsenic ($_{74.92}As^{33}$) loading into rice plants, based on our two-year field trial we propose adopting alternating wetting and drying (AWD) irrigation as a sustainable water management strategy allowing greater silicon ($_{28.08}Si^{14}$) availability. Our field-based project is the first report on AWD's impact on As-Si distribution in fluvio-alluvial soils of the entire Ganga valley (24 study sites, six divisions), seasonal variance (pre-monsoon and monsoon), rice plant anatomy and productivity, soil microbial diversity, microbial gene ontology profiling and associated metabolic pathways. Under AWD to flooded and pre-monsoon to monsoon cultivations, respectively, As-bioavailability was reduced by 8.71±0.014–9.25±0.019% and 25.68±0.088–26.13±0.0921%. In the pre-monsoon and monsoon seasons, the rice grain yield under AWD improved by 8.41±0.075% and 9.96±0.069%, proving the economic profitability. Compared to waterlogging, AWD evidences as an optimal soil condition for supporting soil microbial communities in rice fields, allowing diverse metabolic activities, including As-resistance, and active expression of As-responsive genes and gene products. Finally, we propose that by using AWD, the use of groundwater can be reduced, lowering the cost of pumping and field management and generating an economic profit for farmers. These combined assessments prove the acceptability of AWD for the establishment of multiple sustainable development goals (SDGs).

Keywords- Alternate wetting-drying; sustainable agriculture; rice productivity; economic profit; high throughput sequencing; gene ontology; microbial metabolism

Synopsis statement- Sustainable water management in rice cultivation reduces arsenic contamination and increases productivity while promoting soil microbial metabolic activities, gene expressions and economic profit for the farmers.

Introduction

In the soil-water-rice agro-ecosystem, both geogenic as well as anthropogenic factors contribute to arsenic (As) build-up in paddy fields[1–3]. However, the As-hotspot areas spread across the globe, where the As content was reportedly exceeding permissible limits[4,5]. Multifactorial influence (e.g., rice variety, soil elemental biogeochemistry, agro-environmental parameters, agronomic practices etc.) ultimately determines the susceptibility of rice varieties to As stress[6,7]. The bioavailability of As is usually governed by pH, the proportion of cationic and anionic species, its association with soil minerals as well as the actions of the soil microbiome[8]. Considering rice production on a global scale, observations have projected demand of 550.0 Mt rice production to cope with the issue to feed increasing global rice consumers and maintain the pace of economic growth too[9]. For optimal growth and yield, rice plant physiology and structural integrity must tolerate adverse environmental effects, made possible by high silicon (Si) accumulation in rice plants[10]. As and Si are structurally similar and inversely correlated[11]. Under frequent alterations of soil pH and redox state, the release of labile soil Si can occur[12], ready for rice plant uptake. Flooded conditions in rice cultivation results in significant water loss through seepage, surface runoff, evaporation, and deep percolation[13]. However, alternate wetting and drying (AWD) was found to be sufficient in minimizing As load in grain by reducing the bioavailability of As to rice plants leading to reductions in As translocation into the above-ground part[14,15]. This AWD practice can greatly influence soluble Si percentage and also influence soil microbial communities to thrive[11,16]. The Gangetic Plain is one of the enriched fluvial-alluvial valleys in the world producing the bulk of India's rice[17,18]. Loading of As in rice needs to be managed while increasing productivity and future food storage. A fluvio-alluvial soil can harbour diverse microbial communities that are naturally resistant towards As[19,20], and under differential soil status, microbial communities can express their complex network of metabolic activities relevant to As stress and agro-environmental practices[21,22].

In the fluvial-alluvial soil, As and Si dynamics are yet to be understood together in the context of rice productivity, socio-economic profit to the farmers, soil health quality via microbial active metabolisms and their diversity. This study is the first report from the Indian subcontinent involving the whole Ganga Valley to establish proposed practices in rice cultivation. Objectives of this study were to define- (i) As and Si status and distribution pattern in fluvio-alluvial soils of different geographic and topographic locations, (ii) how AWD practice can make a difference in As bioavailability in the soil to rice plants when Si is counteracting in the field, (iii) generated profit in AWD practice from the difference of rice productivity and minimized water usage, (iv) soil microbial community alterations under AWD and their expression of active metabolic pathways, (v) triggered As-resistance ability in soil microbes under AWD and helping in the reduction of As bioavailability in the soil. The project specifically was designed to unite many Sustainable Development Goals SDGs specifically SDG 2, SDG 3, SDG 6, SDG 9, SDG 12 and SDG 15[23]. Outcomes allow the promotion of SDGs based on holistic sets of field study data applicable to global SDGs perspectives as well, as discussed in this report.

■ Materials and method

Sampling site selection and experimental design. Soils at the bank of Ganga are mostly fluvial-alluvial type[24] and allow easy translocation of As from soil to rice plants while cultivated anaerobically[25]. The whole Gangetic plain was divided into six sections including four states- upper Ganga (Uttarakhand), upper-middle Ganga (Uttar Pradesh), middle Ganga (Uttar Pradesh), middle Ganga (Bihar), middle-lower Ganga (West Bengal) and lower Ganga (West Bengal). Based on previous reports, these sites are selected[24,26]. Each section was again marked for four sampling points where the field setups were engaged making a total of 24 study sites which were within a radius of 1 km from the river bed. **Fig. S1** shows the sampling points with their specific coordinates. The experimental design of the study site follows similarly as in Majumdar et al[27] (**supplementary method**).

Soil-rice plant analysis for total and bioavailable arsenic and silicon. Total and bioavailable As concentrations were measured using wavelength dispersive X-ray fluorescence spectroscopy (WD-XRF, S8 Tiger, Bruker, Germany) and inductively-coupled plasma mass spectrophotometer (ICP-MS, Nexion 300X Parkin Elmer, US) respectively, according to the standardized method of Majumdar et al[28,29]. Total Si in soil was measured using the WD-XRF method while bioavailable and plant Si concentrations were analyzed following the established method by Majumdar et al[30] and Mu et al[31] (**supplementary method**). Standard reference materials (SRM) used in these analyses were SDC-1, JSD-3, MESS3 and NIST2711a and quality-checked data is provided in **Table S1**. Rice plants were analyzed for total As concentrations followed by the di-acid digestion-dilution method using ICP-MS and calibrated using the SRM NIST1568c.

Soil physico-chemical parameters and rice productivity. Oakton Waterproof PCS Testr35 and ORP Testr 10 were used as portable meters for pH and ORP testing in the fields whereas samples were analyzed for soil organic matter (SOM) and microbial biomass carbon (MBC) using the method described in Walkley and Black[32]. Soil textures were assessed considering the ASTM sieve plate method, standardized by Sarkar et al[33]. To prove the effect of AWD unbiasedly, the study did not choose any specific rice cultivar during these trials and locally grown rice cultivars were considered. Each of the 800m^2 areas was assessed for rice grain yield and converted to hectare equivalent.

Economic profit validity and social acceptance. Rice yield per hectare under AWD and flooded practices were compared. The average of the minimum support price (MSP) of common and Grade A variety of paddy was used to estimate the price of paddy yield per hectare and national reports by Ministry of Agriculture-Govt. of India, were used to estimate the cultivable areas for rice in the Gangetic valley. The total economic value per hectare yield along the study cites for pre-monsoonal and monsoonal using AWD technology is estimated for the entire Ganga valley.

Secondary analyses of As-Si association and plant physiology. Soil samples were analyzed for the possible oxy/hydroxygenic As and Si ions present in the soil during AWD or flooded conditions using 'The Materials Project' (an online database of NERSC Scientific Computing Center and Computational Research Division under Lawrence Berkeley National Library)[30,34]. The pourbaix diagram, X-ray diffractogram and bubble plot analysis were generated based on the field data and database files together **(supplementary method).** Rice plant physiology was analyzed using field-emission scanning electron microscopy (FE-SEM, Carl Zeiss SUPRA 55VP) following the standardized method by Majumdar et al[29].

Soil microbial diversity assessment and next-generation sequencing. High-throughput sequencing was performed using isolated DNA samples from collected soils using a Qiagen DNeasy Powersoil kit **(supplementary method)**. These finally retrieved raw data were implemented in making microbial diversity assessments, gene ontology, metabolic pathways identification using the Kyoto Encyclopedia of Genes and Genomes (KEGG), As-responsive gene activity and occurrences[35].

Statistical justifications and microbial data analysis. All soil analyses were performed in triplicates and tested for statistical significance at $p \leq 0.05$ using one-way analysis of variance (ANOVA). To confirm the factual significance level, Bonferroni Correction was performed as a post-hoc assessment of all the soil-plant data obtained[36]. Experimental sites were 24, hence the considered variables were 24 to generate α-corrected p-value ≤ 0.00208 in Bonferroni Correction. For statistical analyses, graphical representations, microbial diversity assessments, gene ontology and KEGG analyses, GraphPad Prism 6, R Studio 2022, OriginPro 2018, SigmaPlot (ver. 12), ClustVis (ver 2.0 online), ShinyGO (ver 0.77 online), Cytoscape (ver. 3.8.2) and PAST (ver. 3.2.1) were used.

▪ Results

Distribution of As-Si content in different geographic locations. Soil textures were found to be similar with minor variations in the composition of soil, silt and clay percentage of all 24 sites from four states and six Gangetic divisions (**Table S2**). Silt predominates at the middle to lower Gangetic belt, however, overall, the whole Ganga valley was found to be silty clay in nature. A higher amount of clay in soil-sediment poses a barrier to As translocation to the rice plant[37]. In **Fig. S2 (a-h)**, a contour plot of As-Si distribution related to their site-specific pH and ORP is shown. These graphs represent the mean data of 24 sites from two years together revealing the bulk elemental change with pH and ORP getting altered in the field. A lower ORP state can be found in anaerobic flooded conditions compared to the aerobic dry soils[38], supporting our findings as well. These lower ORP and comparatively high pH (7.6-8.9) resulted in the higher release of total As content from soil-associated minerals to the aqueous phase (**Fig. S2a-d**). High Si concentrations were found within higher ORP values that become predominant in soil under the AWD cycle as shown in **Fig. S2e-h**, irrespective of seasonal changes. Pre-monsoonal soil Si, although, gets more frequent AWD transition than the monsoonal soil Si, hence a difference of 5-20g kg^{-1} was found between seasonal changes.

Fig. S3a-b shows the percentage area stacked plots of pre-monsoon and monsoon phases to understand the range of this As-Si distribution in individual Gangetic divisions (marked as divisions A-F). The upper Gangetic area showed minimum As concentrations in soil which comes from its lower As-contained groundwater[24] than the other states of the Ganga valley. The percentage plot clearly indicates the percent ratio of flooded soil As was greater than flooded soil Si and vice versa in AWD, during both seasons. Correlative plots of AWD and flooded soil physico-chemical parameters are emphasizing the relationship of bioavailable As-Si content to other influencing factors (**Fig. 1a-b**). This is a tri-parameter-based correlative analysis which indicates a positive or negative relationship based on color (red to violet), direction (upward or downward) and shape (slender to oval). Mean data of pH, ORP, OM, MBC and bioavailable As-Si were used for both pre-monsoon and monsoon during two consecutive years. ORP showed negative relation with As and positive relation with Si. During frequent ORP change, it contradicts soil pH values, as found in the pre-monsoon phase and AWD application[12] which in turn triggers the pulse release of available soil Si while entrapping the As content, reducing its bioavailability[39,40]. Soil OM and MBC both displayed a positive effect on the soil Si availability while restricting the mobility of available As content. MBC can modulate OM which in turn contributes to the Si concentration[30] and found during the AWD applications.

The experiment used 24 sites and the average per hectare yield of paddy through AWD is 5774.02 kg/hectare compared to 2809 kg/hectare for the production for the country (**Fig. 2a**). Interestingly, the average per hectare water consumption consumed for paddy cultivation through AWD is one-fifth compared to the traditional methods used for paddy cultivation. The per hectare average water consumption for paddy cultivation through ADW and FL, were 258437.5 litres, and 1316875 litres, respectively. If 10% of the Ganga valley used AWD technology for paddy cultivation the total annual water can be saved in the range of 1.354×10^{12} to 1.873×10^{12} litres. The water saving through AWD could act as a paradigm shift in a country like India where many of its states are water stress by 2030. This really helps to reduce the problem of water scarcity and helpful to achieve SDG 6 to clean water and sanitation and also economic benefits to the farmers[23].

Socio-economic validation and profitability analysis. The average per hectare revenue for AWD technology is estimated as INR 118367.4 (1442.14 USD) compared to INR 57584.5 (701.59 USD) for the country average, making farmer's per hectare average revenue increased by INR 60782.9 (740.55 USD) (**Fig. 2b**). The total increase in revenue for the farmers if 10% of the Ganga valley is used AWD is estimated as INR 82056.9 million (1000 million USD). The AWD technology is useful in terms of an increase in yield per hectare as a result an increase in total revenue. As a result, the farmers are gaining an increase in revenue, reducing the consumption of water, reducing the issues of food inequality and helping to achieve various sustainable goals through the use of ADW in paddy cultivation. **Table S5** and **S6** shows the details of economic profit from AWD implementation.

Secondary analyses and plant productivity in AWD and flooded cultivations. Soil As and Si were analyzed for the potential ionic species and their data-based molecular structures. Using 'The Materials Project', four molecular structures were simulated for As hydroxides and As-Si complexes (**Fig. S4a-b**). Field-obtained analyzed concentration range and other physical properties were provided as modelling input to generate these structures ($SiAs_2$, Si_3As_4, $As_3(HO_2)_5$ and As_3HO_6) emphasizing the stability of these compounds in the natural environments. Furthermore, a pourbaix diagram was generated (**Fig. S4c**) using the concentration range in molar values[41]. The generated graph suggests the predominant species of As and Si independently within a pH range of 6.4 to 8.7 and ORP of -185 to +290 mV. Predominant ionic species of As and Si were found to be $H_2AsO_4^-$, $HAsO_4^{2-}$, $HAsO_2$, and SiO_2 within this range, as marked by the red-colored box in the figure. The generated structures were further validated using the 'The Materials Project' database of elemental confirmatory XRD assessments (**Fig. S5a**). The XRD graphs were generated by comparing our experimental data to the online database of these four compounds mentioned. The graph shows single peak lines and a brown-colored reference line to show the exact match of these compounds, indicating the acceptability of these structures as valid naturally present compounds[42]. Bubble plots of soil As and Si compounds were obtained under AWD and flooded conditions in both seasons where OM was considered as the influencing factor. It appears that the AWD has a marked effect on As capture and Si release[15] (**Fig. S5b**).

Plant internal anatomy and ultra-structure of vascular systems were observed using FE-SEM from 24 study sites (six Gangetic divisions) under both AWD and flooded and presented in **Fig. S6**. Xylem (Xy) and Phloem (Ph) are marked in the figures to elucidate the prominent difference between the vasculature of AWD-grown plants and flooded-grown plants[30,43]. Improved rice internal anatomy is due to the fact of higher Si and lower As accumulation which directly correlates with the bioavailable amount of soil As and Si under AWD and flooded field conditions (**Fig. S7a-f**). A distinct and consistent pattern of As bioavailability was observed in pre-monsoonal AWD for all 24 sites while the highest plant available As was recorded in flooded soils during monsoonal season. However, higher plant-available Si was observed in pre-monsoonal AWD soils. Higher Si and lower As increase the rice plant cellulose synthase gene expressions for CESA3 and CESA4, resulting in higher cellulose production and therefore better structural rigidity[44]. These combined effects of bioavailability and structural betterments proved the plant's positive response towards AWD, resulted in greater rice grain productivity in all Gangetic divisions. Rice productivity was measured in kg ha^{-1} and shown in **Fig. S7g-l.** The data trend clearly reflects the effectivity of AWD practice over the flooded condition with greater statistical significance as marked in the figure. The highest range of rice yield was assessed in lower-middle and lower Gangetic divisions under the West Bengal district.

Microbial diversity and KEGG metabolic pathway assessments. Soil microbial communities are sensitive to any change in soil status and agronomic practices[16,19] which triggers their gene expressions, metabolic activities, and tolerance towards abiotic stresses. Soil microbial diversity was assessed using a next-generation sequencing technique which allows us to find variance in the microbial predominance in soil under different circumstances[27]. **Fig. S8** shows the predominant microbial classes under AWD and flooded conditions with seasonal changes. Among the 94-107 classes, 74 classes are presented in this color-coded heatmap which was present in all soil samples but differed in their number and degree of occurrence. It is evident that most of these microbial communities were well established under the dry-wet condition of the pre-monsoonal phase followed by the monsoonal dry-wet cultivation. Flooded conditions in both seasons were lower in harbouring microbial diversity. How AWD soil might promote microbial growth, communities and their metabolism has been suggested in some earlier studies[27,45]. Microbial diversity can be estimated by analyzing their alpha and beta diversity indices as given in **Table S3**. Mean values are presented in this table for all six Gangetic divisions for three different species richness indices- Shannon, Simpson and Chao1. These indices show that a higher species richness and microbial diversity were present in AWD soils compared to the flooded soils and pre-monsoonal phase had a greater richness overall than the monsoonal richness.

Irrespective of geographical locations, soil microbial metabolism showed greater expressions and activities when AWD was implemented. **Fig. 3a-b** shows a color-coded heat map of the analyzed and counted KEGG modules from all 24 sites of the six Gangetic divisions. A total of 164 metabolism-related pathways are presented in two different graphs for better visibility. These KEGG modules are presented with their KEGG numbers which can further tell us the details of the pathway compositions and counter-parts. The color distribution clearly indicates the dominance of pre-monsoonal dry-wet soil had a greater impact on the microbial communities which triggered most of the metabolic pathways to be active and expressed[46]. By way of illustration, 26 pathways from these KEGG modules are presented in **Fig. S9**, which are essential for the viability and stability of microbial growth and metabolism. Purine and pyrimidine metabolism; biosynthesis and degradation of fatty acids; glycolysis/gluconeogenesis; metabolisms of amino acids; carbohydrate metabolisms including pentose sugar and galactose; metabolic activities of Kreb's cycle; synthesis of other essential bio-molecules including lipopolysaccharides, pantothenate, co-enzyme A, and folic acid; metabolism of other essential bio-molecules including nicotinamide, lipoic acid, thiamine, riboflavin, and biotin are presented in a database-dependent pathway marking manner[47]. The red color indicates active enzymes, precursors, and their metabolic products within a pathway chart from our given input. Several pathways were found to be less active under flooded soil, as shown also in **Fig. 3a-b**. Greater occurrence and activities of microbial metabolic activities under AWD likely contribute to prove healthier soil compared to flooded soil[20,46].

Microbial gene ontology and arsenic resistance. Gene ontology is used to understand which gene clusters and their representative molecular functions are active under AWD and flooded soils and getting altered with seasonal changes[27,46]. Again, an average data of gene ontology obtained from next-generation sequencing has been presented in **Fig. 4a-b**. High frequency and low frequency genes are counted at the Illumina platform. It was evident that the highest gene ontological encounter in dry-wet soils compared to the flooded soils was found in both high-frequency and low-frequency genes. Similarly, another color-coded heat map distribution of these high-frequency and low-frequency gene ontological terms is presented in **Fig. S10**.

These heat maps show the intensity of these high-frequency and low-frequency gene ontological terms for AWD and flooded soil microbiomes. These combined ontology assessments prove the efficiency of microbial genes and their respective activities which comes under three different categories- Biological processes (GO:0008150), Cellular components (GO:0005575) and Molecular functions (GO:0003674)[48].

This further encouraged us to define the arsenic-responsive genes and their relationship with microbial diversity distribution under these altered soil statuses[49]. Some of these genes can govern the microbial ability to modulate total and bioavailable As concentration in soil depending on the environmental factors. From the obtained data of gene-specific high throughput sequencing and microbial distribution, a networking analysis is presented in **Fig. S11a-d**. Genes including *arsA, arsB, arsC, arsD, arsH, arsM, arsR, arsT, aioA/aoxB, aioE, aioS/aoxS, aioR/aoxR, aioX/aoxX, arrA, arrB, pstA_1, pstB, pstC_1, pstS1, glpF_1, ctaF,* and *pgpA/ltpgpA* were more connected to an extensive microbial genus network in AWD soils both under pre-monsoon and monsoonal changes compared to the flooded soil microbial genera. Cytoscape 'String' network has been implemented here which allows to visualize of gene-translated protein PDB (protein database) structures from these networks[50]. A number of microbial genera connected to each of these genes within these networks strongly suggests the involvement of microbial diversity expressing As-responsive genes profoundly under AWD which results in the As transformation and its reduced mobilization into the soil system.

The arsenic response and tolerance in microbes are one of the primitive cellular activities[51] which is also related to other cellular functions. In another set of analysis, *arrB, aioA, arrA, arsR, arsB, arsC, arsA, arsR, arsD, arsH, aioE, arsT, arrB, pstS, pstC, pstB, pstA, pgpA, arsP, arsM, aioX, aioS, aioR, aioA, aoxX, aoxS, aoxR, aoxB, ltpgpA,* and *aoxB* genes are presented with their corresponding cellular and physiological activity profiling in **Fig. 5**. Physiological responses including protein functions are mentioned in **Fig. 5** which has some direct or indirect link to As metabolism and/or tolerance. The color-coded fold enrichment values and types of parameters suggest that phosphate transporters, arsenical transporters, and arsenical efflux proteins are more expressed under AWD soil microbes in both pre-monsoonal and monsoonal phases while a higher expressions of phosphate transporter, arsenic transporter proteins, cell membrane proteins and other membrane stabilizing proteins under flooded soil microbes in both the seasons. This indicates additional cell-stressing activities are being managed by the microbial cells by producing and expressing different membrane-stabilizing proteins and bio-molecules under flooded conditions[52]. Further, a networking analysis of these genes and their products or their molecular functions is presented in **Fig. S12**. Various secondary ion transporters, phosphate transporters, arsenical transporters proteins, arsenic efflux proteins, anion and cation transporters, As-resistance biomolecules, redox-active centers and membrane-associated proteins are interconnected showing the complex inter-relationship of these bio-molecules depending on their degree of expression under AWD and flooded conditions with seasonal changes[53]. A gradient of network complexity was observed in the following sequence-pre-monsoon AWD, pre-monsoon flooded, monsoon AWD and monsoon flooded microbiome. These assessments are generated using the GO terms obtained from experimental data, merging with the online database using ShinyGO software to identify the inter-connectivity among these genes and their products[54].

Discussions

The project started with a motto of promoting AWD in the Indian sub-continent and gradually to the rest of the world as much as possible to make common people aware of the scarcity of the freshwater that we need for crop cultivation. Instead of keeping the field waterlogged for the whole time, requiring an average stagnant depth of 14-17cm, the AWD practice needs only 3-5cm waterlogging for 2 days and a drying phase reducing water usage by 52-75% depending on the soil texture and climatic conditions[55,56]. This study also minimized unnecessary groundwater consumption emphasizing **SDG 6** (Clean water and sanitation) and **SDG 12** (Responsible consumption and production) and their promotion to the farmers for future practice. **Table S4** shows the details of water conservation by AWD practice. Excessive extraction of groundwater also increases the risk of As dissolution from the deep aquifer to the groundwater[57], making it contaminated for direct use or for rice cultivation. Also, in the upper Gangetic division, where the annual average temperature is lower than the middle to lower Gangetic divisions, requirements for water were less due to lesser evapotranspiration[56]. This proves again, AWD practice can 'save water' by promoting SDG 6 at a large scale.

SDG 3 (Good health and wellbeing) and **SDG 9** (Industry, innovation, and infrastructure) promote issues related to soil management and their effects on human health. Soil As distribution is a global threat which gets spread through As-contaminated food stuff, primarily rice and rice-based foods[58,59]. More toxic species of As to the rice plant and its consumers, is generated in the flooded field than AWD soils[60]. When soil As bioavailability gets minimized, and rice quality improves, the consumers' health improves and is risk-free[61,62]. While reducing As availability, AWD, on the contrary, influence the plant-available Si to be more labile due to the frequent alterations of pH, redox potentials and OM content[12,39]. This agronomic practice can certainly improve the well-being of our consumers if a proper infrastructure for implementing AWD can be developed by joint ventures of scientists, engineers and policy-makers. **SDG 2** (Zero hunger) urges global researchers and policymakers to develop such practices which will promote higher food production minimizing the hunger ratio and malnutrition status globally[63,64]. Our earlier long-term field experiment has proved the efficacy of AWD in a greater nutritional enrichment in rice grain with higher productivity[27,58] which further has been experimentally established in this project. In **Fig. 2**, rice productivity has been presented indicating the direct effect of AWD on rice grain yield compared to conventional waterlogged cultivation. AWD triggers the development of higher panicle numbers and grain fillings after the inflorescence stage[65]. Better ultra-structure rigidity in AWD-grown plants also indicates a healthier state than the flooded-grown plants (**Fig. S6**). The results establish the fact that irrespective of geographic locations and seasonal changes, AWD can deliver high rice productivity, hence minimizing the crisis of food supply to the market, especially in arid countries[1]. With higher productivity, AWD also ensures greater economic benefit to the farmers and a cost-effective cultivation process (**Fig. S7**). This promotes **SDG 8** (Descent work and economic growth) and appeals to the government or non-government organizations to popularize the AWD practice in crop cultivation which can generate considerable revenue compared to the conventional mode of rice cultivation.

After analyzing soil microbiomes for their diversity depending on the water management practices, and seasonal variations, it becomes evident that AWD can induce microbial growth and species richness better than the flooded field conditions (**Table S3**), further supported by the expression of the metabolic pathways obtained by KEGG analysis (**Fig. 3** and **Fig. S9**). Obtained results of KEGG pathway matching of essential metabolic activities from AWD microbiome shows similar results reported in other studies[45,46,66]. AWD implementation can certainly influence microbial molecular responses by triggering their gene expressions[49,51] as found in the GO analysis from altered water regimes and seasonal changes (**Fig. 4** and **Fig. S10**). This can be understood by observing the data presented in Fig. SA where greater microbial genera participated in the As-resistance and phosphate transportation, cell membrane protein function and stability management, other anionic and cationic transfer activities[48]. Microbial cellular responses and physiological traits based on these molecular expressions are triggered under AWD (**Fig. S11** and **Fig. S12**). Under flooded soil, most of the aerobic microbes become dormant or eliminated and the continued prevalence of reducing environment hinders some other soil meso-biota[67]. To promote soil health and soil quality, soil meso- and microbiota must be conserved (**SDG 15**, Life on land) which can be achieved by implementing AWD practice. A complex cycle of biotic-abiotic balance is well preserved and thrived under AWD practice than the flooded conditions[68,69].

Acknowledgements

The authors are thankful to IISER-K for providing infrastructure as well as core facilities (XRF DST-FIST laboratory, FE-SEM Laboratory). AM is thankful to the IISER Kolkata and SERB-Govt. of India for Postdoctoral fellowship and research grant (File no- PDF/2022/001418/LS) for providing fellowship. Authors are also thankful to Genotypic Technology [P] Ltd., Bangalore, and Xcelris Labs Limited, Gujrat, India for the genomics analysis. The authors are also thankful to the junior students from each of these study areas who helped with sample collection and collected the basic information required.

Author credit statement

AM- conceptualization and project development, partial sampling and field management, major lab experiments, supervision, write-up and revisions; MKU- partial sampling and field management, partial write-up; BG- WD-XRF analysis; DM and SS- Metagenomics and high throughput sequencing analysis, partial write-up; BKT- economic value assessments and partial write-up; PY- partial graphics and write-up; KS- FE-SEM analysis; AKS-metagenomics and high throughput sequencing analysis; MKJ- supervision; MB-Metagenomics and high throughput sequencing analysis and supervision; MT- Metagenomics and high throughput sequencing analysis and supervision; TRC- partial write-up and supervision

Declaration for conflict of interest

The authors declare there is no conflict of interest known for this project and manuscript.

References

(1) Moulick, D.; Ghosh, D.; Skalicky, M.; Gharde, Y.; Mazumder, M. K.; Choudhury, S.; Biswas, J. K.; Santra, S. C.; Brestic, M.; Vachova, P. Interrelationship among Rice Grain Arsenic, Micronutrients Content and Grain Quality Attributes: An Investigation from Genotype× Environment Perspective. *Front. Environ. Sci.* **2022**, 180.

(2) Upadhyay, M. K.; Majumdar, A.; Barla, A.; Bose, S.; Srivastava, S. An Assessment of Arsenic Hazard in Groundwater–Soil–Rice System in Two Villages of Nadia District, West Bengal, India. *Environ. Geochem. Health* **2019**, *41*, 2381–2395.

(3) Neumann, R. B.; Pracht, L. E.; Polizzotto, M. L.; Badruzzaman, A. B. M.; Ali, M. A. Sealing Rice Field Boundaries in Bangladesh: A Pilot Study Demonstrating

Reductions in Water Use, Arsenic Loading to Field Soils, and Methane Emissions from Irrigation Water. *Environ. Sci. Technol.* **2014**, *48* (16), 9632–9640.

(4) Shaji, E.; Santosh, M.; Sarath, K. V; Prakash, P.; Deepchand, V.; Divya, B. V. Arsenic Contamination of Groundwater: A Global Synopsis with Focus on the Indian Peninsula. *Geosci. Front.* **2021**, *12* (3), 101079.

(5) Bundschuh, J.; Armienta, M. A.; Morales-Simfors, N.; Alam, M. A.; López, D. L.; Delgado Quezada, V.; Dietrich, S.; Schneider, J.; Tapia, J.; Sracek, O. Arsenic in Latin America: New Findings on Source, Mobilization and Mobility in Human Environments in 20 Countries Based on Decadal Research 2010-2020. *Crit. Rev. Environ. Sci. Technol.* **2021**, *51* (16), 1727–1865.

(6) Singh, S.; Rajput, V. D.; Upadhyay, S. K.; Minkina, T. Arsenic Contamination in Rice Agro-Ecosystems: Mitigation Strategies for Safer Crop Production. *J. Plant Growth Regul.* **2022**, 1–12.

(7) Harine, I. J.; Islam, M. R.; Hossain, M.; Afroz, H.; Jahan, R.; Siddique, A. B.; Uddin, S.; Hossain, M. A.; Alamri, S.; Siddiqui, M. H.; Henry, R. J. Arsenic Accumulation in Rice Grain as Influenced by Water Management: Human Health Risk Assessment. *Agronomy* **2021**, *11* (9), 1–13. https://doi.org/10.3390/agronomy11091741.

(8) Abedin, J.; Cresser, M. S.; Meharg, A. A.; Feldmann, J.; Cotter-Howells, J. Arsenic Accumulation and Metabolism in Rice (Oryza Sativa L.). *Environ. Sci. Technol.* **2002**, *36* (5), 962–968. https://doi.org/10.1021/es0101678.

(9) Yuan, S.; Linquist, B. A.; Wilson, L. T.; Cassman, K. G.; Stuart, A. M.; Pede, V.; Miro, B.; Saito, K.; Agustiani, N.; Aristya, V. E. Sustainable Intensification for a Larger Global Rice Bowl. *Nat. Commun.* **2021**, *12* (1), 7163.

(10) Raturi, G.; Sharma, Y.; Rana, V.; Thakral, V.; Myaka, B.; Salvi, P.; Singh, M.; Dhar, H.; Deshmukh, R. Exploration of Silicate Solubilizing Bacteria for Sustainable Agriculture and Silicon Biogeochemical Cycle. *Plant Physiol. Biochem.* **2021**, *166*, 827–838.

(11) Liu, W.-J.; McGrath, S. P.; Zhao, F.-J. Silicon Has Opposite Effects on the Accumulation of Inorganic and Methylated Arsenic Species in Rice. *Plant Soil* **2014**, *376*, 423–431.

(12) Kabata-Pendias, A. *Trace Elements in Soils and Plants*; CRC press, 2010.

(13) Vories, E.; Rhine, M.; Straatmann, Z. Investigating Irrigation Scheduling for Rice Using Variable Rate Irrigation. *Agric. Water Manag.* **2017**, *179*, 314–323.

(14) Li, C.; Carrijo, D. R.; Nakayama, Y.; Linquist, B. A.; Green, P. G.; Parikh, S. J. Impact of Alternate Wetting and Drying Irrigation on Arsenic Uptake and Speciation in Flooded Rice Systems. *Agric. Ecosyst. Environ.* **2019**, *272*, 188–198.

(15) Rokonuzzaman, M. D.; Ye, Z.; Wu, C.; Li, W. Arsenic Accumulation in Rice: Alternative Irrigation Regimes Produce Rice Safe from Arsenic Contamination. *Environ. Pollut.* **2022**, *310*, 119829.

(16) Cao, X.; Zhang, J.; Yu, Y.; Ma, Q.; Kong, Y.; Pan, W.; Wu, L.; Jin, Q. Alternate Wetting–Drying Enhances Soil Nitrogen Availability by Altering Organic Nitrogen Partitioning in Rice-Microbe System. *Geoderma* **2022**, *424*, 115993.

(17) Sekar, I.; Pal, S. Rice and Wheat Crop Productivity in the Indo-Gangetic Plains of India: Changing Pattern of Growth and Future Strategies. *Indian J. Agric. Econ.* **2012**, *67* (902-2016–67295).

(18) Ahamed, S.; Sengupta, M. K.; Mukherjee, A.; Hossain, M. A.; Das, B.; Nayak, B.; Pal, A.; Mukherjee, S. C.; Pati, S.; Dutta, R. N. Arsenic Groundwater Contamination and Its Health Effects in the State of Uttar Pradesh (UP) in Upper and Middle Ganga Plain, India: A Severe Danger. *Sci. Total Environ.* **2006**, *370* (2–3), 310–322.

(19) Zheng, T.; Deng, Y.; Wang, Y.; Jiang, H.; O'Loughlin, E. J.; Flynn, T. M.; Gan, Y.; Ma, T. Seasonal Microbial Variation Accounts for Arsenic Dynamics in Shallow Alluvial Aquifer Systems. *J. Hazard. Mater.* **2019**, *367*, 109–119.

(20) Jeong, S.; Hong, J. K.; Jho, E. H.; Nam, K. Interaction among Soil Physicochemical Properties, Bacterial Community Structure, and Arsenic Contamination: Clay-Induced Change in Long-Term Arsenic Contaminated Soils. *J. Hazard. Mater.* **2019**, *378*, 120729.

(21) Jia, Y.; Huang, H.; Chen, Z.; Zhu, Y.-G. Arsenic Uptake by Rice Is Influenced by Microbe-Mediated Arsenic Redox Changes in the Rhizosphere. *Environ. Sci. Technol.* **2014**, *48* (2), 1001–1007.

(22) Reid, M. C.; Maillard, J.; Bagnoud, A.; Falquet, L.; Le Vo, P.; Bernier-Latmani, R. Arsenic Methylation Dynamics in a Rice Paddy Soil Anaerobic Enrichment Culture. *Environ. Sci. Technol.* **2017**, *51* (18), 10546–10554.

(23) Lal, R.; Bouma, J.; Brevik, E.; Dawson, L.; Field, D. J.; Glaser, B.; Hatano, R.; Hartemink, A. E.; Kosaki, T.; Lascelles, B. Soils and Sustainable Development Goals of the United Nations: An International Union of Soil Sciences Perspective. *Geoderma Reg.* **2021**, *25*, e00398.

(24) Singh, M.; Singh, A. K.; Swati; Srivastava, N.; Singh, S.; Chowdhary, A. K. Arsenic Mobility in Fluvial Environment of the Ganga Plain, Northern India. *Environ. Earth Sci.* **2010**, *59*, 1703–1715.

(25) Upadhyay, M. K.; Majumdar, A.; Suresh Kumar, J.; Srivastava, S. Arsenic in Rice Agro-Ecosystem: Solutions for Safe and Sustainable Rice Production. *Front. Sustain. Food Syst.* **2020**, *4* (May). https://doi.org/10.3389/fsufs.2020.00053.

(26) Tyagi, N.; Upadhyay, M. K.; Majumdar, A.; Pathak, S. K.; Giri, B.; Jaiswal, M. K.; Srivastava, S. An Assessment of Various Potentially Toxic Elements and Associated Health Risks in Agricultural Soil along the Middle Gangetic Basin, India. *Chemosphere* **2022**, *300*, 134433.

(27) Majumdar, A.; Dubey, P. K.; Giri, B.; Moulick, D.; Srivastava, A. K.; Roychowdhury, T.; Bose, S.; Jaiswal, M. K. Combined Effects of Dry-Wet Irrigation, Redox Changes and Microbial Diversity on Soil Nutrient Bioavailability in the Rice Field. *Soil Tillage Res.* **2023**, *232*, 105752.

(28) Majumdar, A.; Upadhyay, M. K.; Giri, B.; Karwadiya, J.; Bose, S.; Jaiswal, M. K. Iron Oxide Doped Rice Biochar Reduces Soil-Plant Arsenic Stress, Improves Nutrient Values: An Amendment towards Sustainable Development Goals. *Chemosphere* **2023**, *312*, 137117.

(29) Majumdar, A.; Upadhyay, M. K.; Ojha, M.; Afsal, F.; Giri, B.; Srivastava, S.; Bose, S.

Enhanced Phytoremediation of Metal (Loid) s via Spiked ZVI Nanoparticles: An Urban Clean-up Strategy with Ornamental Plants. *Chemosphere* **2022**, *288*, 132588.

(30) Majumdar, A.; Upadhyay, M. K.; Kumar, J. S.; Barla, A.; Srivastava, S.; Jaiswal, M. K.; Bose, S. Ultra-Structure Alteration via Enhanced Silicon Uptake in Arsenic Stressed Rice Cultivars under Intermittent Irrigation Practices in Bengal Delta Basin. *Ecotoxicol. Environ. Saf.* **2019**, *180*, 770–779.

(31) Mu, J.; Hu, Z.; Huang, L.; Xie, Z.; Holm, P. E. Preparation of a Silicon-Iron Amendment from Acid-Extracted Copper Tailings for Remediating Multi-Metal-Contaminated Soils. *Environ. Pollut.* **2020**, *257*, 113565.

(32) Walkley, A.; Black, I. A. An Examination of the Degtjareff Method for Determining Soil Organic Matter, and a Proposed Modification of the Chromic Acid Titration Method. *Soil Sci.* **1934**, *37* (1), 29–38.

(33) Sarkar, S. R.; Majumdar, A.; Barla, A.; Pradhan, N.; Singh, S.; Ojha, N.; Bose, S. A Conjugative Study of Typha Latifolia for Expunge of Phyto-Available Heavy Metals in Fly Ash Ameliorated Soil. *Geoderma* **2017**, *305*, 354–362.

(34) Jain, A.; Montoya, J.; Dwaraknath, S.; Zimmermann, N. E. R.; Dagdelen, J.; Horton, M.; Huck, P.; Winston, D.; Cholia, S.; Ong, S. P. The Materials Project: Accelerating Materials Design through Theory-Driven Data and Tools. *Handb. Mater. Model. Methods Theory Model.* **2020**, 1751–1784.

(35) Kakui, K.; Fleming, J. F.; Mori, M.; Fujiwara, Y.; Arakawa, K. Comprehensive Transcriptome Sequencing of Tanaidacea with Proteomic Evidences for Their Silk. *Genome Biol. Evol.* **2021**, *13* (12), evab281.

(36) Li, W.; Liu, Q.; Xie, L.; Yin, C. Interspecific Plant-Plant Interactions Increase the Soil Microbial Network Stability, Shift Keystone Microbial Taxa, and Enhance Their Functions in Mixed Stands. *For. Ecol. Manage.* **2023**, *533*, 120851.

(37) Liu, W. J.; Zhu, Y. G.; Hu, Y.; Williams, P. N.; Gault, A. G.; Meharg, A. A.; Charnock, J. M.; Smith, F. A. Arsenic Sequestration in Iron Plaque, Its Accumulation and Speciation in Mature Rice Plants (Oryza Sativa L.). *Environ. Sci. Technol.* **2006**, *40* (18), 5730–5736. https://doi.org/10.1021/es060800v.

(38) Khan, S. U.; Hooda, P. S.; Blackwell, M. S. A.; Busquets, R. Effects of Drying and Simulated Flooding on Soil Phosphorus Dynamics from Two Contrasting UK Grassland Soils. *Eur. J. Soil Sci.* **2022**, *73* (1), e13196.

(39) Savant, N. K.; Snyder, G. H.; Datnoff, L. E. Silicon Management and Sustainable Rice Production. *Adv. Agron.* **1996**, *58*, 151–199.

(40) Khan, I.; Awan, S. A.; Rizwan, M.; Ali, S.; Hassan, M. J.; Brestic, M.; Zhang, X.; Huang, L. Effects of Silicon on Heavy Metal Uptake at the Soil-Plant Interphase: A Review. *Ecotoxicol. Environ. Saf.* **2021**, *222*, 112510.

(41) Wang, Z.; Guo, X.; Montoya, J.; Nørskov, J. K. Predicting Aqueous Stability of Solid with Computed Pourbaix Diagram Using SCAN Functional. *npj Comput. Mater.* **2020**, *6* (1), 160.

(42) Lee, B. Do; Lee, J.-W.; Park, W. B.; Park, J.; Cho, M.-Y.; Pal Singh, S.; Pyo, M.; Sohn, K.-S. Powder X-Ray Diffraction Pattern Is All You Need for Machine-Learning-Based Symmetry Identification and Property Prediction. *Adv. Intell. Syst.* **2022**, *4* (7),

2200042.

(43) Concenço, G.; de Brito, G. G.; Fagundes, P. R. R.; Scivittaro, W. B.; Parfitt, J. M. B.; Melo, T. S.; da SILVA, L. B. X.; Deuner, S. Contribution for Improvement of Rice Breeding Programs through Morphoanatomical Traits. **2021**.

(44) Srivastava, A. K.; Pandey, M.; Ghate, T.; Kumar, V.; Upadhyay, M. K.; Majumdar, A.; Sanjukta, A. K.; Agrawal, A. K.; Bose, S.; Srivastava, S. Chemical Intervention for Enhancing Growth and Reducing Grain Arsenic Accumulation in Rice. *Environ. Pollut.* **2021**, *276*, 116719.

(45) Hester, E. R.; Vaksmaa, A.; Valè, G.; Monaco, S.; Jetten, M. S. M.; Lüke, C. Effect of Water Management on Microbial Diversity and Composition in an Italian Rice Field System. *FEMS Microbiol. Ecol.* **2022**, *98* (3), fiac018.

(46) Wu, J.; Ma, C.; Li, F. Microbial Community Structure and Function in Paddy Soil as Affected by Water-Saving Irrigation Mode. *Eur. J. Soil Biol.* **2022**, *113*, 103450.

(47) Kanehisa, M.; Furumichi, M.; Sato, Y.; Ishiguro-Watanabe, M.; Tanabe, M. KEGG: Integrating Viruses and Cellular Organisms. *Nucleic Acids Res.* **2021**, *49* (D1), D545–D551.

(48) Behera, B. K.; Chakraborty, H. J.; Patra, B.; Rout, A. K.; Dehury, B.; Das, B. K.; Sarkar, D. J.; Parida, P. K.; Raman, R. K.; Rao, A. R. Metagenomic Analysis Reveals Bacterial and Fungal Diversity and Their Bioremediation Potential from Sediments of River Ganga and Yamuna in India. *Front. Microbiol.* **2020**, *11*, 556136.

(49) Yuan, C.; Qiao, J.; Li, F.; Zhang, X.; Du, Y.; Hu, M.; Sun, W. Community Dynamics of As (V)-Reducing and As (III)-Oxidizing Genes during a Wet–Dry Cycle in Paddy Soil Amended with Organic Matter, Gypsum, or Iron Oxide. *J. Hazard. Mater.* **2020**, *393*, 122485.

(50) Doncheva, N. T.; Morris, J. H.; Gorodkin, J.; Jensen, L. J. Cytoscape StringApp: Network Analysis and Visualization of Proteomics Data. *J. Proteome Res.* **2018**, *18* (2), 623–632.

(51) Ben Fekih, I.; Zhang, C.; Li, Y. P.; Zhao, Y.; Alwathnani, H. A.; Saquib, Q.; Rensing, C.; Cervantes, C. Distribution of Arsenic Resistance Genes in Prokaryotes. *Front. Microbiol.* **2018**, *9*, 2473.

(52) Randle-Boggis, R. J.; Ashton, P. D.; Helgason, T. Increasing Flooding Frequency Alters Soil Microbial Communities and Functions under Laboratory Conditions. *Microbiologyopen* **2018**, *7* (1), e00548.

(53) Anawar, H. M.; Rengel, Z.; Damon, P.; Tibbett, M. Arsenic-Phosphorus Interactions in the Soil-Plant-Microbe System: Dynamics of Uptake, Suppression and Toxicity to Plants. *Environ. Pollut.* **2018**, *233*, 1003–1012.

(54) Ge, S. X.; Jung, D.; Yao, R. ShinyGO: A Graphical Gene-Set Enrichment Tool for Animals and Plants. *Bioinformatics* **2020**, *36* (8), 2628–2629.

(55) Ishfaq, M.; Farooq, M.; Zulfiqar, U.; Hussain, S.; Akbar, N.; Nawaz, A.; Anjum, S. A. Alternate Wetting and Drying: A Water-Saving and Ecofriendly Rice Production System. *Agric. Water Manag.* **2020**, *241*, 106363.

(56) Pande, C. B.; Moharir, K. N.; Varade, A. Water Conservation Structure as an

Unconventional Method for Improving Sustainable Use of Irrigation Water for Soybean Crop under Rainfed Climate Condition. In *Climate change impacts on natural resources, ecosystems and agricultural systems*; Springer, 2023; pp 629–641.

(57) Saftner, D. M.; Bacon, S. N.; Arienzo, M. M.; Robtoy, E.; Schlauch, K.; Neveux, I.; Grzymski, J. J.; Carbone, M. Predictions of Arsenic in Domestic Well Water Sourced from Alluvial Aquifers of the Western Great Basin, USA. *Environ. Sci. Technol.* **2023**, *57* (8), 3124–3133.

(58) Chowdhury, N. R.; Das, A.; Joardar, M.; Mridha, D.; De, A.; Majumder, S.; Mandal, J.; Majumdar, A.; Roychowdhury, T. Distribution of Arsenic in Rice Grain from West Bengal, India: Its Relevance to Geographical Origin, Variety, Cultivars and Cultivation Season. In *Global Arsenic Hazard: Ecotoxicology and Remediation*; Springer, 2022; pp 509–531.

(59) Zhao, F. J.; Zhu, Y. G.; Meharg, A. A. Methylated Arsenic Species in Rice: Geographical Variation, Origin, and Uptake Mechanisms. *Environ. Sci. Technol.* **2013**, *47* (9), 3957–3966. https://doi.org/10.1021/es304295n.

(60) Chen, C.; Yu, Y.; Wang, Y.; Gao, A.; Yang, B.; Tang, Z.; Zhao, F.-J. Reduction of Dimethylarsenate to Highly Toxic Dimethylarsenite in Paddy Soil and Rice Plants. *Environ. Sci. Technol.* **2022**, *57* (1), 822–830.

(61) Joardar, M.; Mukherjee, P.; Das, A.; Mridha, D.; De, A.; Chowdhury, N. R.; Majumder, S.; Ghosh, S.; Das, J.; Alam, M. R. Different Levels of Arsenic Exposure through Cooked Rice and Its Associated Benefit-Risk Assessment from Rural and Urban Populations of West Bengal, India: A Probabilistic Approach with Sensitivity Analysis. *Environ. Sci. Pollut. Res.* **2023**, *30* (27), 70950–70973.

(62) Nunes, L. M.; Li, G.; Chen, W.-Q.; Meharg, A. A.; O'Connor, P.; Zhu, Y.-G. Embedded Health Risk from Arsenic in Globally Traded Rice. *Environ. Sci. Technol.* **2022**, *56* (10), 6415–6425.

(63) Blesh, J.; Hoey, L.; Jones, A. D.; Friedmann, H.; Perfecto, I. Development Pathways toward "Zero Hunger." *World Dev.* **2019**, *118*, 1–14.

(64) Kumar, K. A.; Rajitha, G. Alternate Wetting and Drying (AWD) Irrigation-a Smart Water Saving Technology for Rice: A Review. *Int. J. Curr. Microbiol. Appl. Sci.* **2019**, *8* (3), 2561–2571.

(65) Shrivastava, A.; Barla, A.; Majumdar, A.; Singh, S.; Bose, S. Arsenic Mitigation in Rice Grain Loading via Alternative Irrigation by Proposed Water Management Practices. *Chemosphere* **2020**, *238*, 124988.

(66) Min, D.; Cheng, L.; Liu, D.-F.; Liu, J.-Q.; Li, W.-W.; Yu, H.-Q. Single Strain-Triggered Biogeochemical Cycle of Arsenic. *Environ. Sci. Technol.* **2022**, *56* (22), 16410–16418.

(67) Bambaradeniya, C. N. B.; Amerasinghe, F. P. Biodiversity Associated with the Rice Field Agroecosystem in Asian Countries: A Brief Review. **2004**.

(68) Afsal, F.; Majumdar, A.; Kumar, J. S.; Bose, S. Microbial Inoculation to Alleviate the Metal Toxicity in Crop Plants and Subsequent Growth Promotion. *Sustain. Solut. Elem. Defic. Excess Crop Plants* **2020**, 451–479. https://doi.org/10.1007/978-981-15-8636-1_17.

(69) Plum, N. Terrestrial Invertebrates in Flooded Grassland: A Literature Review. *Wetlands* **2005**, *25* (3), 721–737.

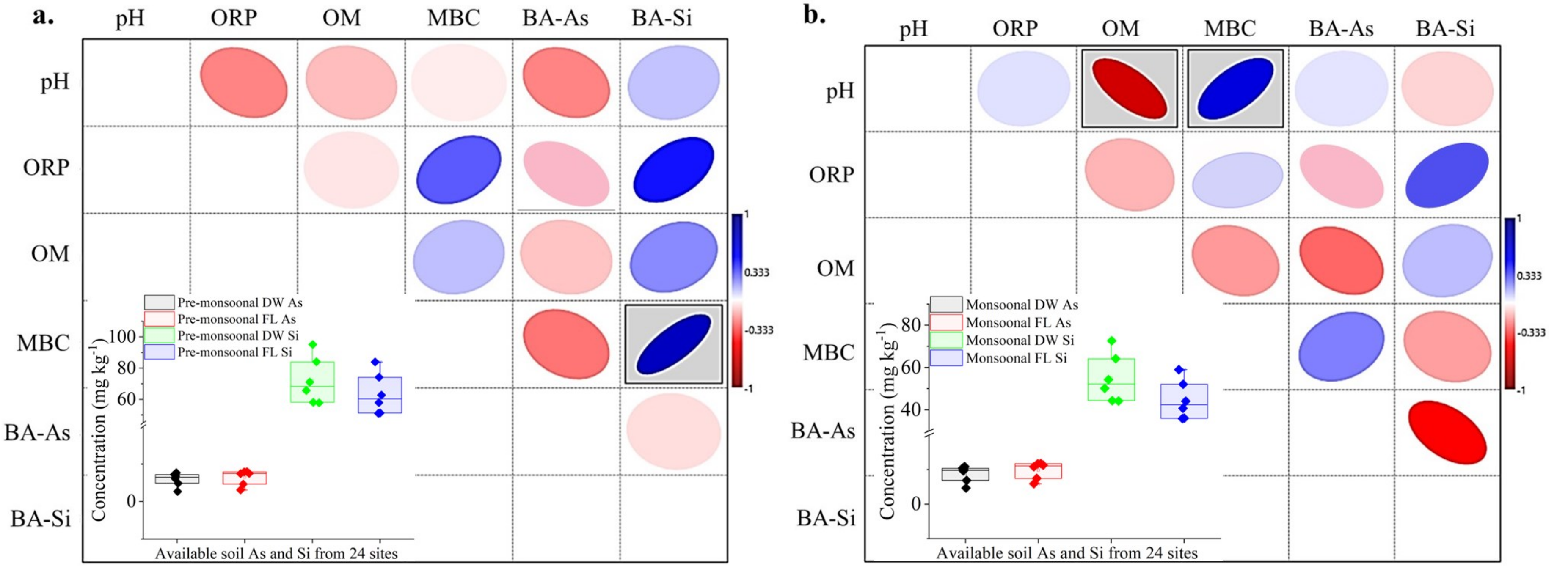

Fig. 1. Irrigation-influenced bioavailable As and Si concentration in all 24 sites and correlation with soil properties. The concentration range of soil As and Si has been presented in a box plot. Both pre-monsoonal **(a)** and monsoonal **(b)** results are presented with physico-chemical parameter-dependent correlative plots.

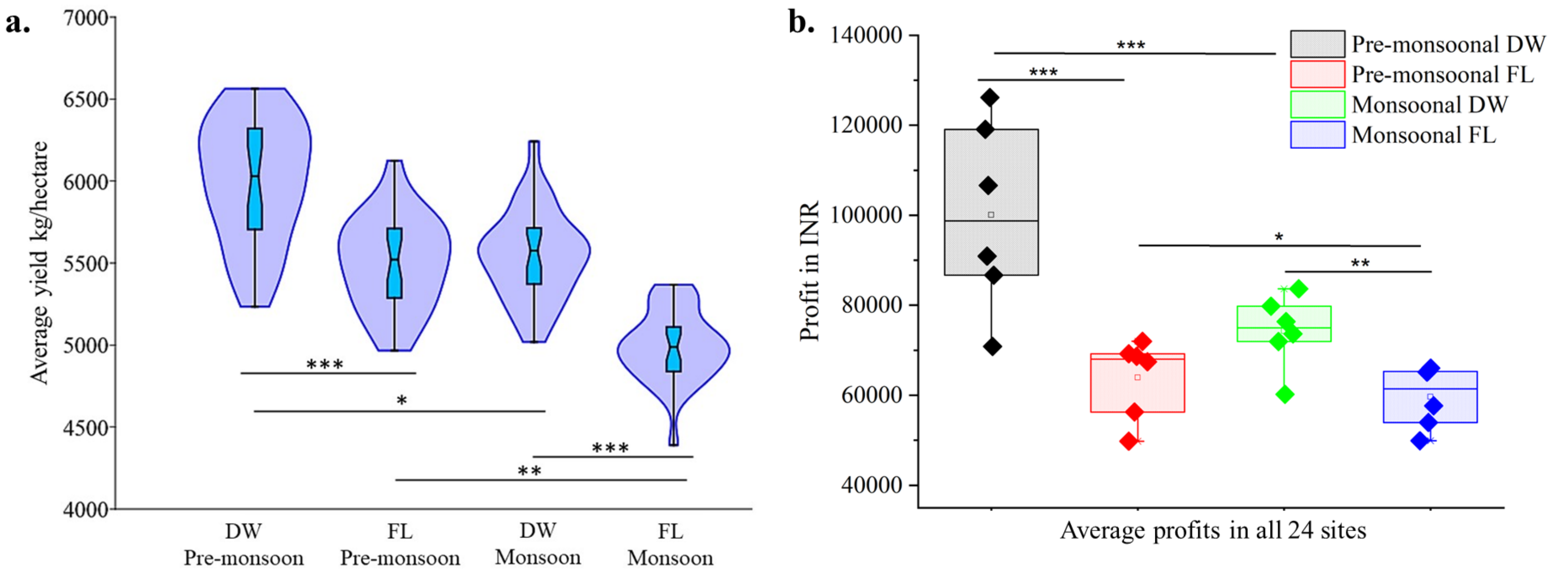

Fig. 2. Average rice yield and relative profit generated from all 24 sites under the compared practices. The average rice yield (kg/hectare) in all 24 sites under six Gangetic divisions is given in the form of a violin plot **(a).** Based on these productivity records, monitory profit has been calculated for all 24 sites **(b)** indicating a much higher revenue generation using this AWD practice.


a.
1.5
1
0.5
0
-0.5
-1
K1000590 Arachidonic acid metabolism
K1000472 D-Arginine and D-ornithine metabolism
K1000565 Ether lipid metabolism
K1000591 Linoleic acid metabolism
K1000531 Glycosaminoglycan degradation
K1000121 Secondary bile acid biosynthesis
K1000196 Photosynthesis - antenna proteins
K1000410 beta-Alanine metabolism
K1000061 Fatty acid biosynthesis
K1000053 Ascorbate and aldarate metabolism
K1000140 Steroid hormone biosynthesis
K1000730 Thiamine metabolism
K1000480 Glutathione metabolism
K1000430 Taurine and hypotaurine metabolism
K1000740 Riboflavin metabolism
K1000052 Galactose metabolism
K1000510 N-Glycan biosynthesis
K1000550 Peptidoglycan biosynthesis
K1000051 Fructose and mannose metabolism
K1000500 Starch and sucrose metabolism
K1000190 Oxidative phosphorylation
K1000785 Lipoic acid metabolism
K1000750 Vitamin B6 metabolism
K1000020 Citrate cycle (TCA cycle)
K1000720 Carbon fixation pathways in prokaryotes
K1000910 Nitrogen metabolism
K1000010 Glycolysis / Gluconeogenesis
K1000520 Amino sugar and nucleotide sugar metabolism
K1000040 Pentose and glucuronate interconversions
K1000564 Glycerophospholipid metabolism
K1000680 Methane metabolism
K1000290 Valine, leucine and isoleucine biosynthesis
K1000473 D-Alanine metabolism
K1000540 Lipopolysaccharide biosynthesis
K1000360 Phenylalanine metabolism
K1000460 Cyanoamino acid metabolism
K1000660 C5-Branched dibasic acid metabolism
K1000195 Photosynthesis
K1000592 alpha-Linolenic acid metabolism
K1000300 Lysine biosynthesis
K1000310 Lysine degradation
K1000240 Pyrimidine metabolism
K1000760 Nicotinate and nicotinamide metabolism
K1000350 Tyrosine metabolism
K1000072 Synthesis and degradation of ketone bodies
K1000380 Tryptophan metabolism
K1000071 Fatty acid degradation
K1000600 Sphingolipid metabolism
K1000650 Butanoate metabolism
K1000640 Propanoate metabolism
K1001040 Biosynthesis of unsaturated fatty acids
K1000340 Histidine metabolism
K1000630 Glyoxylate and dicarboxylate metabolism
K1000250 Alanine, aspartate and glutamate metabolism
K1000120 Primary bile acid biosynthesis
K1000280 Valine, leucine and isoleucine degradation
K1000620 Pyruvate metabolism
K1000562 Inositol phosphate metabolism
K1000710 Carbon fixation in photosynthetic organisms
K1000561 Glycerolipid metabolism
K1000400 Phenylalanine, tyrosine and tryptophan biosynthesis
K1000230 Purine metabolism
K1000030 Pentose phosphate pathway
K1000270 Cysteine and methionine metabolism
K1000100 Steroid biosynthesis
K1000450 Selenocompound metabolism
K1000260 Glycine, serine and threonine metabolism
K1000770 Pantothenate and CoA biosynthesis
K1000330 Arginine and proline metabolism
K1000920 Sulfur metabolism
K1000670 One carbon pool by folate
K1000780 Biotin metabolism
K1000471 D-Glutamine and D-glutamate metabolism
K1000790 Folate biosynthesis
K1000603 Glycosphingolipid biosynthesis - globo series
K1000511 Other glycan degradation
K1000062 Fatty acid elongation
K1000440 Phosphonate and phosphinate metabolism
K1000604 Glycosphingolipid biosynthesis - ganglio series
Pre-monsoon DW
Monsoon DW
Pre-monsoon FL
Monsoon FL
b.
1
0.5
0
-0.5
-1
K1004113 Meiosis - yeast
K1000363 Bisphenol degradation
K1004210 Apoptosis
K1000791 Atrazine degradation
K1000623 Toluene degradation
K1004011 MAPK signaling pathway - yeast
K1000980 Metabolism of xenobiotics by cytochrome P450
K1000982 Drug metabolism - cytochrome P450
K1000830 Retinol metabolism
K1004115 p53 signaling pathway
K1004510 Focal adhesion
K1003050 Proteasome
K1000364 Fluorobenzoate degradation
K1004621 NOD-like receptor signaling pathway
K1000311 Penicillin and cephalosporin biosynthesis
K1000625 Chloroalkane and chloroalkene degradation
K1001055 Biosynthesis of vancomycin group antibiotics
K1000524 Butirosin and neomycin biosynthesis
K1004142 Lysosome
K1001056 Biosynthesis of type II polyketide backbone
K1000627 Aminobenzoate degradation
K1004626 Plant-pathogen interaction
K1000523 Polyketide sugar unit biosynthesis
K1004070 Phosphatidylinositol signaling system
K1000906 Carotenoid biosynthesis
K1003410 Base excision repair
K1000860 Porphyrin and chlorophyll metabolism
K1003018 RNA degradation
K1000960 Tropane, piperidine and pyridine alkaloid biosynthesis
K1000130 Ubiquinone and other terpenoid-quinone biosynthesis
K1000401 Novobiocin biosynthesis
K1002010 ABC transporters
K1000281 Geraniol degradation
Benzoate degradation via CoA ligation
K1000983 Drug metabolism - other enzymes
K1000940 Phenylpropanoid biosynthesis
Carbazole degradation
K1003010 Ribosome
K1002060 Phosphotransferase system (PTS)
K1000633 Nitrotoluene degradation
K1003420 Nucleotide excision repair
K1003430 Mismatch repair
K1003440 Homologous recombination
K1003030 DNA replication
K1002030 Bacterial chemotaxis
K1000622 Xylene degradation
K1003070 Bacterial secretion system
K1002020 Two-component system
K1000970 Aminoacyl-tRNA biosynthesis
K1004146 Peroxisome
K1000900 Terpenoid backbone biosynthesis
K1002040 Flagellar assembly
K1000521 Streptomycin biosynthesis
K1003060 Protein export
K1001051 Biosynthesis of ansamycins
K1003020 RNA polymerase
K1004112 Cell cycle - Caulobacter
K1000903 Limonene and pinene degradation
3-Chloroacrylic acid degradation
1,2-Dichloroethane degradation
K1003022 Basal transcription factors
K1001053 Biosynthesis of siderophore group nonribosomal peptides
K1000624 Polycyclic aromatic hydrocarbon degradation
K1000930 Caprolactam degradation
K1000361 Chlorocyclohexane and chlorobenzene degradation
K1000908 Zeatin biosynthesis
K1000945 Stilbenoid, diarylheptanoid and gingerol biosynthesis
K1000943 Isoflavonoid biosynthesis
K1000944 Flavone and flavonol biosynthesis
K1000253 Tetracycline biosynthesis
K1000626 Naphthalene degradation
K1000232 Caffeine metabolism
Fluorene degradation
K1003040 Spliceosome
K1000941 Flavonoid biosynthesis
K1000642 Ethylbenzene degradation
K1000621 Dioxin degradation
K1004150 mTOR signaling pathway
K1000950 Isoquinoline alkaloid biosynthesis
K1000362 Benzoate degradation
K1000901 Indole alkaloid biosynthesis
K1000965 Betalain biosynthesis
K1000643 Styrene degradation
K1003450 Non-homologous end-joining
Monsoon FL
Pre-monsoon FL
Pre-monsoon DW
Monsoon DW

Fig. 3. Microbial Kyoto Encyclopaedia of Genes and Genomes (KEGG) metabolic pathways expressed differentially under dry-wet cycle and flooded cultivation. The KEGG database has been used to compare the obtained data from our high throughput sequencing to generate these heatmaps. To avoid excessive input in one file, the KEGG metabolic pathways are expressed in two separate images **(a, b)**.

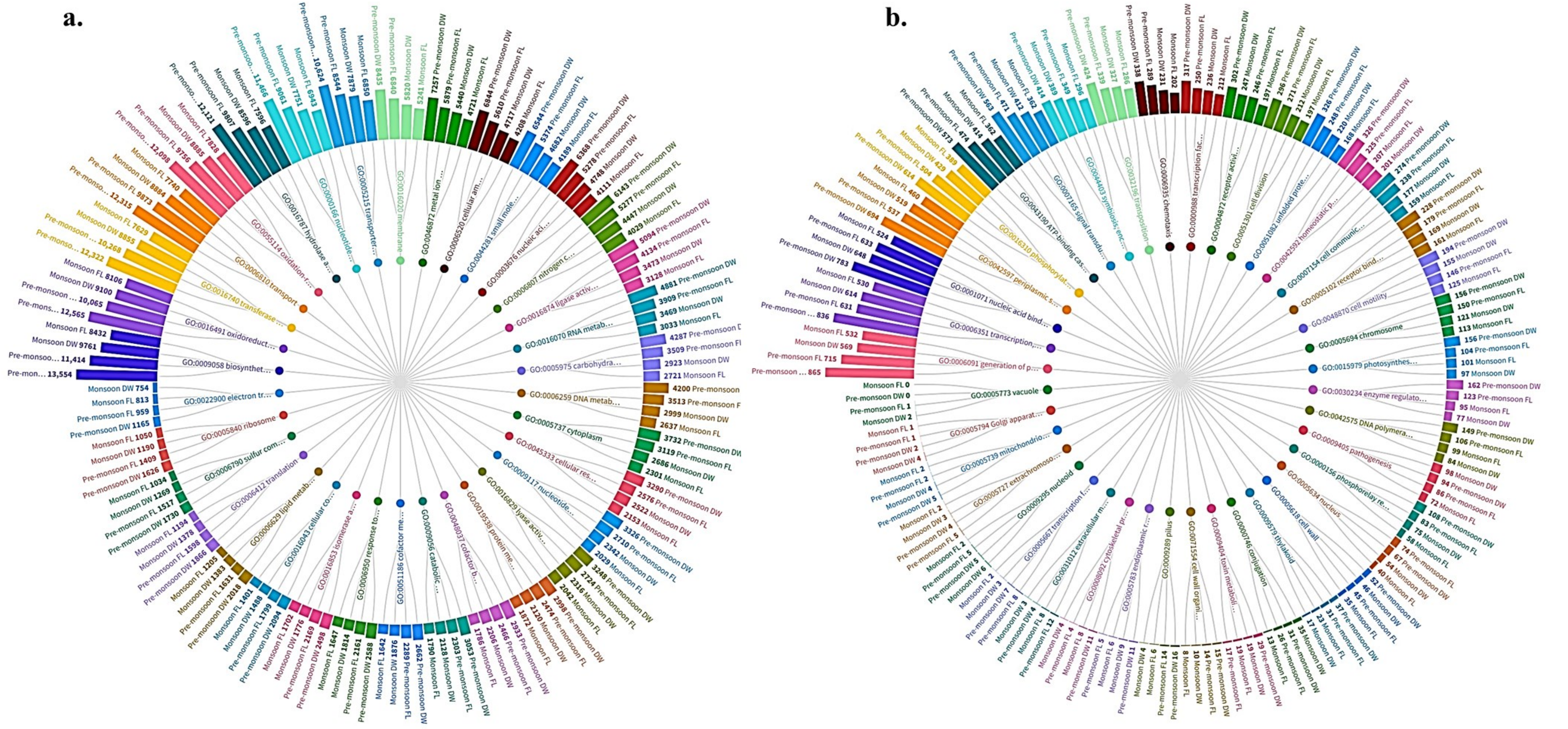

Fig. 4. Gene ontology analysis of high-frequency genes and low-frequency genes. The figure shows high-frequency GO **(a)** terms and low-frequency GO terms **(b)**. Specific reads are given aside indicating the identified reads or counts of these GO terms from each of the soil microbial communities. Data are representative of mean read counts from 24 sampling sites.

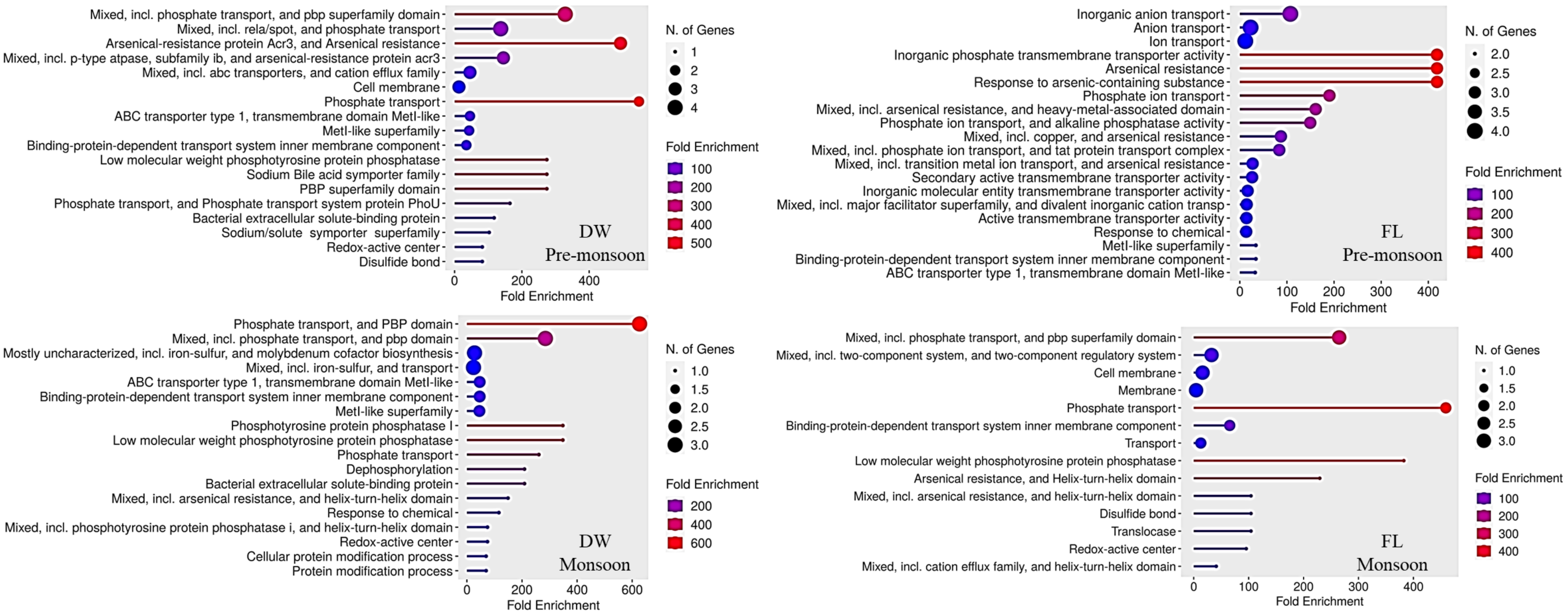

Fig. 5. Microbial arsenic-responsive and related gene activity with fold-change analysis. Arsenic-responsive and related gene prevalence, activity and fold-change occurrence in pre-monsoonal dry-wet and flooded along with monsoonal dry-wet and flooded microbes are presented in this figure.

Sustainable water management in rice cultivation reduces arsenic contamination, increases productivity, microbial molecular response, and profitability

Supplementary contents-

1. Additional methodologies.
2. Supplementary Figure S1. Study areas with sampling points of Upper middle to lower Gangetic delta of Indian subcontinent.
3. Supplementary Figure S2. Parametric-dependent pre-monsoonal and monsoonal distribution of soil As (a-d), Si (e-h).
4. Supplementary Figure S3. Stacked area plot for 24 sites with concentration rage distribution of soil As and Si with altered irrigation. Part (a) indicates the results from pre-monsoonal sampling and (b) represents monsoonal sampling.
5. Supplementary Figure S4. Modelled soil As-Si complexation (a1-a2), modelled arsenic species (b-arsenate, b1-arsenite) and pourbaix diagram (c) of probable redox status within pH range 6.2 to 8.5.
6. Supplementary Figure S5. Database-made XRD analysis (a) and experimentally-proved As-Si association and availability depending on the organic matter (b) content in the soil.
7. Supplementary Figure S6. Rice plant vascular ultra-structure (Xy= xylem; Ph= phloem) under AWD and flooded conditions from 6 Gangetic divisions with 24 sampling sites (one figure from each site) indicating the role of higher Si and lower As accumulation effect on plant physiology.
8. Supplementary Figure S7. Rice yield productivity (a-f) and plant bioavailable As-Si concentrations (g-l) with spatial variation at 24 sites.
9. Supplementary Figure S8. Heatmap analysis of pre-monsoonal and monsoonal microbial class occurrence under two irrigation types.
10. Supplementary Figure S9. KEGG Metabolic pathway analysis with predominant biochemical modules as superimposed models of earlier reports. Our analysed pathways are highlighted with red lines in each diagram.
11. Supplementary Figure S10. Gene Ontology (GO) profiling of dominant microbial metabolisms with higher frequency (a) and lower frequency (b) activities.
12. Supplementary Figure S11. Arsenic responsive gene-dependent dominant microbial network analysis in pre-monsoonal dry-wet/flooded (a,b) and monsoonal dry-wet/flooded (c,d) phases respectively.
13. Supplementary Figure S12. Network relationship of As-responsive and related genes under pre-monsoonal dry-wet and flooded soils (a-b) and monsoonal dry-wet and flooded soils (c-d). The genes are named within the figure.
14. Supplementary Table S1. Standard reference material values as analyzed for quality assurance.
15. Supplementary Table S2. Soil texture analysis by ASTM sieve method of all 24 sites within a radius of 1km from the Ganga bed.
16. Supplementary Table S3. Alpha and Beta diversity indices of soil microbiome under different field setups and seasonal changes.

17. Supplementary Table S4. The volume of water (in L) which can be saved in AWD practice compared to the flooded.
18. Supplementary Table S5. Profit calculation based on the rice productivity per hectare (H) in dry-wet (DW) and flooded (FL) fields. Average data for India has been used collected from the Ministry of Agriculture database.
19. Supplementary Table S6. Profit calculations based on the average income per hectare from dry-wet and flooded fields.

Additional methodologies-

Experimental site design- Briefly, each field was 800m^2 in area and irrigated with groundwater during the pre-monsoonal season while rainwater was used in the monsoonal phase. Water stagnancy of 10cm was maintained for 2 days followed by a drying cycle with 60% soil moisture (time varied due to weather conditions) and repeated till the late inflorescence stage. During the monsoonal season, maintaining AWD was difficult but manageable, resulting in a marked difference.

Soil-plant Si analysis- Briefly, soil extracts were mixed up with ammonium sulfomolybdate [$(NH_4)_6Mo_7O_{24}.4H_2O)+H_2SO_4$], tartaric acid ($C_4H_6O_6$) and ascorbic acid ($C_6H_8O_6$) at different concentrations as per the method and measured at 660nm using a spectrophotometer (Specord 210, AnalytikJena, Germany). Plant extracts were mixed up with hydrochloric acid (HCl), ammonium heptamolybdate [$(NH_4)_6Mo_7O_{24}$. $4H_2O$], and oxalic acid [$(COOH)_2{\cdot}2H_2O$] and measured at 410nm. As a standard material for calibration, silicon tetrachloride ($SiCl_4$), NIST2711a and NIST1568c were used.

Secondary analyses- The pourbaix diagram of pH and ORP making a graph of the oxyhydroxide ions of As and Si in the soil-water interphase and during the transition phase (Majumdar et al., 2019). This online database allows generation of a single or multi-element molecular structure from obtained data and available crystal structures online. **Supplementary Figure S2** shows four such predicted As-Si molecular structures and a pourbaix diagram with predominant ions marked within the area of interest (red colored box). For further assessment of these oxyhydroxide ions of As and Si, experimentally obtained data were used to generate X-ray diffractograms on The Materials Project (**Supplementary Figure S3**). Generated peaks in these graphs were deduced further for the identification of the elemental groups present in the samples. The complementary part of Fig. S3 represents a bubble plot which was made using field-obtained OM, total soil As and Si data.

High throughput sequencing- High-throughput sequencing was performed using isolated DNA samples from collected soils using a Qiagen DNeasy Powersoil kit (Cat# 12888-50). Eluted DNAs in Nuclease-free water (Ambion Cat# AM9938) were further checked in Nanodrop 2000 for quality assurance. A Ligation sequencing kit (Oxford Nanopore Technologies, SQK-LSK109) and PCR Barcoding kit (Oxford Nanopore

Technologies, EXP-PCR096) were used for the library preparation for which purified amplicon DNAs were end-repaired by NEBnext Ultra II End Repair kit (New England Biolabs, MA, USA) followed by a cleaning step using AmPure beads (Beckmann Coulter, USA). Barcoded DNA samples were further pooled and quantified using NEBnext Ultra II End repair/dA-Tailing Module (New England Biolabs, MA, USA). Another set of cleaning and adapter ligation was done using AmPure beads and NEB blunt/TA Ligase (New England Biolabs, MA, USA). Finally, the sequencing was conducted on GridION X5 (Oxford Nanopore Technologies, Oxford, UK) using SpotON flow cell R9.4 (FLO-MIN106). Nanopore raw reads (‘fast5’ format) were basecalled (‘fastq’ format) and demultiplexed using Guppy v2.3.4. These processed data are used further for the microbial expressions of metabolic and gene ontological status.

Supplementary Figure S1. Study areas with sampling points of Upper middle to lower Gangetic delta of Indian subcontinent.

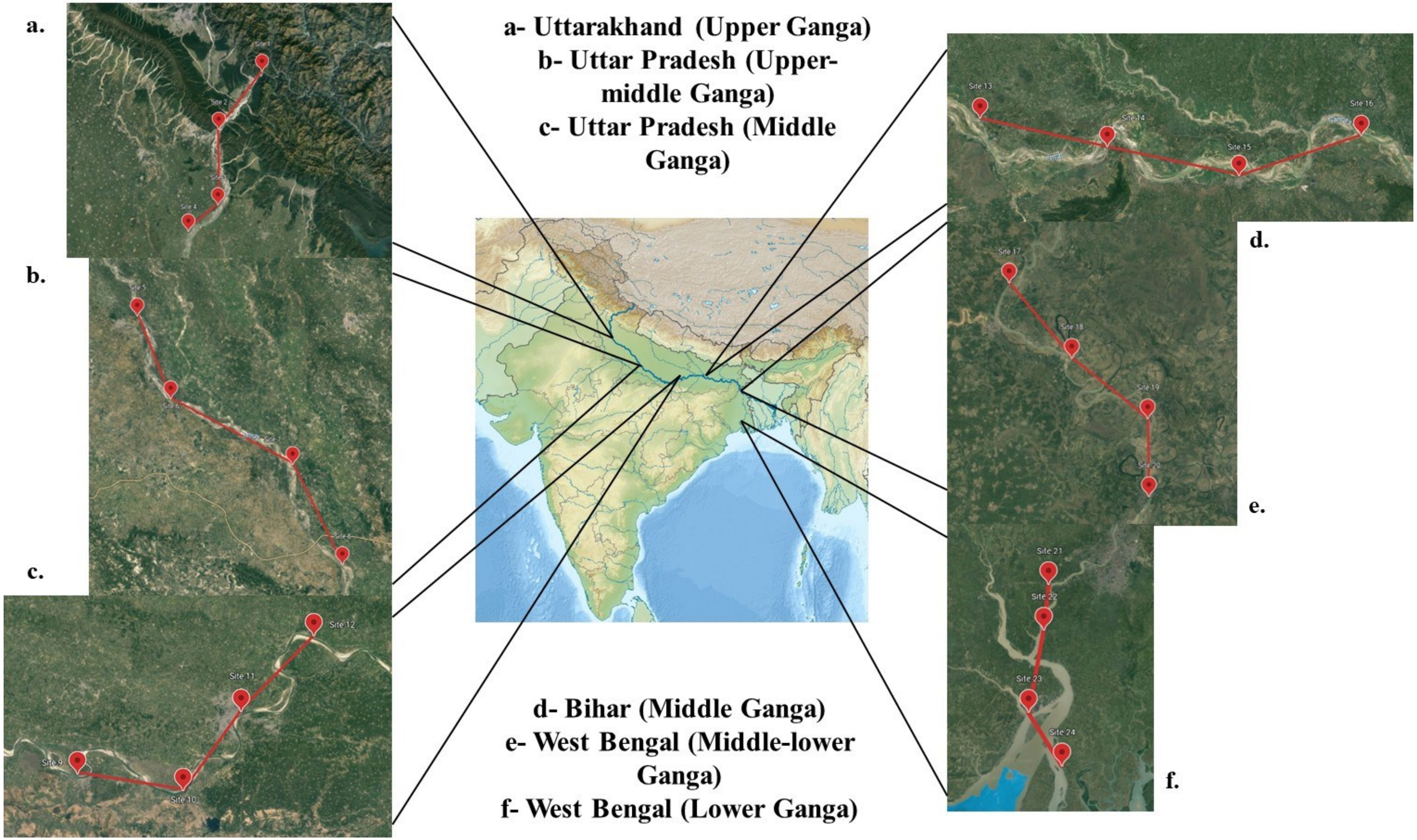

The coordinates of these 24 sampling sites are given below, which have been divided into six Gangetic divisions- Upper Ganga, Upper-middle Ganga, Middle Ganga 1, Middle Ganga 2, Lower-middle Ganga and Lower Ganga. Sampling sites are in Uttarakhand, Uttar Pradesh, Bihar and West Bengal.

Upper Ganga	Upper-middle Ganga	Middle Ganga 1	Middle Ganga 2	Middle-lower Ganga
30D08'24"N 78D19'53"E	27D24'29"N 79D36'54"E	25D10'00"N 82D33'12"E	25D28'29"N 85D57'22"E	23D42'10"N 88D08'44"E
29D57'24"N 78D09'17"E	27D14'52"N 79D41'59"E	25D07'26"N 82D50'36"E	25D22'12"N 86D27'58"E	23D36'02"N 88D15'14"E
29D42'30"N 78D09'29"E	27D06'52"N 79D58'46"E	25D20'03"N 83D01'45"E	25D16'48"N 86D58'33"E	23D30'58"N 88D22'05"E
29D37'19"N 78D03'10"E	26D53'14"N 80D06'45"E	25D32'03"N 83D14'16"E	25D24'16"N 87D27'08"E	23D25'18"N 88D22'59"E

Lower Ganga
22D28'17"N 88D06'43"E
22D18'38"N 88D06'13"E
22D01'15"N 88D03'32"E
21D50'12"N 88D11'46"E

Three random replicates have been sampled from each of these sites to maintain the sampling process's heterogeneity.

Supplementary Figure S2. Parametric-dependent pre-monsoonal and monsoonal distribution of soil As (a-d), Si (e-h).

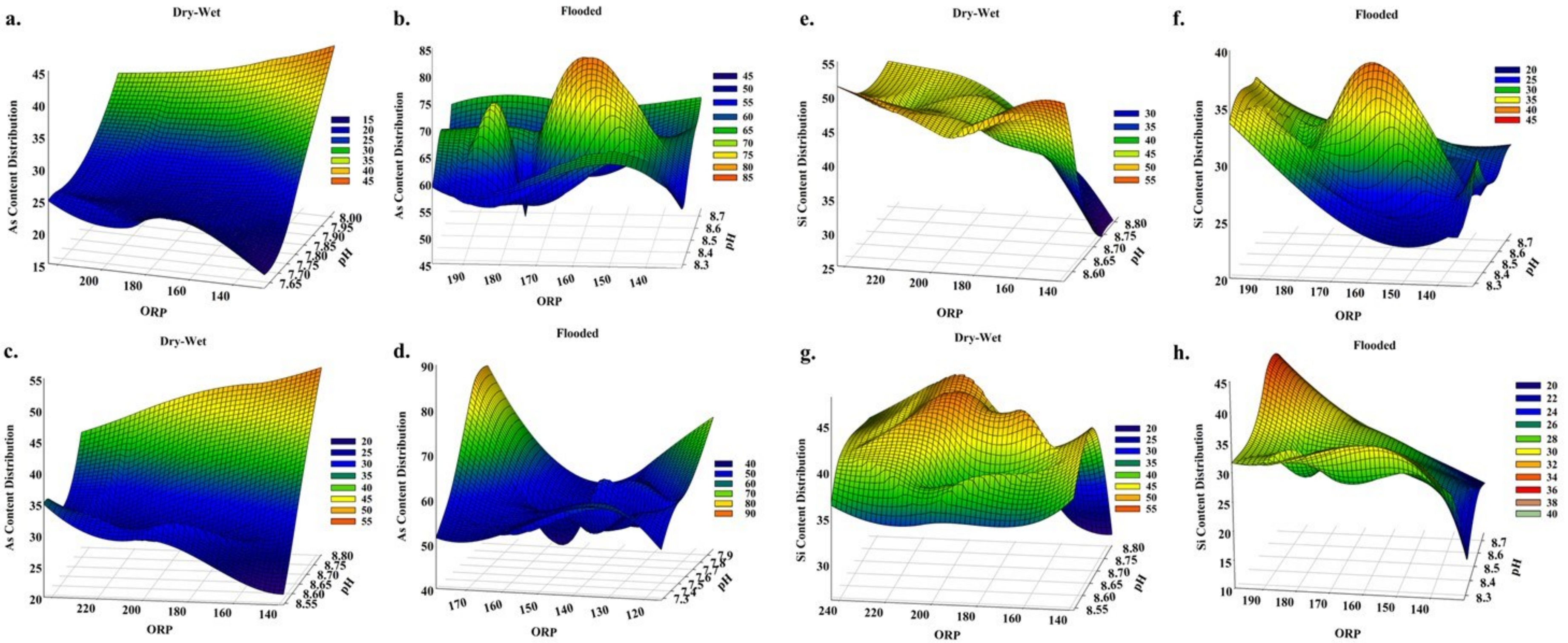

Figures 1a-b and 1c-d show pre-monsoonal and monsoonal soil As data in dry-wet and flooded conditions. Figures 1e-f and 1g-h show pre-monsoonal and monsoonal soil Si data in dry-wet and flooded conditions.

Supplementary Figure S3. Stacked area plot for 24 sites with concentration rage distribution of soil As and Si with altered irrigation. Part (a) indicates the results from pre-monsoonal sampling and (b) represents monsoonal sampling.

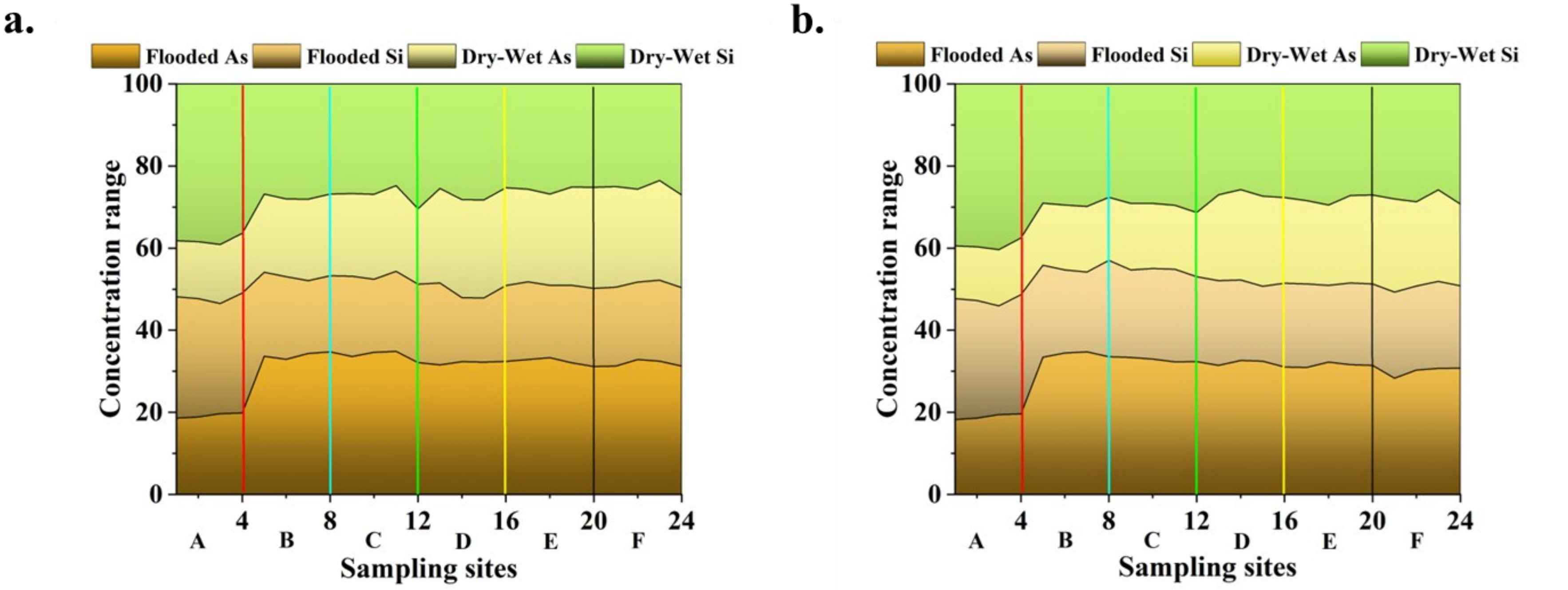

Supplementary Figure S4. Modelled soil As-Si complexation (a1-a2), modelled arsenic species (b-arsenate, b1-arsenite) and pourbaix diagram (c) of probable redox status within pH range 6.2 to 8.5.

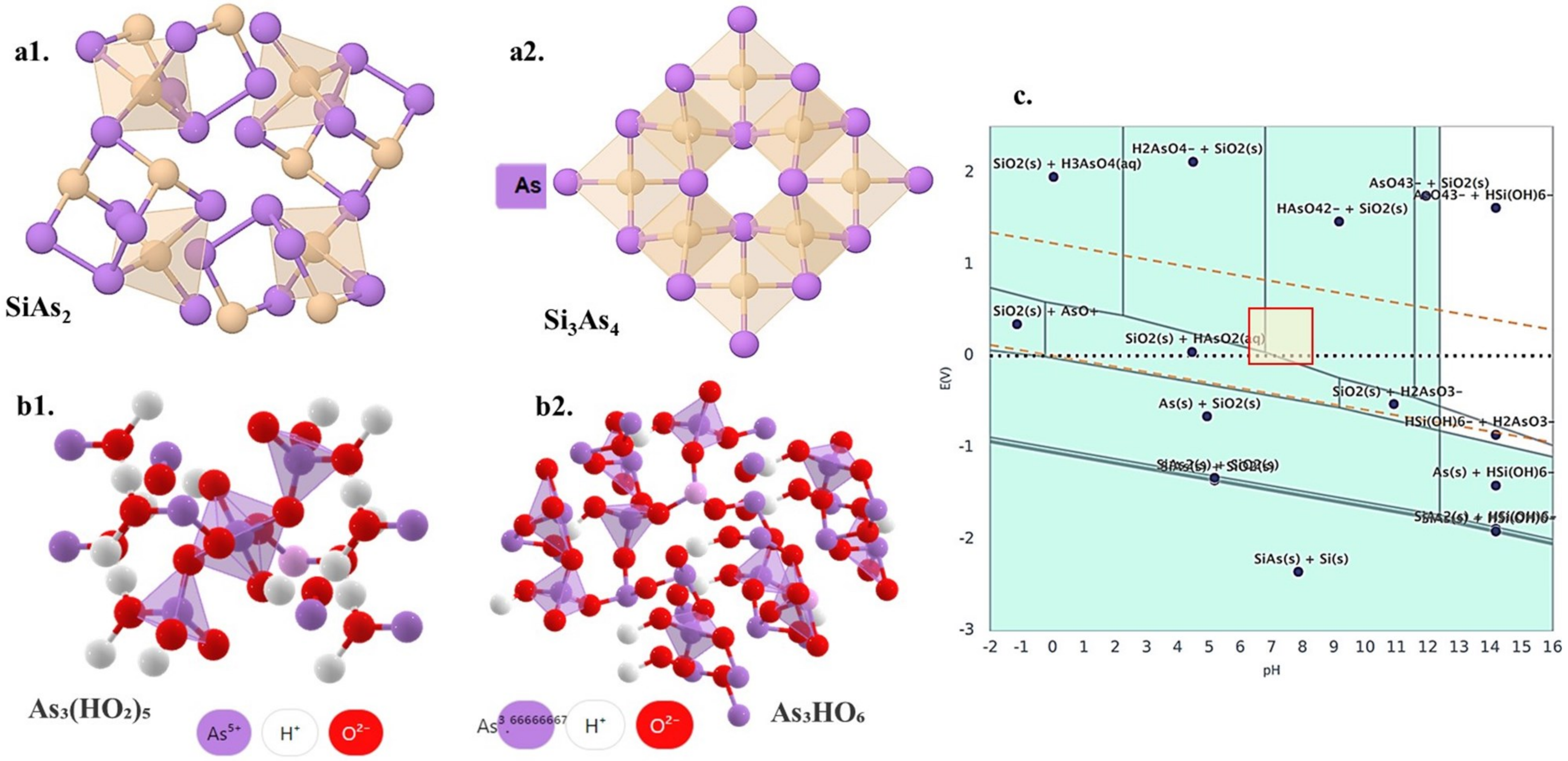

Supplementary Figure S5. Database-made XRD analysis (a) and experimentally-proved As-Si association and availability depending on the organic matter (b) content in the soil.

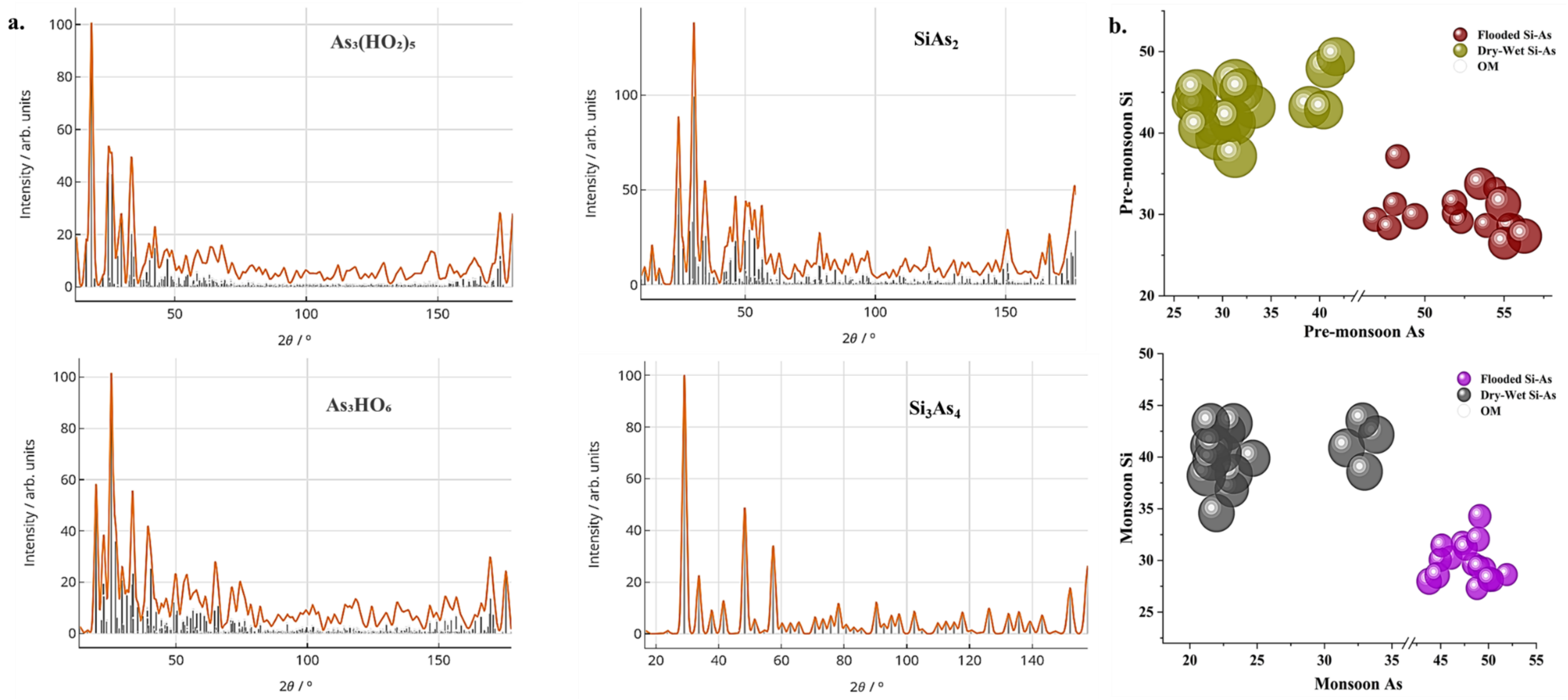

Supplementary Figure S6. Rice plant vascular ultra-structure (Xy= xylem; Ph= phloem) under AWD and flooded conditions from 6 Gangetic divisions with 24 sampling sites (one figure from each site) indicating the role of higher Si and lower As accumulation effect on plant physiology.

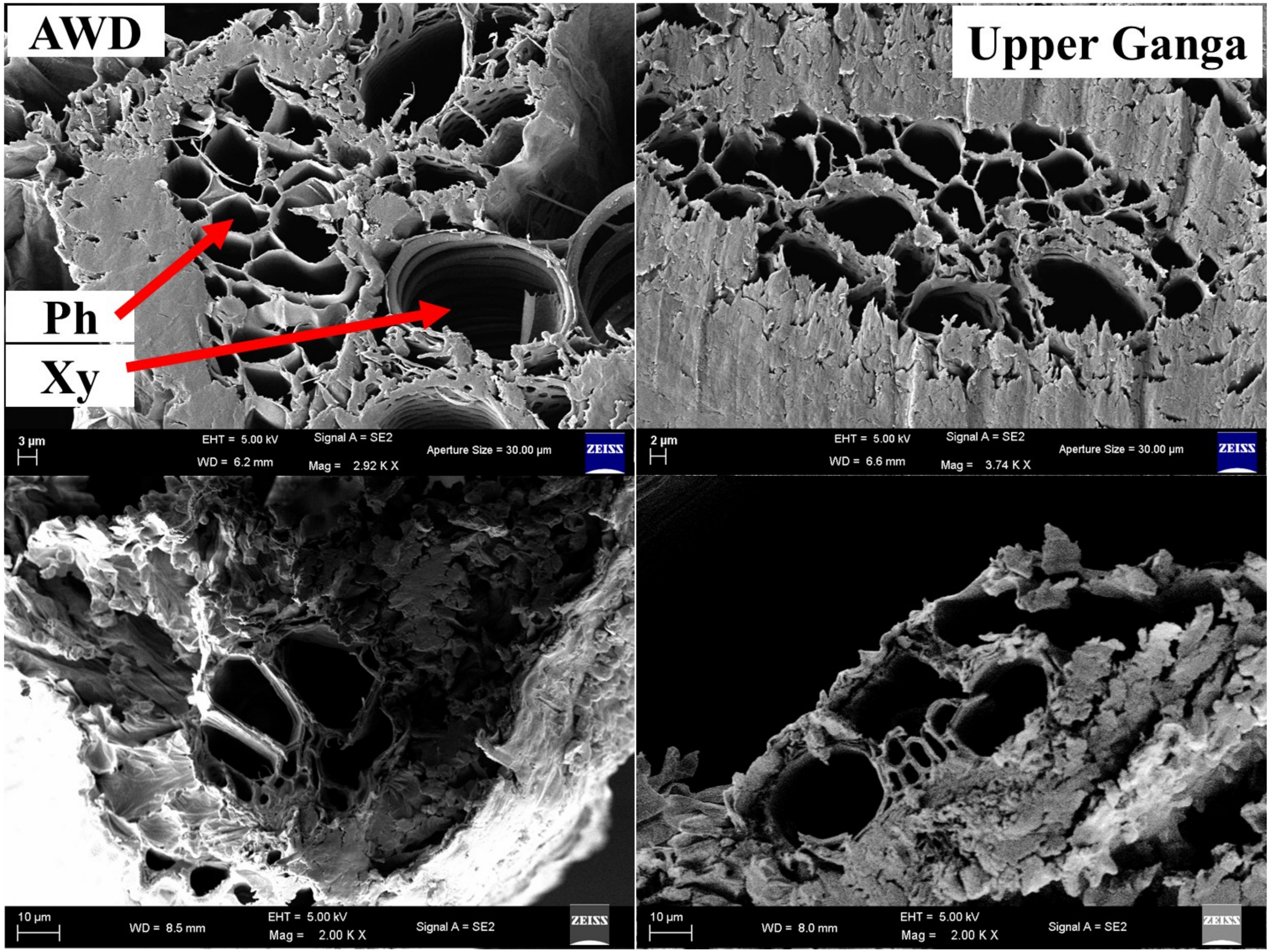

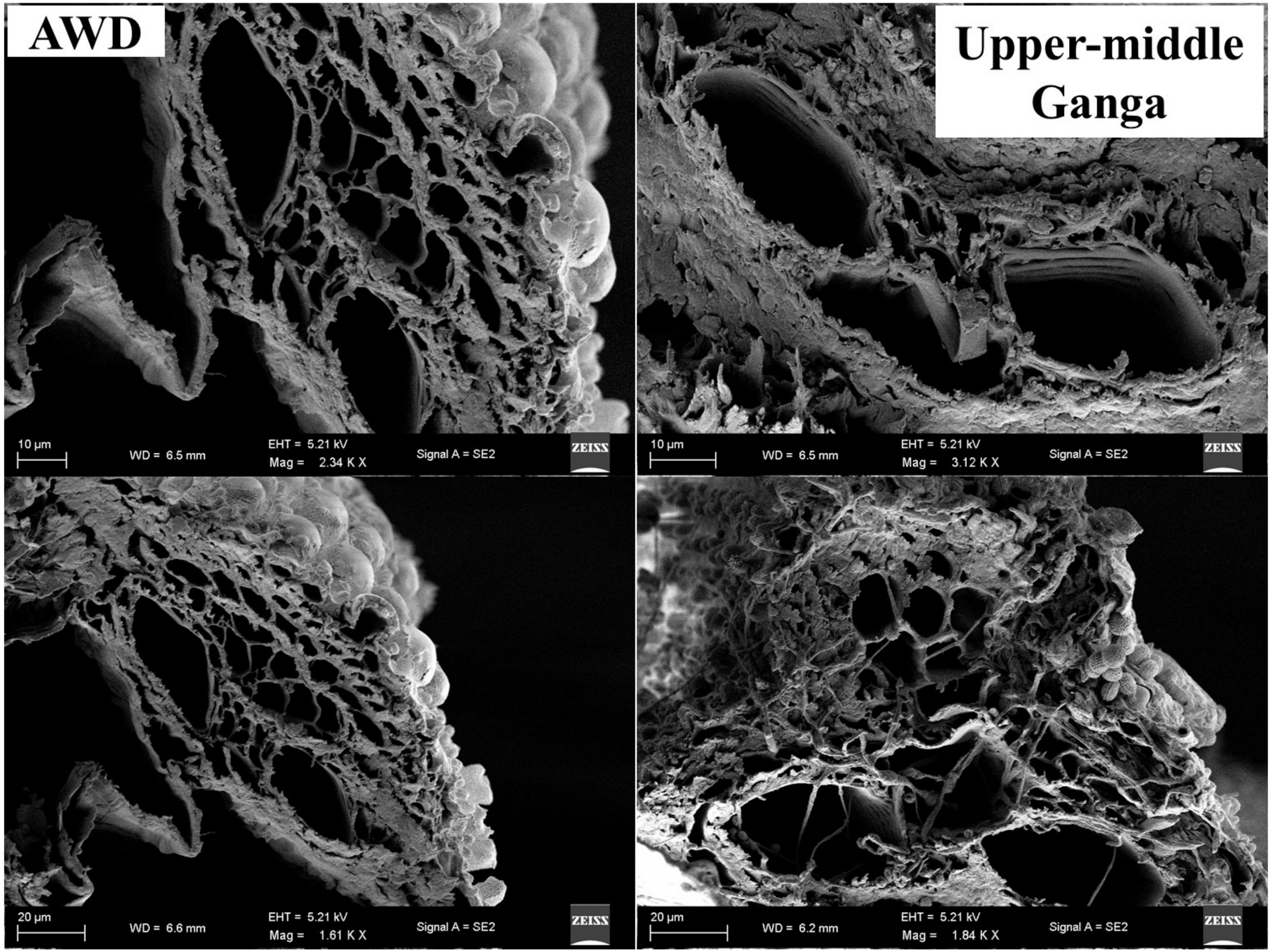
AWD
Upper-middle Ganga
10 µm
WD = 6.5 mm
EHT = 5.21 kV
Mag = 2.34 K X
Signal A = SE2
ZEISS
10 µm
WD = 6.5 mm
EHT = 5.21 kV
Mag = 3.12 K X
Signal A = SE2
ZEISS
20 µm
WD = 6.6 mm
EHT = 5.21 kV
Mag = 1.61 K X
Signal A = SE2
ZEISS
20 µm
WD = 6.2 mm
EHT = 5.21 kV
Mag = 1.84 K X
Signal A = SE2
ZEISS

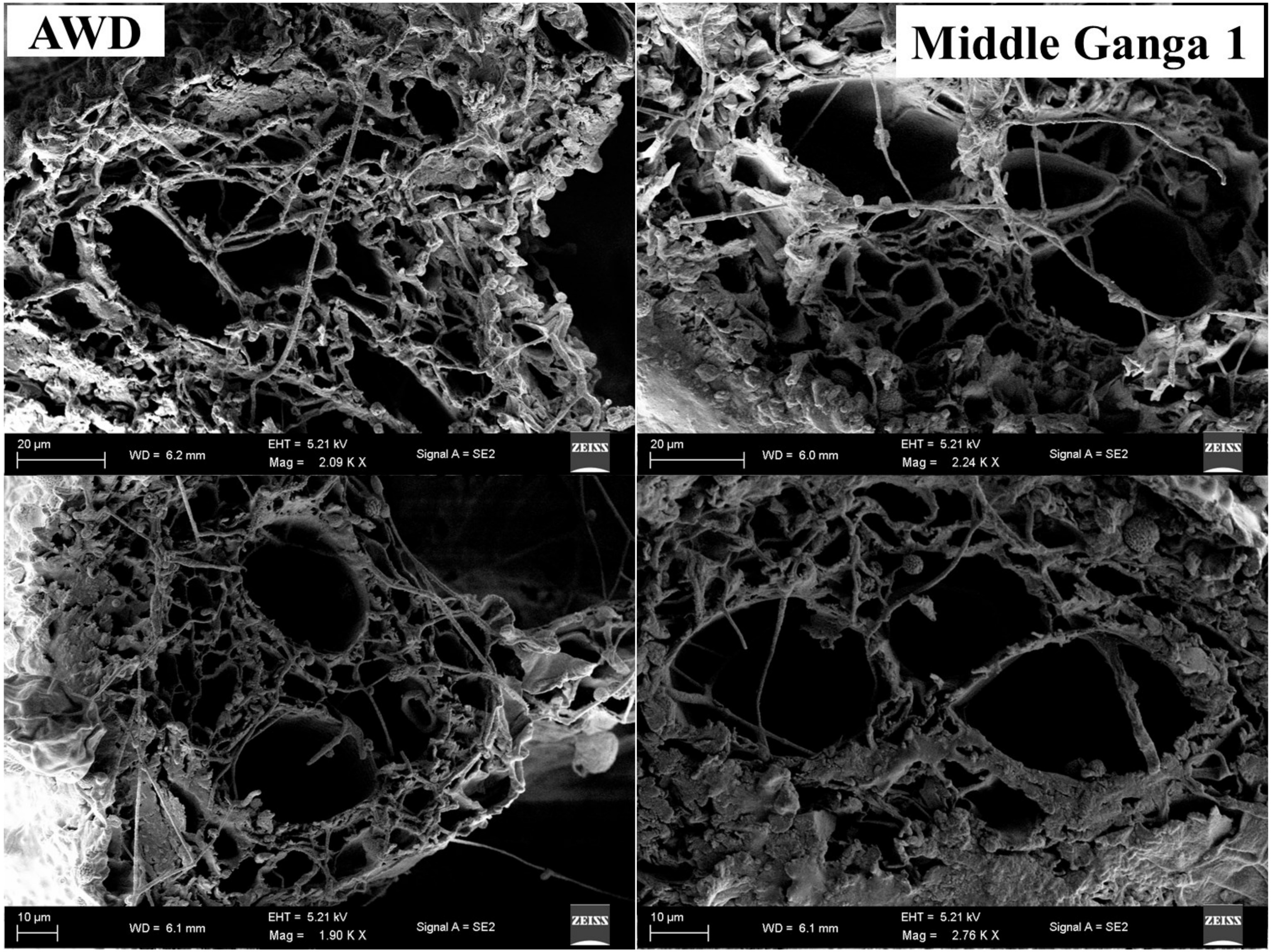
AWD
Middle Ganga 1
20 µm
WD = 6.2 mm
EHT = 5.21 kV
Mag = 2.09 K X
Signal A = SE2
ZEISS
20 µm
WD = 6.0 mm
EHT = 5.21 kV
Mag = 2.24 K X
Signal A = SE2
ZEISS
10 µm
WD = 6.1 mm
EHT = 5.21 kV
Mag = 1.90 K X
Signal A = SE2
ZEISS
10 µm
WD = 6.1 mm
EHT = 5.21 kV
Mag = 2.76 K X
Signal A = SE2
ZEISS

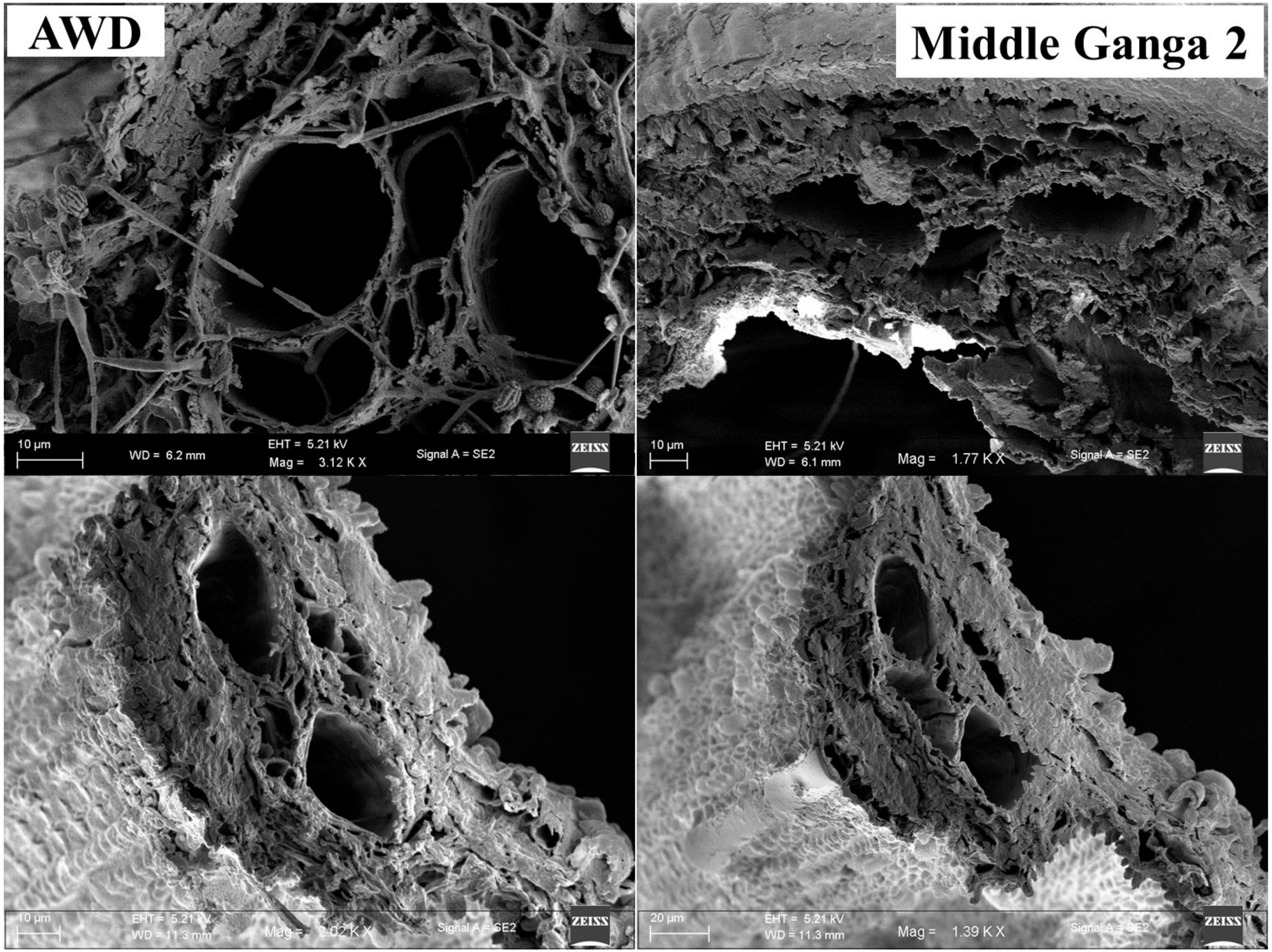
AWD
Middle Ganga 2
10 µm
WD = 6.2 mm
EHT = 5.21 kV
Mag = 3.12 K X
Signal A = SE2
ZEISS
10 µm
EHT = 5.21 kV
WD = 6.1 mm
Mag = 1.77 K X
Signal A = SE2
ZEISS
10 µm
EHT = 5.21 kV
WD = 11.3 mm
Mag = 2.02 K X
Signal A = SE2
ZEISS
20 µm
EHT = 5.21 kV
WD = 11.3 mm
Mag = 1.39 K X
Signal A = SE2
ZEISS

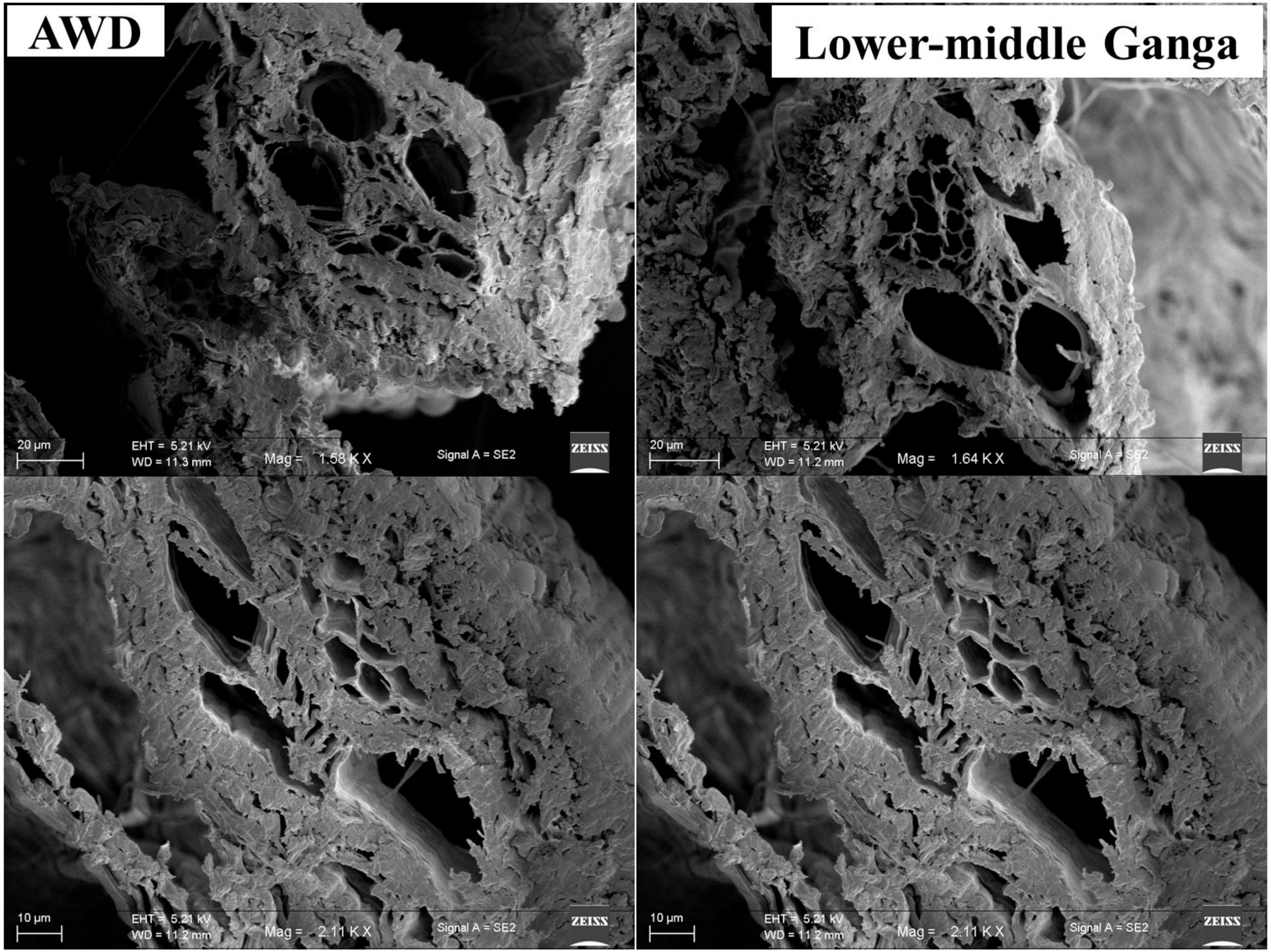
AWD
Lower-middle Ganga
20 µm
EHT = 5.21 kV
WD = 11.3 mm
Mag = 1.58 K X
Signal A = SE2
ZEISS
20 µm
EHT = 5.21 kV
WD = 11.2 mm
Mag = 1.64 K X
Signal A = SE2
ZEISS
10 µm
EHT = 5.21 kV
WD = 11.2 mm
Mag = 2.11 K X
Signal A = SE2
ZEISS
10 µm
EHT = 5.21 kV
WD = 11.2 mm
Mag = 2.11 K X
Signal A = SE2
ZEISS

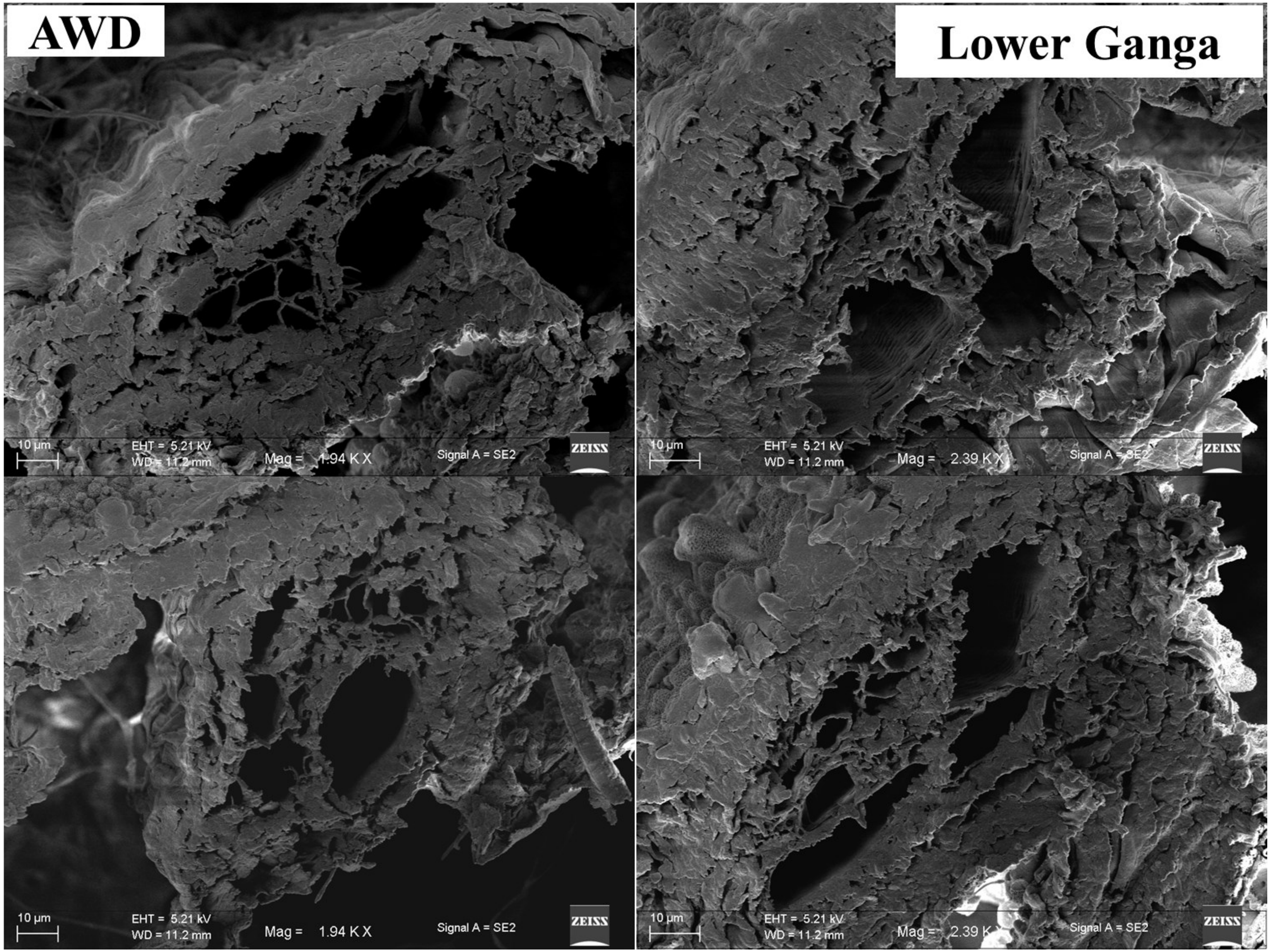
AWD
Lower Ganga
10 µm
EHT = 5.21 kV
WD = 11.2 mm
Mag = 1.94 K X
Signal A = SE2
ZEISS
10 µm
EHT = 5.21 kV
WD = 11.2 mm
Mag = 2.39 K X
Signal A = SE2
ZEISS
10 µm
EHT = 5.21 kV
WD = 11.2 mm
Mag = 1.94 K X
Signal A = SE2
ZEISS
10 µm
EHT = 5.21 kV
WD = 11.2 mm
Mag = 2.39 K X
Signal A = SE2
ZEISS

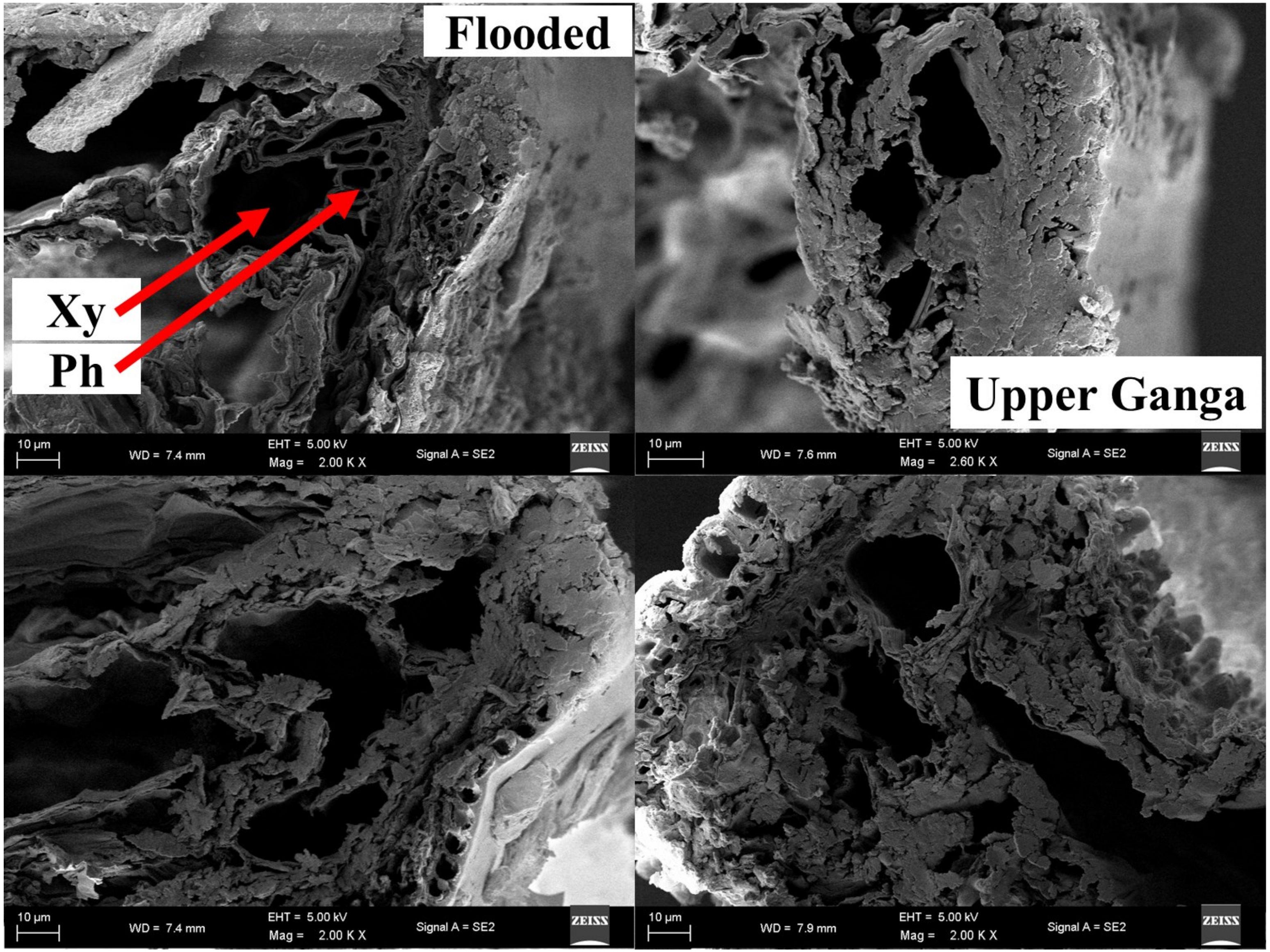
Flooded
Xy
Ph
10 µm
WD = 7.4 mm
EHT = 5.00 kV
Mag = 2.00 K X
Signal A = SE2
ZEISS
Upper Ganga
10 µm
WD = 7.6 mm
EHT = 5.00 kV
Mag = 2.60 K X
Signal A = SE2
ZEISS
10 µm
WD = 7.4 mm
EHT = 5.00 kV
Mag = 2.00 K X
Signal A = SE2
ZEISS
10 µm
WD = 7.9 mm
EHT = 5.00 kV
Mag = 2.00 K X
Signal A = SE2
ZEISS

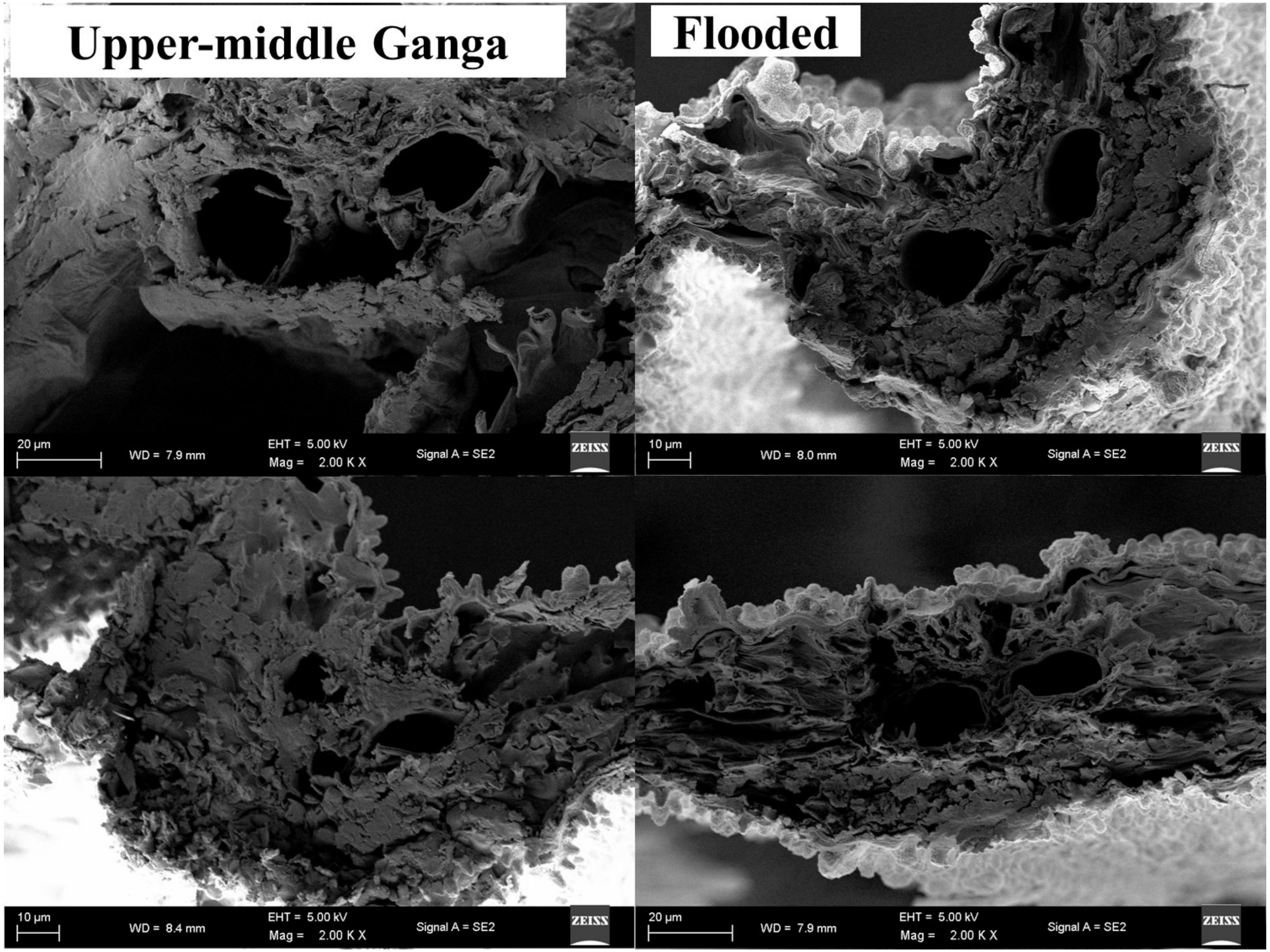
Upper-middle Ganga
Flooded
20 µm
WD = 7.9 mm
EHT = 5.00 kV
Mag = 2.00 K X
Signal A = SE2
ZEISS
10 µm
WD = 8.0 mm
EHT = 5.00 kV
Mag = 2.00 K X
Signal A = SE2
ZEISS
10 µm
WD = 8.4 mm
EHT = 5.00 kV
Mag = 2.00 K X
Signal A = SE2
ZEISS
20 µm
WD = 7.9 mm
EHT = 5.00 kV
Mag = 2.00 K X
Signal A = SE2
ZEISS

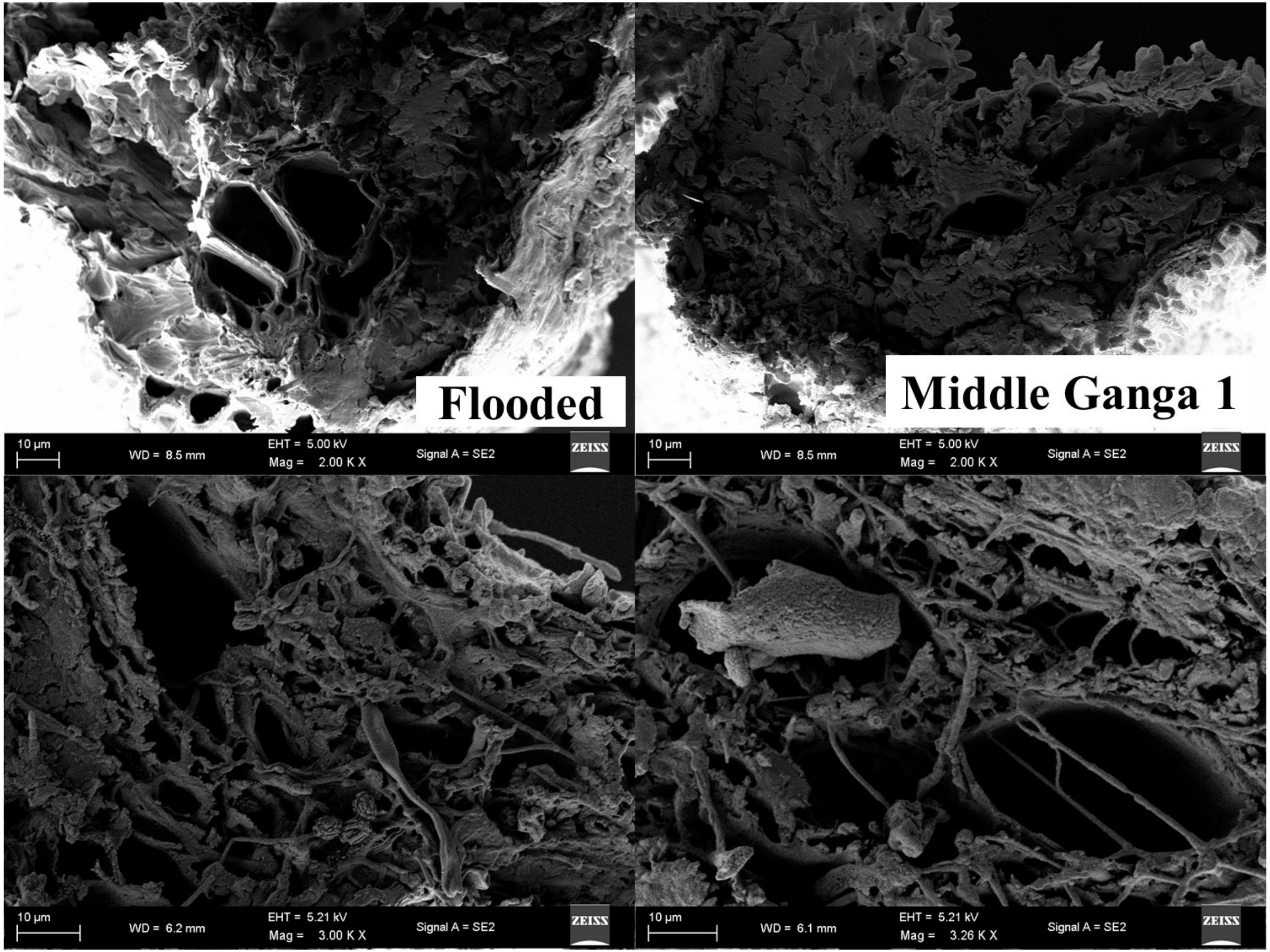
Flooded
Middle Ganga 1
10 µm
WD = 8.5 mm
EHT = 5.00 kV
Mag = 2.00 K X
Signal A = SE2
ZEISS
10 µm
WD = 8.5 mm
EHT = 5.00 kV
Mag = 2.00 K X
Signal A = SE2
ZEISS
10 µm
WD = 6.2 mm
EHT = 5.21 kV
Mag = 3.00 K X
Signal A = SE2
ZEISS
10 µm
WD = 6.1 mm
EHT = 5.21 kV
Mag = 3.26 K X
Signal A = SE2
ZEISS

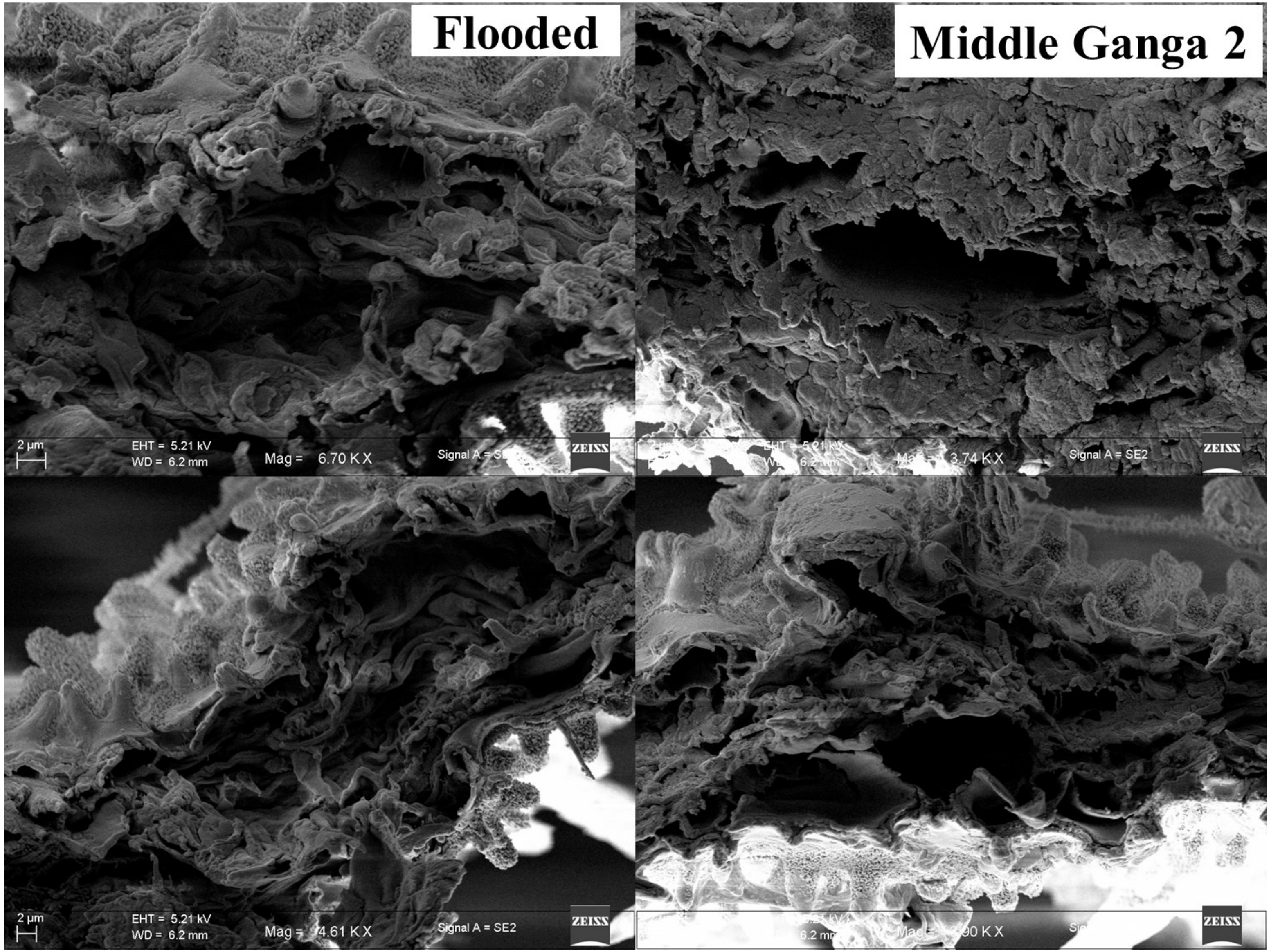
Flooded
Middle Ganga 2
2 µm
EHT = 5.21 kV
WD = 6.2 mm
Mag = 6.70 K X
Signal A = SE2
EHT = 5.21 kV
WD = 6.2 mm
Mag = 3.74 K X
Signal A = SE2
2 µm
EHT = 5.21 kV
WD = 6.2 mm
Mag = 4.61 K X
Signal A = SE2
6.2 mm
Mag = 90 K X

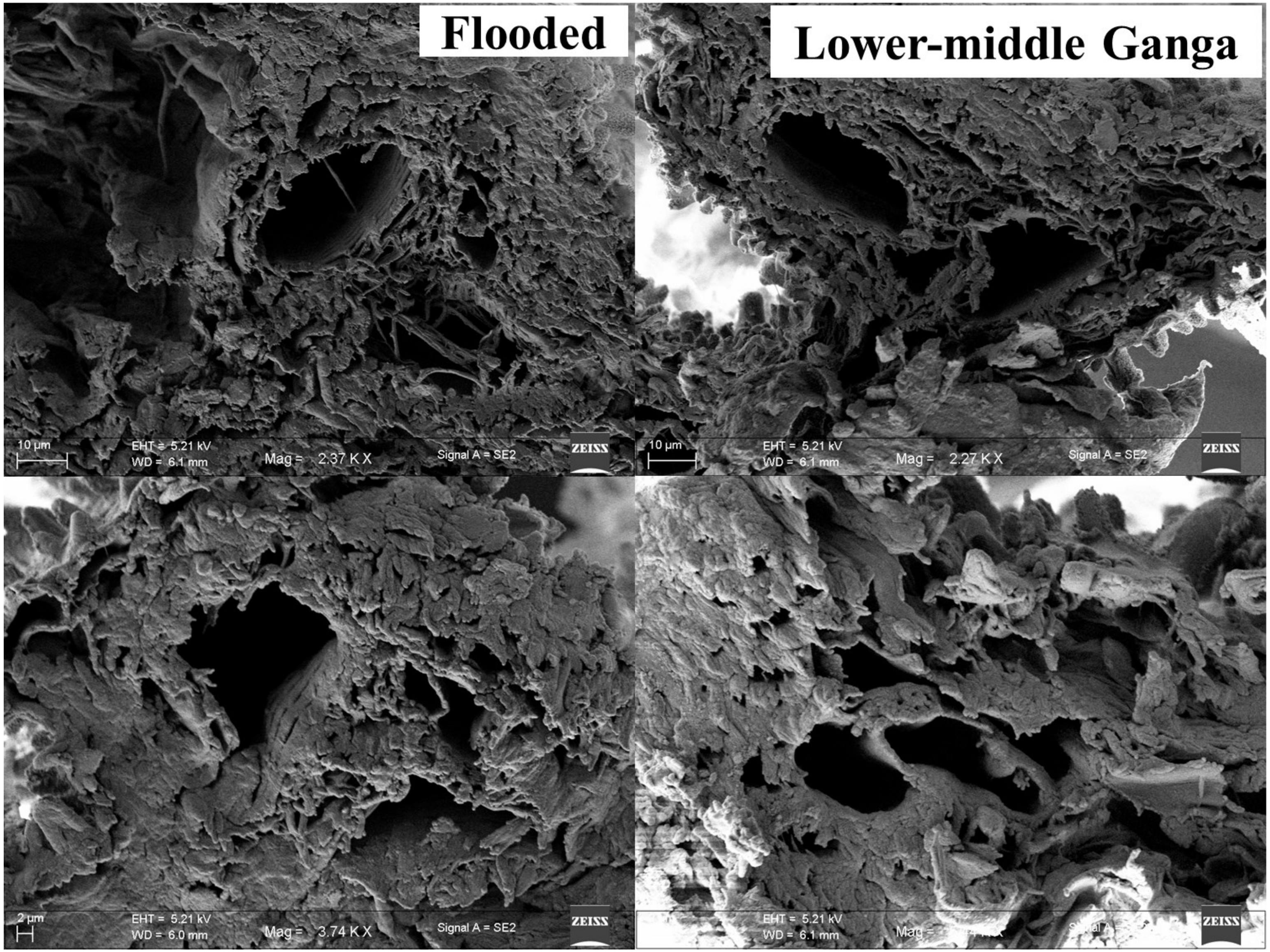
Flooded
Lower-middle Ganga
10 µm
EHT = 5.21 kV
WD = 6.1 mm
Mag = 2.37 K X
Signal A = SE2
ZEISS
10 µm
EHT = 5.21 kV
WD = 6.1 mm
Mag = 2.27 K X
Signal A = SE2
ZEISS
2 µm
EHT = 5.21 kV
WD = 6.0 mm
Mag = 3.74 K X
Signal A = SE2
ZEISS
EHT = 5.21 kV
WD = 6.1 mm
ZEISS

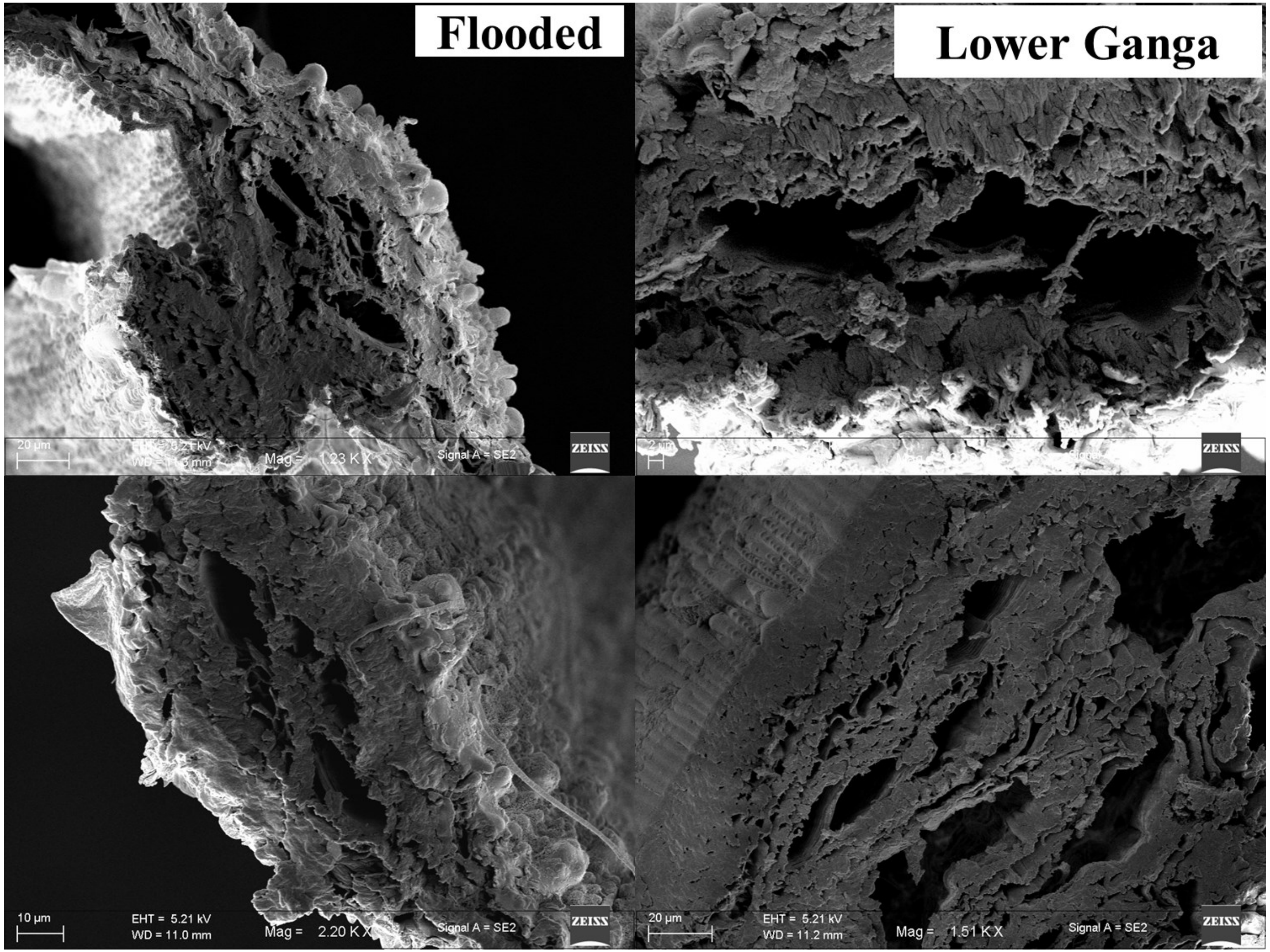
Flooded
Lower Ganga
20 µm
EHT = 5.21 kV
WD = 11.0 mm
Mag = 1.23 K X
Signal A = SE2
ZEISS
2 µm
ZEISS
10 µm
EHT = 5.21 kV
WD = 11.0 mm
Mag = 2.20 K X
Signal A = SE2
ZEISS
20 µm
EHT = 5.21 kV
WD = 11.2 mm
Mag = 1.51 K X
Signal A = SE2
ZEISS

Supplementary Figure S7. Rice yield productivity (a-f) and plant bioavailable As-Si concentrations (g-l) with spatial variation at 24 sites.

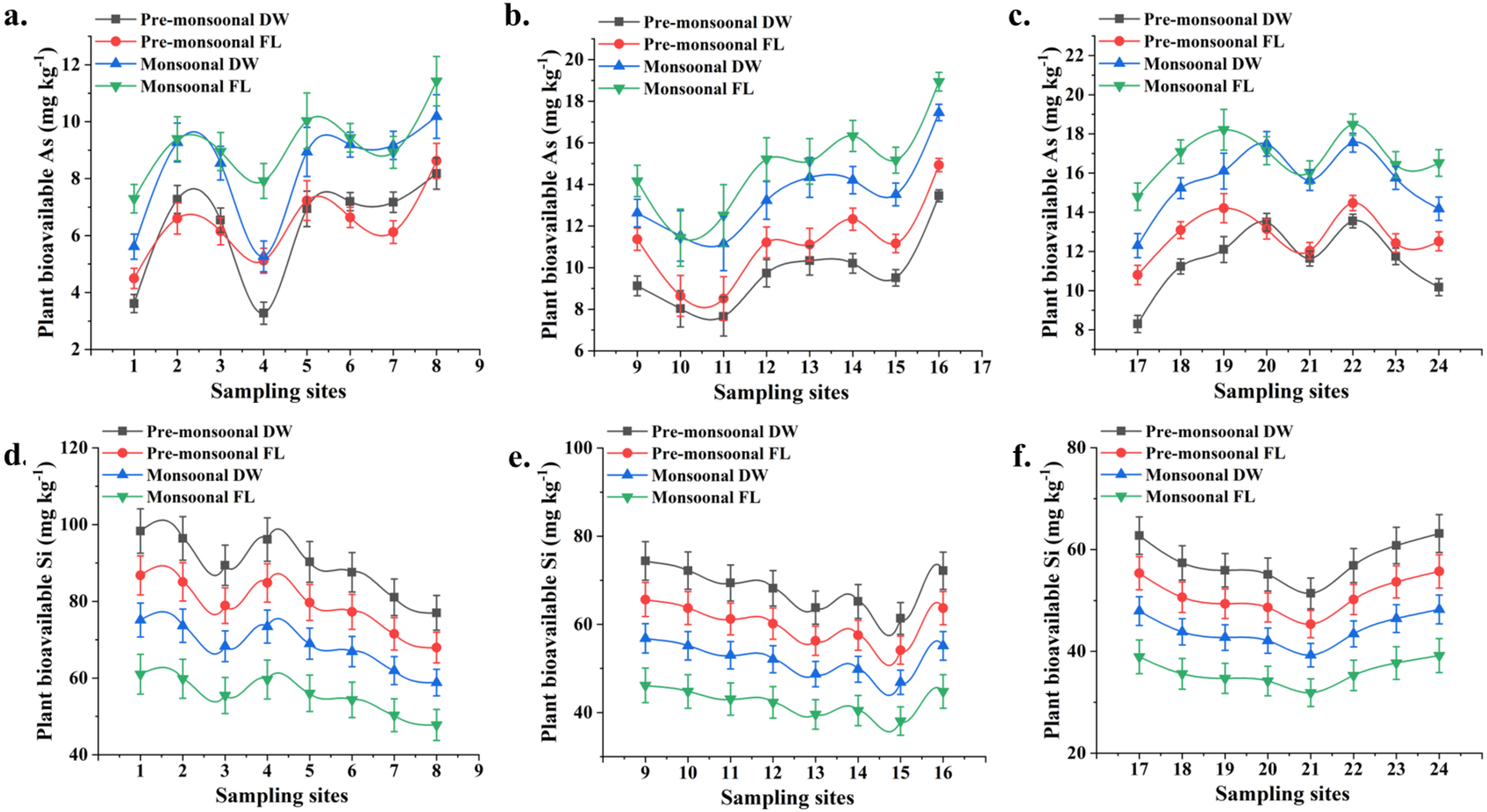

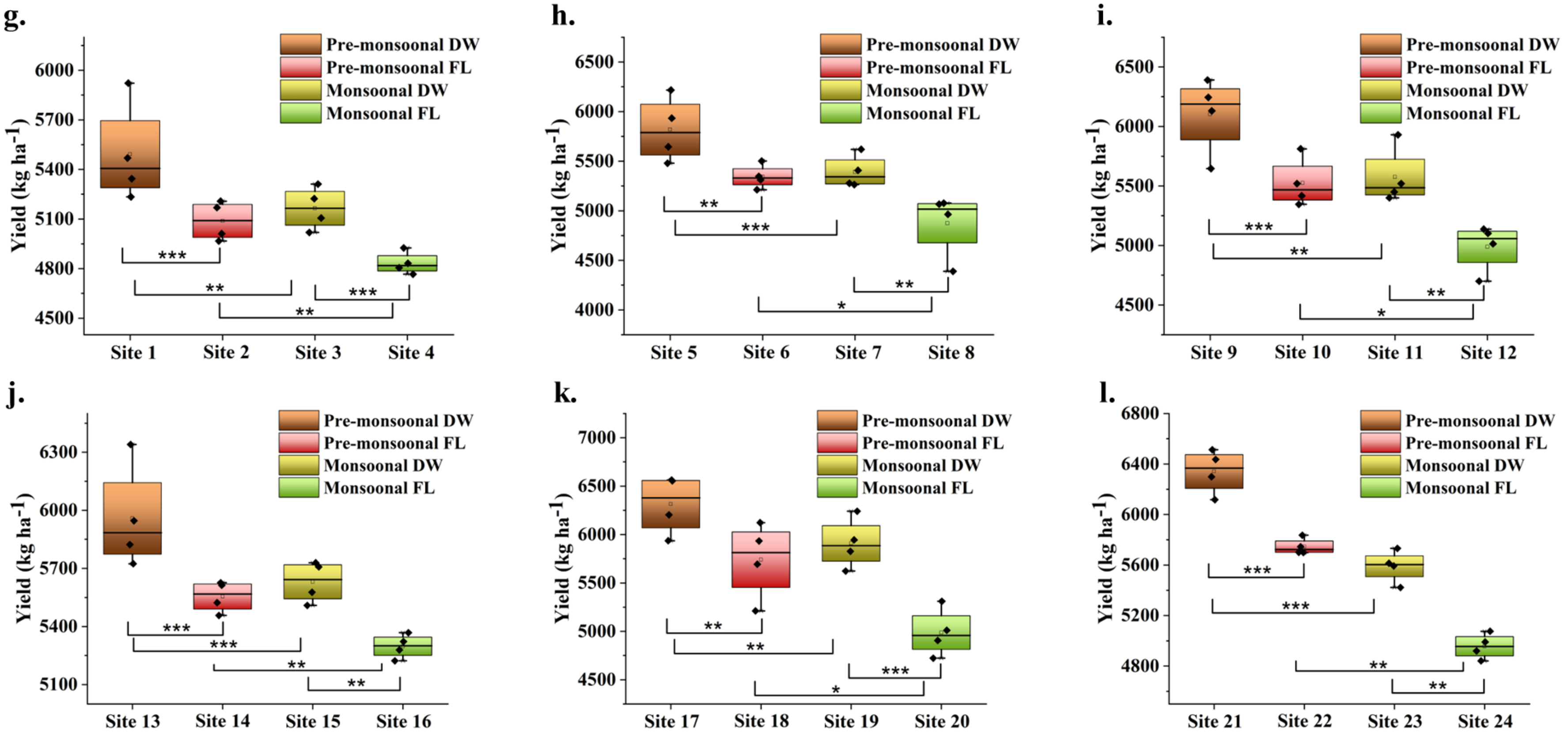

Figure 1a-f shows the As and Si bioavailable concentrations in soil under both the irrigation regimes and seasonal change. Each site represents the mean yield data (1g-l) of triplicate sampling points where significant variance has been presented with ‘***’ to be highly significant, ‘**’ moderate significance and ‘*’ low significance. Graphs are representative of triplicate data with standard deviation.

Supplementary Figure S8. Heatmap analysis of pre-monsoonal and monsoonal microbial class occurrence under two irrigation types.

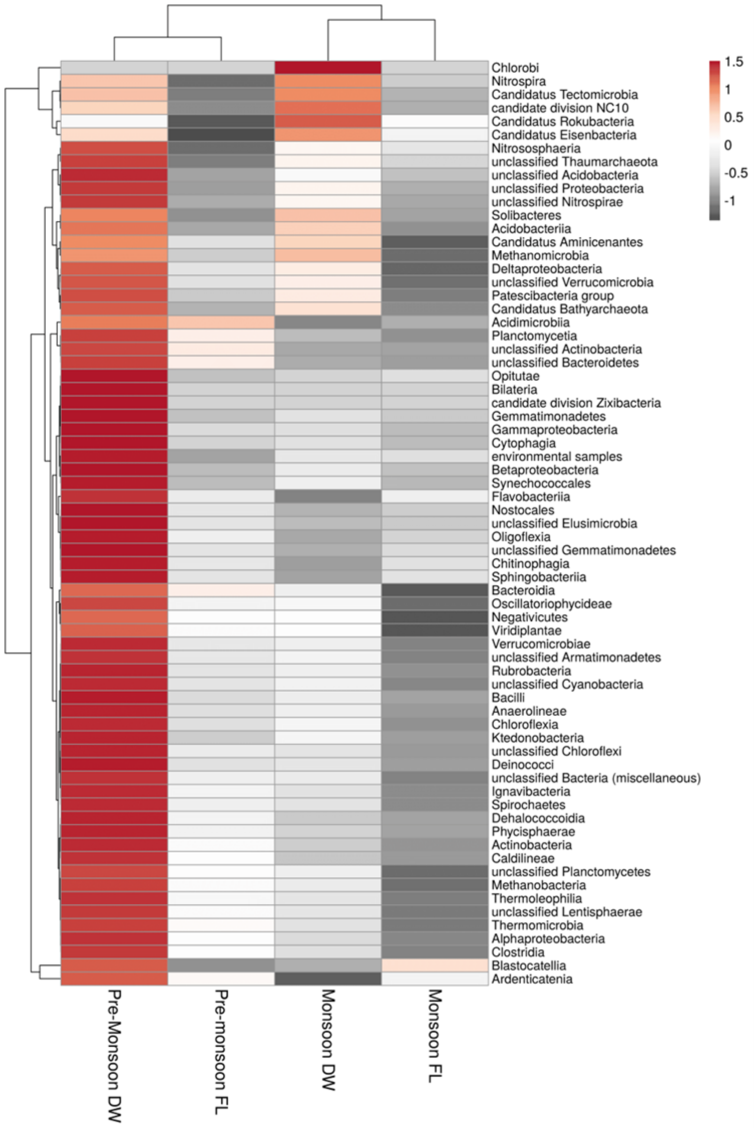

Supplementary Figure S9. KEGG Metabolic pathway analysis with predominant biochemical modules as superimposed models of earlier reports. Our analysed pathways are highlighted with red lines in each diagram.

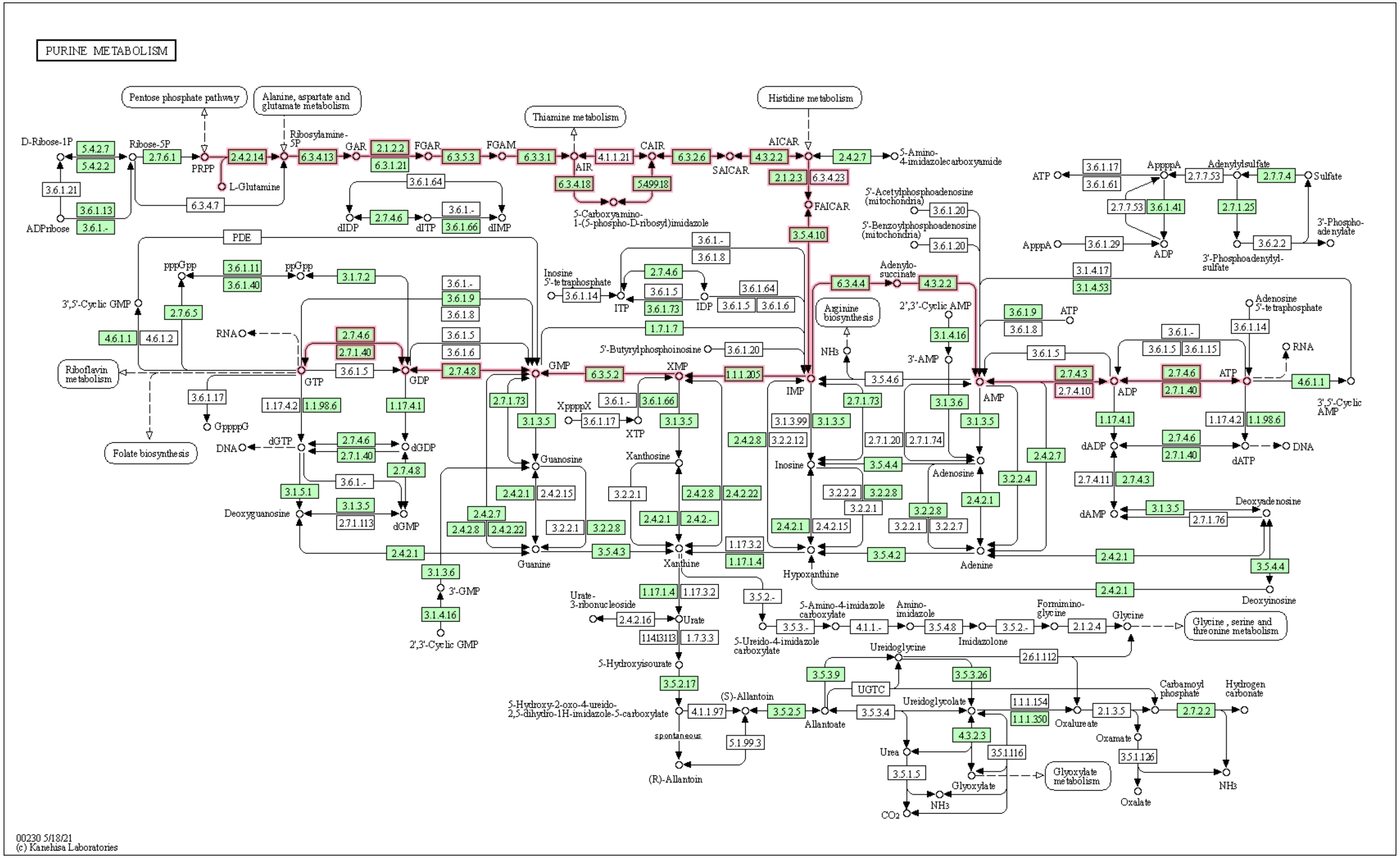

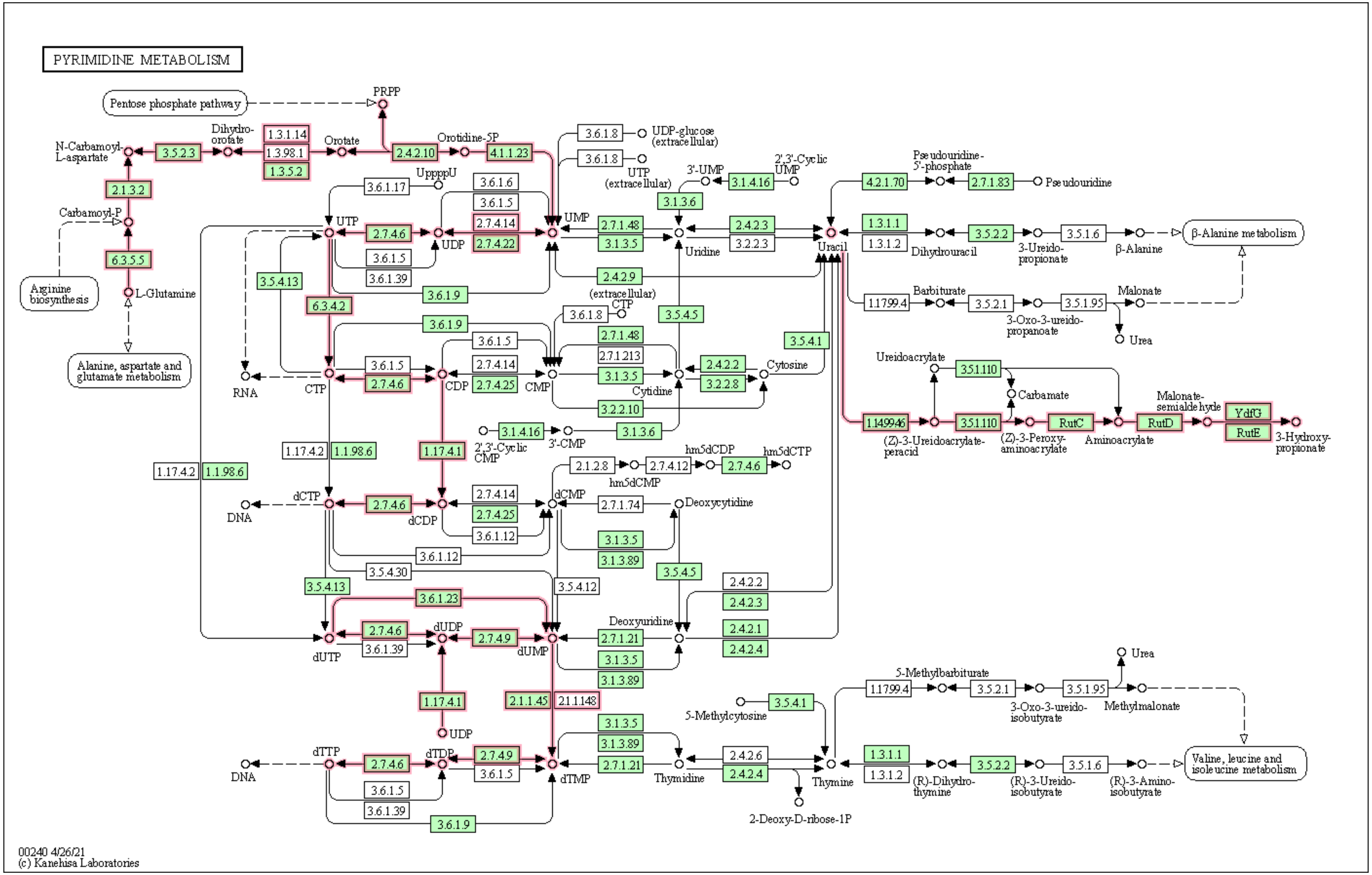
PYRIMIDINE METABOLISM
Pentose phosphate pathway
PRPP
N-Carbamoyl-L-aspartate
3.5.2.3
Dihydro-orotate
1.3.1.14
1.3.98.1
1.3.5.2
Orotate
2.4.2.10
Orotidine-5P
4.1.1.23
2.1.3.2
Carbamoyl-P
6.3.5.5
L-Glutamine
Arginine biosynthesis
Alanine, aspartate and glutamate metabolism
3.6.1.8
UDP-glucose (extracellular)
3.6.1.8
UTP (extracellular)
3'-UMP
3.1.4.16
2',3'-Cyclic UMP
Pseudouridine-5'-phosphate
4.2.1.70
2.7.1.83
Pseudouridine
UppppU
3.6.1.17
3.6.1.6
3.6.1.5
2.7.4.14
2.7.4.22
UTP
2.7.4.6
UDP
UMP
2.7.1.48
3.1.3.5
3.1.3.6
Uridine
2.4.2.3
3.2.2.3
Uracil
1.3.1.1
1.3.1.2
Dihydrouracil
3.5.2.2
3-Ureido-propionate
3.5.1.6
β-Alanine
β-Alanine metabolism
3.6.1.5
3.6.1.39
3.5.4.13
3.6.1.9
2.4.2.9
6.3.4.2
(extracellular) CTP
3.6.1.8
3.5.4.5
3.5.4.1
1.17.99.4
Barbiturate
3.5.2.1
3.5.1.95
Malonate
3-Oxo-3-ureido-propanoate
Urea
3.6.1.9
3.6.1.5
2.7.1.48
2.7.1.213
3.6.1.5
2.7.4.14
2.4.2.2
Cytosine
RNA
CTP
2.7.4.6
CDP
2.7.4.25
CMP
3.1.3.5
3.2.2.8
Cytidine
3.2.2.10
Ureidoacrylate
3.5.1.110
Carbamate
Malonate-semialdehyde
YdfG
RutE
3.1.4.16
3'-CMP
2',3'-Cyclic CMP
3.1.3.6
1.14.99.46
3.5.1.110
RutC
RutD
3-Hydroxy-propionate
(Z)-3-Ureidoacrylate-peracid
(Z)-3-Peroxy-aminoacrylate
Aminoacrylate
1.17.4.2
1.1.98.6
1.17.4.2
1.1.98.6
1.17.4.1
2.1.2.8
2.7.4.12
2.7.4.6
hm5dCDP
hm5dCTP
hm5dCMP
DNA
dCTP
2.7.4.6
dCDP
2.7.4.14
2.7.4.25
3.6.1.12
dCMP
2.7.1.74
Deoxycytidine
3.1.3.5
3.1.3.89
3.6.1.12
3.5.4.30
3.5.4.12
3.5.4.5
2.4.2.2
2.4.2.3
3.5.4.13
3.6.1.23
Deoxyuridine
2.4.2.1
2.4.2.4
dUTP
2.7.4.6
3.6.1.39
dUDP
2.7.4.9
dUMP
2.7.1.21
3.1.3.5
3.1.3.89
Urea
5-Methylbarbiturate
1.17.99.4
3.5.2.1
3.5.1.95
3-Oxo-3-ureido-isobutyrate
Methylmalonate
1.17.4.1
UDP
2.1.1.45
2.1.1.148
5-Methylcytosine
3.5.4.1
3.1.3.5
3.1.3.89
DNA
dTTP
2.7.4.6
dTDP
2.7.4.9
3.6.1.5
dTMP
2.7.1.21
Thymidine
2.4.2.6
2.4.2.4
Thymine
1.3.1.1
1.3.1.2
3.5.2.2
(R)-Dihydro-thymine
(R)-3-Ureido-isobutyrate
3.5.1.6
(R)-3-Amino-isobutyrate
Valine, leucine and isoleucine metabolism
3.6.1.5
3.6.1.39
3.6.1.9
2-Deoxy-D-ribose-1P
00240 4/26/21
(c) Kanehisa Laboratories

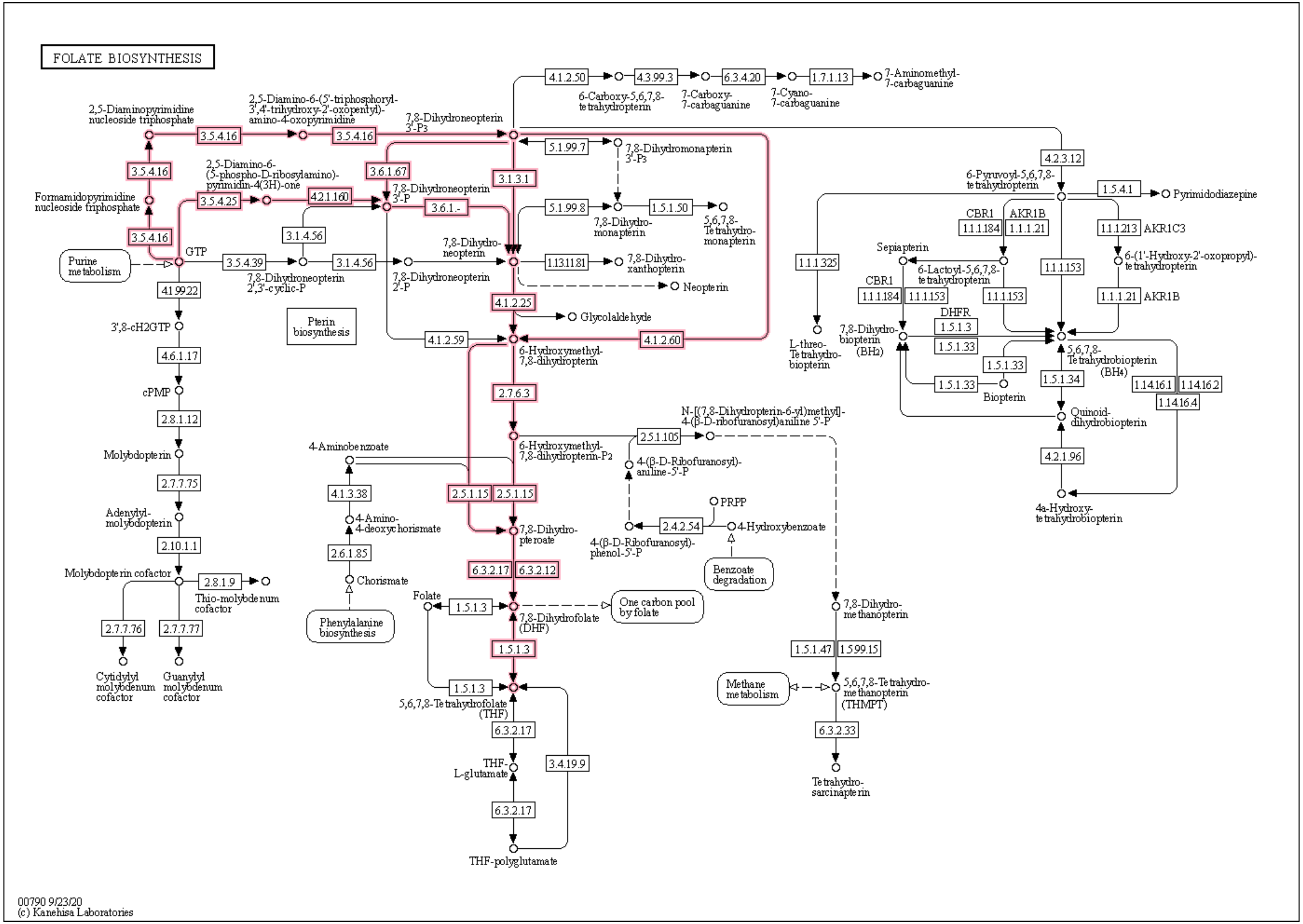

00790 9/23/20
(c) Kanehisa Laboratories

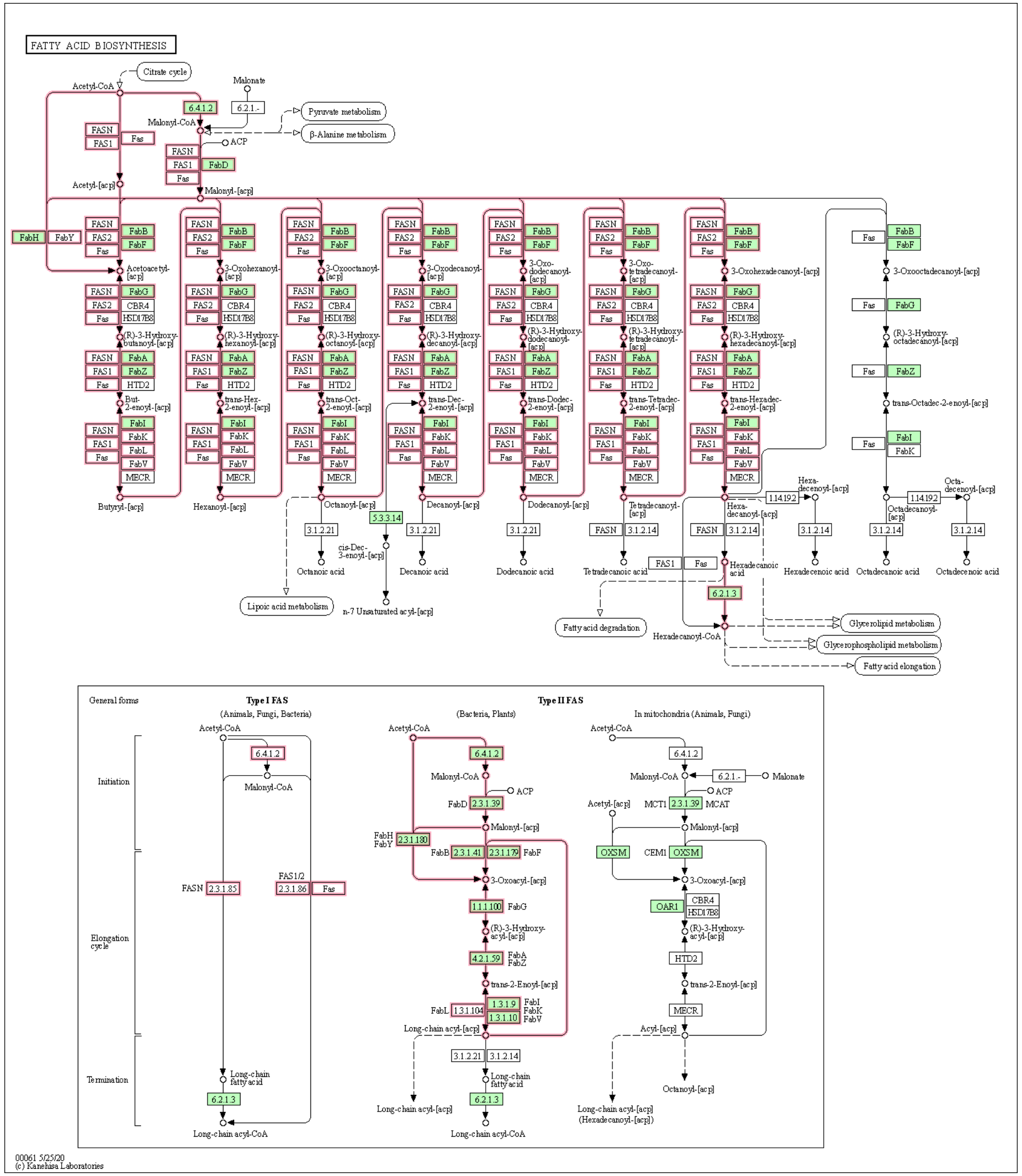
FATTY ACID BIOSYNTHESIS
Citrate cycle
Acetyl-CoA
Malonate
6.4.1.2
6.2.1.-
Pyruvate metabolism
β-Alanine metabolism
Malonyl-CoA
ACP
FASN
FAS1
FAS2
Fas
FabD
Acetyl-[acp]
Malonyl-[acp]
FabH
FabY
FabB
FabF
FabG
CBR4
HSD17B8
FabA
FabZ
HTD2
FabI
FabK
FabL
FabV
MECR
Acetoacetyl-[acp]
(R)-3-Hydroxy-butanoyl-[acp]
But-2-enoyl-[acp]
Butyryl-[acp]
3-Oxohexanoyl-[acp]
(R)-3-Hydroxy-hexanoyl-[acp]
trans-Hex-2-enoyl-[acp]
Hexanoyl-[acp]
3-Oxooctanoyl-[acp]
(R)-3-Hydroxy-octanoyl-[acp]
trans-Oct-2-enoyl-[acp]
Octanoyl-[acp]
3-Oxodecanoyl-[acp]
(R)-3-Hydroxy-decanoyl-[acp]
trans-Dec-2-enoyl-[acp]
Decanoyl-[acp]
3-Oxo-dodecanoyl-[acp]
(R)-3-Hydroxy-dodecanoyl-[acp]
trans-Dodec-2-enoyl-[acp]
Dodecanoyl-[acp]
3-Oxo-tetradecanoyl-[acp]
(R)-3-Hydroxy-tetradecanoyl-[acp]
trans-Tetradec-2-enoyl-[acp]
Tetradecanoyl-[acp]
3-Oxohexadecanoyl-[acp]
(R)-3-Hydroxy-hexadecanoyl-[acp]
trans-Hexadec-2-enoyl-[acp]
Hexa-decanoyl-[acp]
3-Oxooctadecanoyl-[acp]
(R)-3-Hydroxy-octadecanoyl-[acp]
trans-Octadec-2-enoyl-[acp]
Octadecanoyl-[acp]
1.14.19.2
Hexa-decenoyl-[acp]
Octa-decenoyl-[acp]
3.1.2.21
3.1.2.14
5.3.3.14
cis-Dec-3-enoyl-[acp]
n-7 Unsaturated acyl-[acp]
Lipoic acid metabolism
Octanoic acid
Decanoic acid
Dodecanoic acid
Tetradecanoic acid
Hexadecanoic acid
Hexadecenoic acid
Octadecanoic acid
Octadecenoic acid
6.2.1.3
Hexadecanoyl-CoA
Fatty acid degradation
Glycerolipid metabolism
Glycerophospholipid metabolism
Fatty acid elongation
General forms
Type I FAS
(Animals, Fungi, Bacteria)
Type II FAS
(Bacteria, Plants)
In mitochondria (Animals, Fungi)
Initiation
Elongation cycle
Termination
2.3.1.85
FAS1/2
2.3.1.86
Long-chain fatty acid
Long-chain acyl-CoA
2.3.1.39
2.3.1.180
2.3.1.41
2.3.1.179
3-Oxoacyl-[acp]
1.1.1.100
(R)-3-Hydroxy-acyl-[acp]
4.2.1.59
trans-2-Enoyl-[acp]
1.3.1.104
1.3.1.9
1.3.1.10
Long-chain acyl-[acp]
MCT1
MCAT
OXSM
CEM1
OAR1
Acyl-[acp]
Octanoyl-[acp]
Long-chain acyl-[acp] (Hexadecanoyl-[acp])
00061 5/25/20
(c) Kanehisa Laboratories

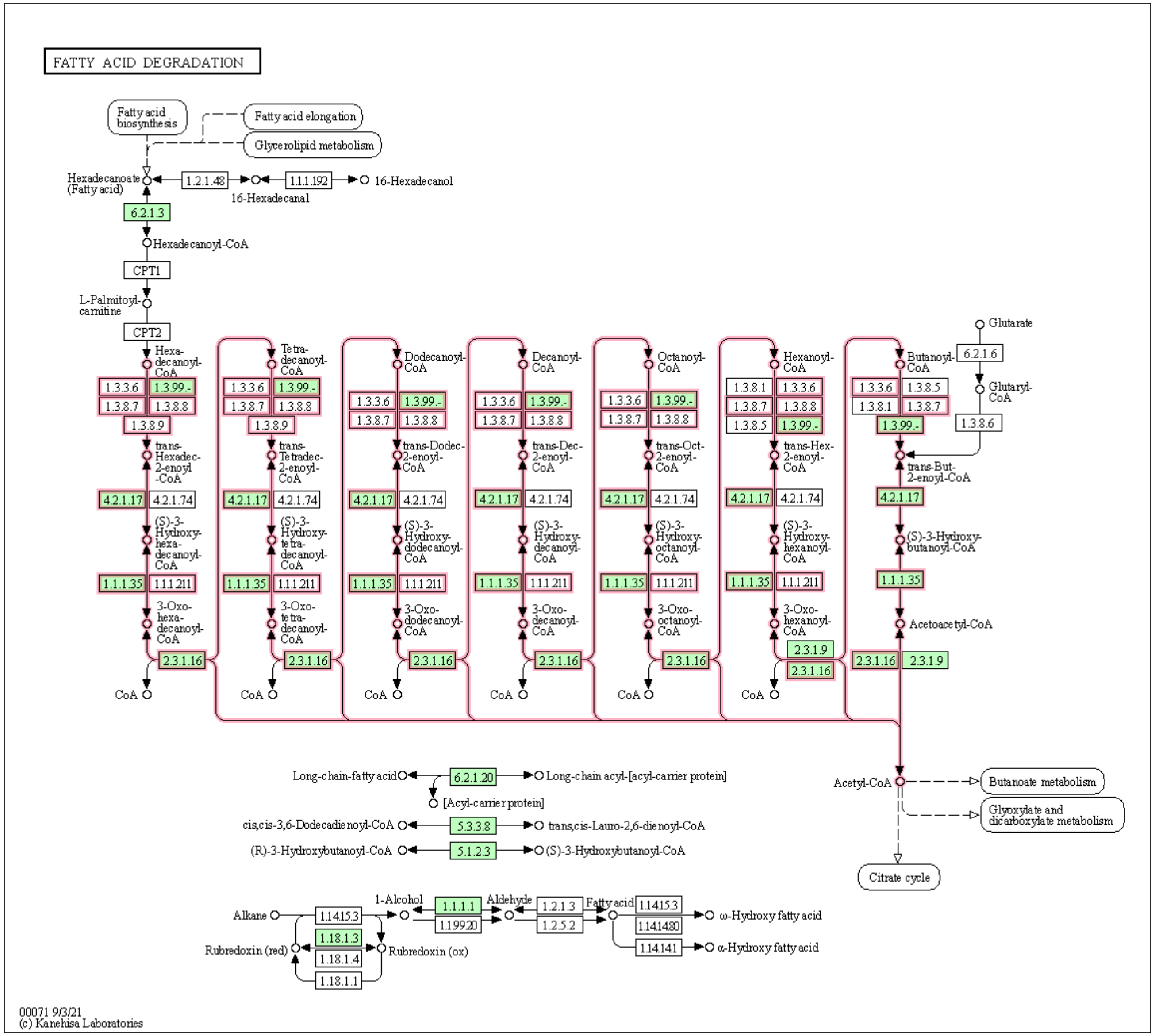
FATTY ACID DEGRADATION
Fatty acid biosynthesis
Fatty acid elongation
Glycerolipid metabolism
Hexadecanoate (Fatty acid)
1.2.1.48
16-Hexadecanal
1.1.1.192
16-Hexadecanol
6.2.1.3
Hexadecanoyl-CoA
CPT1
L-Palmitoyl-carnitine
CPT2
Hexa-decanoyl-CoA
Tetra-decanoyl-CoA
Dodecanoyl-CoA
Decanoyl-CoA
Octanoyl-CoA
Hexanoyl-CoA
Butanoyl-CoA
Glutarate
6.2.1.6
Glutaryl-CoA
1.3.8.6
1.3.3.6
1.3.99.-
1.3.8.7
1.3.8.8
1.3.8.9
1.3.8.1
1.3.8.5
trans-Hexadec-2-enoyl-CoA
trans-Tetradec-2-enoyl-CoA
trans-Dodec-2-enoyl-CoA
trans-Dec-2-enoyl-CoA
trans-Oct-2-enoyl-CoA
trans-Hex-2-enoyl-CoA
trans-But-2-enoyl-CoA
4.2.1.17
4.2.1.74
(S)-3-Hydroxy-hexa-decanoyl-CoA
(S)-3-Hydroxy-tetra-decanoyl-CoA
(S)-3-Hydroxy-dodecanoyl-CoA
(S)-3-Hydroxy-decanoyl-CoA
(S)-3-Hydroxy-octanoyl-CoA
(S)-3-Hydroxy-hexanoyl-CoA
(S)-3-Hydroxy-butanoyl-CoA
1.1.1.35
1.1.1.211
3-Oxo-hexa-decanoyl-CoA
3-Oxo-tetra-decanoyl-CoA
3-Oxo-dodecanoyl-CoA
3-Oxo-decanoyl-CoA
3-Oxo-octanoyl-CoA
3-Oxo-hexanoyl-CoA
Acetoacetyl-CoA
2.3.1.16
2.3.1.9
CoA
Acetyl-CoA
Butanoate metabolism
Glyoxylate and dicarboxylate metabolism
Citrate cycle
Long-chain-fatty acid
6.2.1.20
Long-chain acyl-[acyl-carrier protein]
[Acyl-carrier protein]
cis,cis-3,6-Dodecadienoyl-CoA
5.3.3.8
trans,cis-Lauro-2,6-dienoyl-CoA
(R)-3-Hydroxybutanoyl-CoA
5.1.2.3
(S)-3-Hydroxybutanoyl-CoA
Alkane
1.14.15.3
1.18.1.3
1.18.1.4
1.18.1.1
Rubredoxin (red)
Rubredoxin (ox)
1-Alcohol
1.1.1.1
1.1.99.20
Aldehyde
1.2.1.3
1.2.5.2
Fatty acid
1.14.15.3
1.14.14.80
1.14.14.1
ω-Hydroxy fatty acid
α-Hydroxy fatty acid
00071 9/3/21
(c) Kanehisa Laboratories

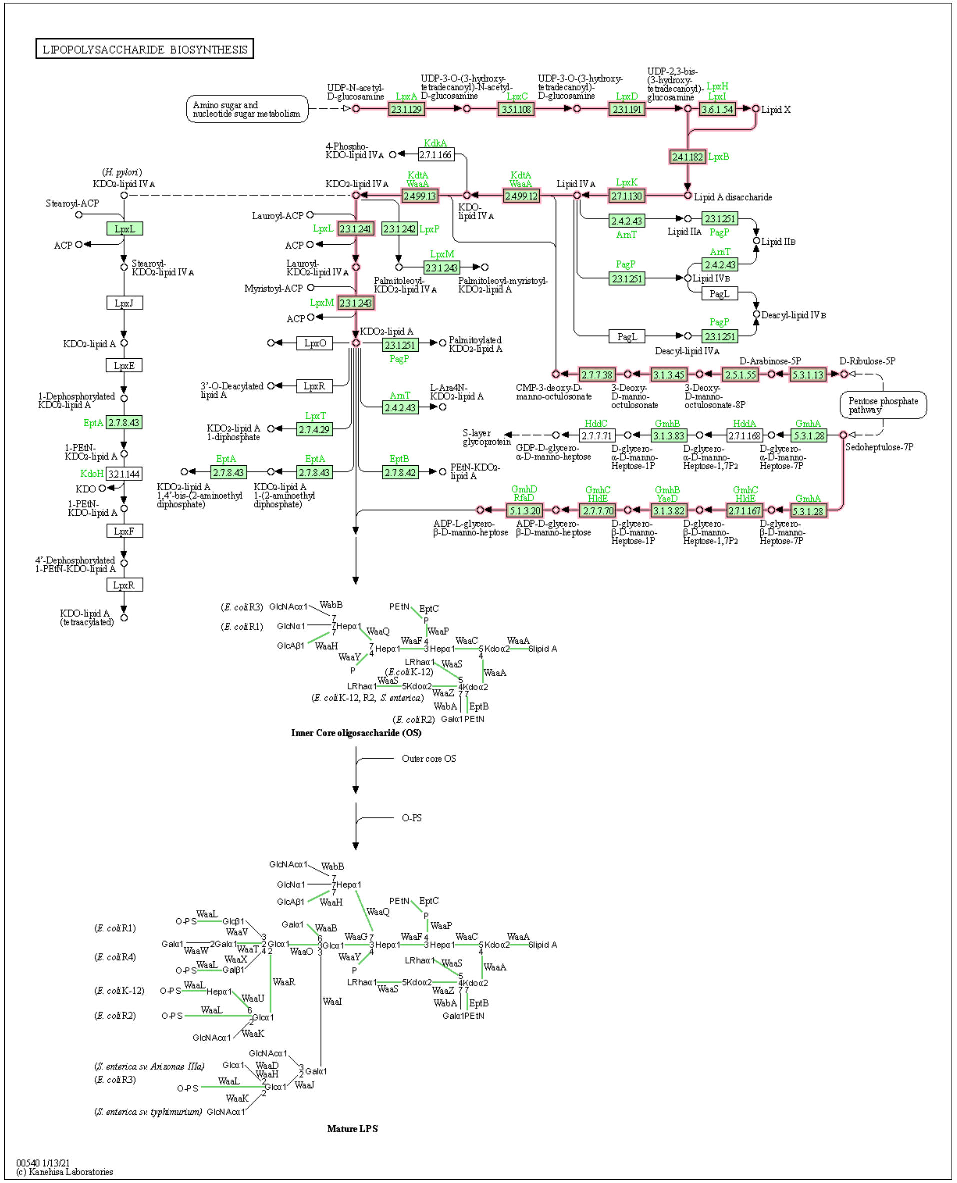
LIPOPOLYSACCHARIDE BIOSYNTHESIS
Amino sugar and nucleotide sugar metabolism
UDP-N-acetyl-D-glucosamine
LpxA 2.3.1.129
UDP-3-O-(3-hydroxy-tetradecanoyl)-N-acetyl-D-glucosamine
LpxC 3.5.1.108
UDP-3-O-(3-hydroxy-tetradecanoyl)-D-glucosamine
LpxD 2.3.1.191
UDP-2,3-bis-(3-hydroxy-tetradecanoyl)-glucosamine
LpxH LpxI 3.6.1.54
Lipid X
2.4.1.182 LpxB
Lipid A disaccharide
LpxK 2.7.1.130
Lipid IVA
KdtA WaaA 2.4.99.12
KDO-lipid IVA
KdtA WaaA 2.4.99.13
KDO2-lipid IVA
KdkA 2.7.1.166
4-Phospho-KDO-lipid IVA
(H. pylori) KDO2-lipid IVA
Stearoyl-ACP
LpxL
ACP
Stearoyl-KDO2-lipid IVA
LpxJ
KDO2-lipid A
LpxE
1-Dephosphorylated KDO2-lipid A
EptA 2.7.8.43
1-PEtN-KDO2-lipid A
KdoH 3.2.1.144
KDO
1-PEtN-KDO-lipid A
LpxF
4'-Dephosphorylated 1-PEtN-KDO-lipid A
LpxR
KDO-lipid A (tetraacylated)
Lauroyl-ACP
LpxL 2.3.1.241
2.3.1.242 LpxP
Lauroyl-KDO2-lipid IVA
LpxM 2.3.1.243
Palmitoleoyl-KDO2-lipid IVA
Palmitoleoyl-myristoyl-KDO2-lipid A
Myristoyl-ACP
LpxM 2.3.1.243
KDO2-lipid A
LpxO
2.3.1.251 PagP
Palmitoylated KDO2-lipid A
3'-O-Deacylated lipid A
LpxR
ArnT 2.4.2.43
L-Ara4N-KDO2-lipid A
LpxT 2.7.4.29
KDO2-lipid A 1-diphosphate
EptA 2.7.8.43
EptA 2.7.8.43
KDO2-lipid A 1,4'-bis-(2-aminoethyl diphosphate)
KDO2-lipid A 1-(2-aminoethyl diphosphate)
EptB 2.7.8.42
PEtN-KDO2-lipid A
2.4.2.43 ArnT
Lipid IIA
2.3.1.251 PagP
Lipid IIB
PagP 2.3.1.251
ArnT 2.4.2.43
Lipid IVB
PagL
Deacyl-lipid IVB
PagL
PagP 2.3.1.251
Deacyl-lipid IVA
CMP-3-deoxy-D-manno-octulosonate
2.7.7.38
3-Deoxy-D-manno-octulosonate
3.1.3.45
3-Deoxy-D-manno-octulosonate-8P
2.5.1.55
D-Arabinose-5P
5.3.1.13
D-Ribulose-5P
Pentose phosphate pathway
Sedoheptulose-7P
S-layer glycoprotein
HddC 2.7.7.71
GDP-D-glycero-α-D-manno-heptose
GmhB 3.1.3.83
D-glycero-α-D-manno-Heptose-1P
HddA 2.7.1.168
D-glycero-α-D-manno-Heptose-1,7P2
GmhA 5.3.1.28
D-glycero-α-D-manno-Heptose-7P
GmhD RfaD 5.1.3.20
ADP-L-glycero-β-D-manno-heptose
GmhC HldE 2.7.7.70
ADP-D-glycero-β-D-manno-heptose
GmhB YaeD 3.1.3.82
D-glycero-β-D-manno-Heptose-1P
GmhC HldE 2.7.1.167
D-glycero-β-D-manno-Heptose-1,7P2
GmhA 5.3.1.28
D-glycero-β-D-manno-Heptose-7P
(E. coli R3)
(E. coli R1)
(E. coli K-12)
(E. coli K-12, R2, S. enterica)
(E. coli R2)
Inner Core oligosaccharide (OS)
Outer core OS
O-PS
(E. coli R1)
(E. coli R4)
(E. coli K-12)
(E. coli R2)
(S. enterica sv. Arizonae IIIa)
(E. coli R3)
(S. enterica sv. typhimurium)
Mature LPS
00540 1/13/21
(c) Kanehisa Laboratories

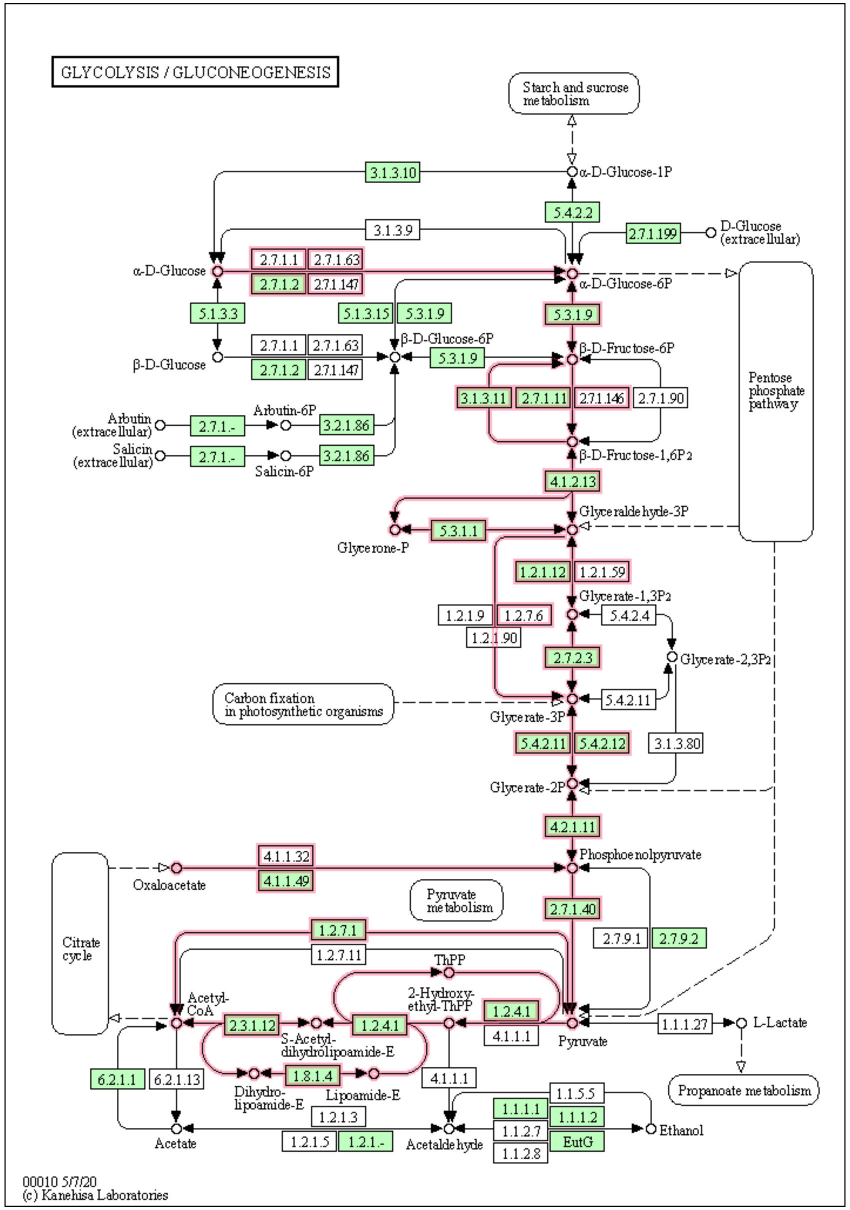
GLYCOLYSIS / GLUCONEOGENESIS
Starch and sucrose metabolism
α-D-Glucose-1P
3.1.3.10
5.4.2.2
3.1.3.9
2.7.1.199
D-Glucose (extracellular)
α-D-Glucose
2.7.1.1
2.7.1.63
2.7.1.2
2.7.1.147
α-D-Glucose-6P
5.1.3.3
5.1.3.15
5.3.1.9
5.3.1.9
β-D-Glucose
2.7.1.1
2.7.1.63
2.7.1.2
2.7.1.147
β-D-Glucose-6P
5.3.1.9
β-D-Fructose-6P
Pentose phosphate pathway
Arbutin (extracellular)
2.7.1.-
Arbutin-6P
3.2.1.86
3.1.3.11
2.7.1.11
2.7.1.146
2.7.1.90
Salicin (extracellular)
2.7.1.-
Salicin-6P
3.2.1.86
β-D-Fructose-1,6P2
4.1.2.13
Glyceraldehyde-3P
5.3.1.1
Glycerone-P
1.2.1.12
1.2.1.59
Glycerate-1,3P2
1.2.1.9
1.2.7.6
5.4.2.4
1.2.1.90
2.7.2.3
Glycerate-2,3P2
Carbon fixation in photosynthetic organisms
5.4.2.11
Glycerate-3P
5.4.2.11
5.4.2.12
3.1.3.80
Glycerate-2P
4.2.1.11
Phosphoenolpyruvate
4.1.1.32
4.1.1.49
Oxaloacetate
Pyruvate metabolism
2.7.1.40
Citrate cycle
1.2.7.1
1.2.7.11
2.7.9.1
2.7.9.2
ThPP
2-Hydroxy-ethyl-ThPP
1.2.4.1
Acetyl-CoA
2.3.1.12
1.2.4.1
S-Acetyl-dihydrolipoamide-E
4.1.1.1
Pyruvate
1.1.1.27
L-Lactate
6.2.1.1
6.2.1.13
1.8.1.4
Dihydro-lipoamide-E
Lipoamide-E
4.1.1.1
1.1.5.5
Propanoate metabolism
1.2.1.3
1.1.1.1
1.1.1.2
Ethanol
1.2.1.5
1.2.1.-
1.1.2.7
EutG
Acetate
Acetaldehyde
1.1.2.8
00010 5/7/20
(c) Kanehisa Laboratories

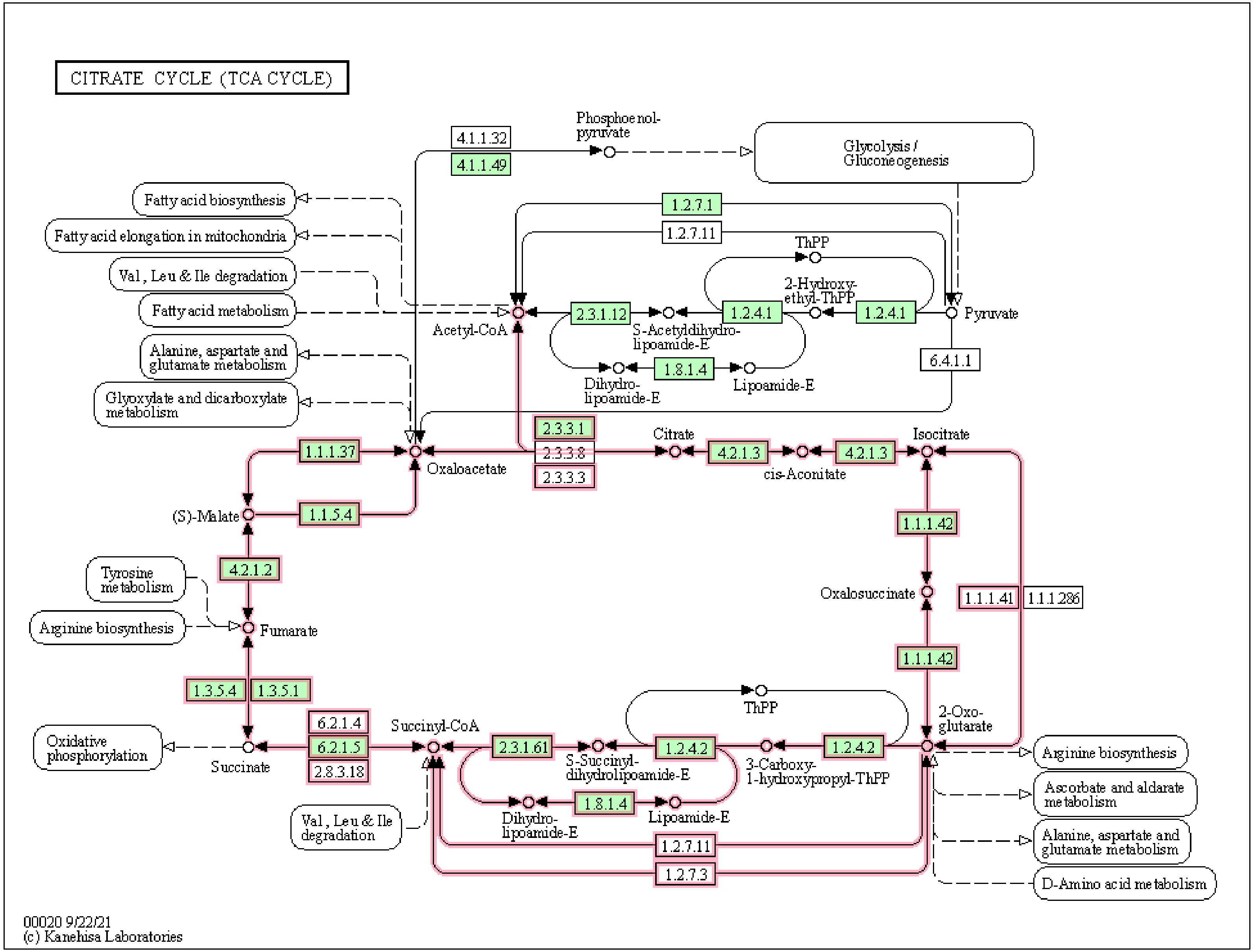
CITRATE CYCLE (TCA CYCLE)
4.1.1.32
4.1.1.49
Phosphoenol-pyruvate
Glycolysis / Gluconeogenesis
Fatty acid biosynthesis
Fatty acid elongation in mitochondria
Val, Leu & Ile degradation
Fatty acid metabolism
Alanine, aspartate and glutamate metabolism
Glyoxylate and dicarboxylate metabolism
1.2.7.1
1.2.7.11
ThPP
2-Hydroxy-ethyl-ThPP
2.3.1.12
1.2.4.1
1.2.4.1
Pyruvate
Acetyl-CoA
S-Acetyldihydro-lipoamide-E
1.8.1.4
Dihydro-lipoamide-E
Lipoamide-E
6.4.1.1
2.3.3.1
2.3.3.8
2.3.3.3
Citrate
4.2.1.3
cis-Aconitate
4.2.1.3
Isocitrate
1.1.1.37
Oxaloacetate
(S)-Malate
1.1.5.4
1.1.1.42
Oxalosuccinate
1.1.1.41
1.1.1.286
4.2.1.2
Tyrosine metabolism
Arginine biosynthesis
Fumarate
1.1.1.42
1.3.5.4
1.3.5.1
ThPP
2-Oxo-glutarate
6.2.1.4
6.2.1.5
2.8.3.18
Succinyl-CoA
2.3.1.61
1.2.4.2
1.2.4.2
Oxidative phosphorylation
Succinate
S-Succinyl-dihydrolipoamide-E
3-Carboxy-1-hydroxypropyl-ThPP
1.8.1.4
Dihydro-lipoamide-E
Lipoamide-E
Val, Leu & Ile degradation
1.2.7.11
1.2.7.3
Arginine biosynthesis
Ascorbate and aldarate metabolism
Alanine, aspartate and glutamate metabolism
D-Amino acid metabolism
00020 9/22/21
(c) Kanehisa Laboratories

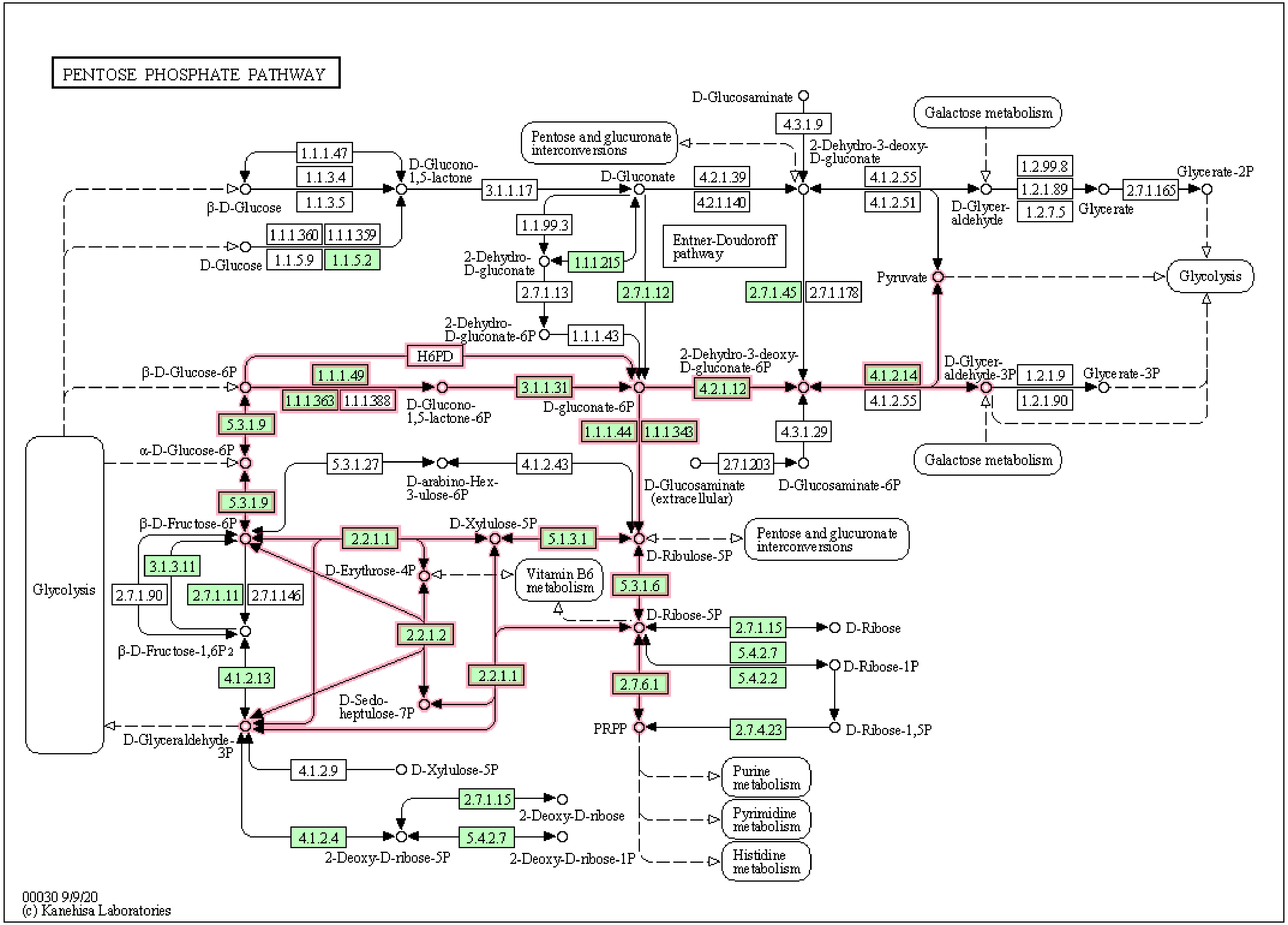
PENTOSE PHOSPHATE PATHWAY
D-Glucosaminate
4.3.1.9
Galactose metabolism
Pentose and glucuronate interconversions
2-Dehydro-3-deoxy-D-gluconate
1.1.1.47
1.1.3.4
1.1.3.5
D-Glucono-1,5-lactone
3.1.1.17
D-Gluconate
4.2.1.39
4.2.1.140
4.1.2.55
4.1.2.51
1.2.99.8
1.2.1.89
1.2.7.5
2.7.1.165
Glycerate-2P
Glycerate
D-Glyceraldehyde
β-D-Glucose
1.1.1.360
1.1.1.359
1.1.5.9
1.1.5.2
D-Glucose
1.1.99.3
2-Dehydro-D-gluconate
1.1.1.215
Entner-Doudoroff pathway
Pyruvate
Glycolysis
2.7.1.13
2.7.1.12
2.7.1.45
2.7.1.178
2-Dehydro-D-gluconate-6P
1.1.1.43
H6PD
2-Dehydro-3-deoxy-D-gluconate-6P
β-D-Glucose-6P
1.1.1.49
1.1.1.363
1.1.1.388
D-Glucono-1,5-lactone-6P
3.1.1.31
D-gluconate-6P
4.2.1.12
4.1.2.14
4.1.2.55
D-Glyceraldehyde-3P
1.2.1.9
1.2.1.90
Glycerate-3P
5.3.1.9
1.1.1.44
1.1.1.343
4.3.1.29
α-D-Glucose-6P
5.3.1.27
4.1.2.43
D-arabino-Hex-3-ulose-6P
2.7.1.203
D-Glucosaminate (extracellular)
D-Glucosamine-6P
Galactose metabolism
5.3.1.9
β-D-Fructose-6P
2.2.1.1
D-Xylulose-5P
5.1.3.1
D-Ribulose-5P
Pentose and glucuronate interconversions
3.1.3.11
2.7.1.90
2.7.1.11
2.7.1.146
D-Erythrose-4P
Vitamin B6 metabolism
5.3.1.6
Glycolysis
D-Ribose-5P
2.7.1.15
D-Ribose
5.4.2.7
5.4.2.2
D-Ribose-1P
β-D-Fructose-1,6P2
2.2.1.2
2.2.1.1
4.1.2.13
2.7.6.1
D-Sedo-heptulose-7P
PRPP
2.7.4.23
D-Ribose-1,5P
D-Glyceraldehyde-3P
4.1.2.9
D-Xylulose-5P
Purine metabolism
2.7.1.15
2-Deoxy-D-ribose
Pyrimidine metabolism
4.1.2.4
5.4.2.7
2-Deoxy-D-ribose-5P
2-Deoxy-D-ribose-1P
Histidine metabolism
00030 9/9/20
(c) Kanehisa Laboratories

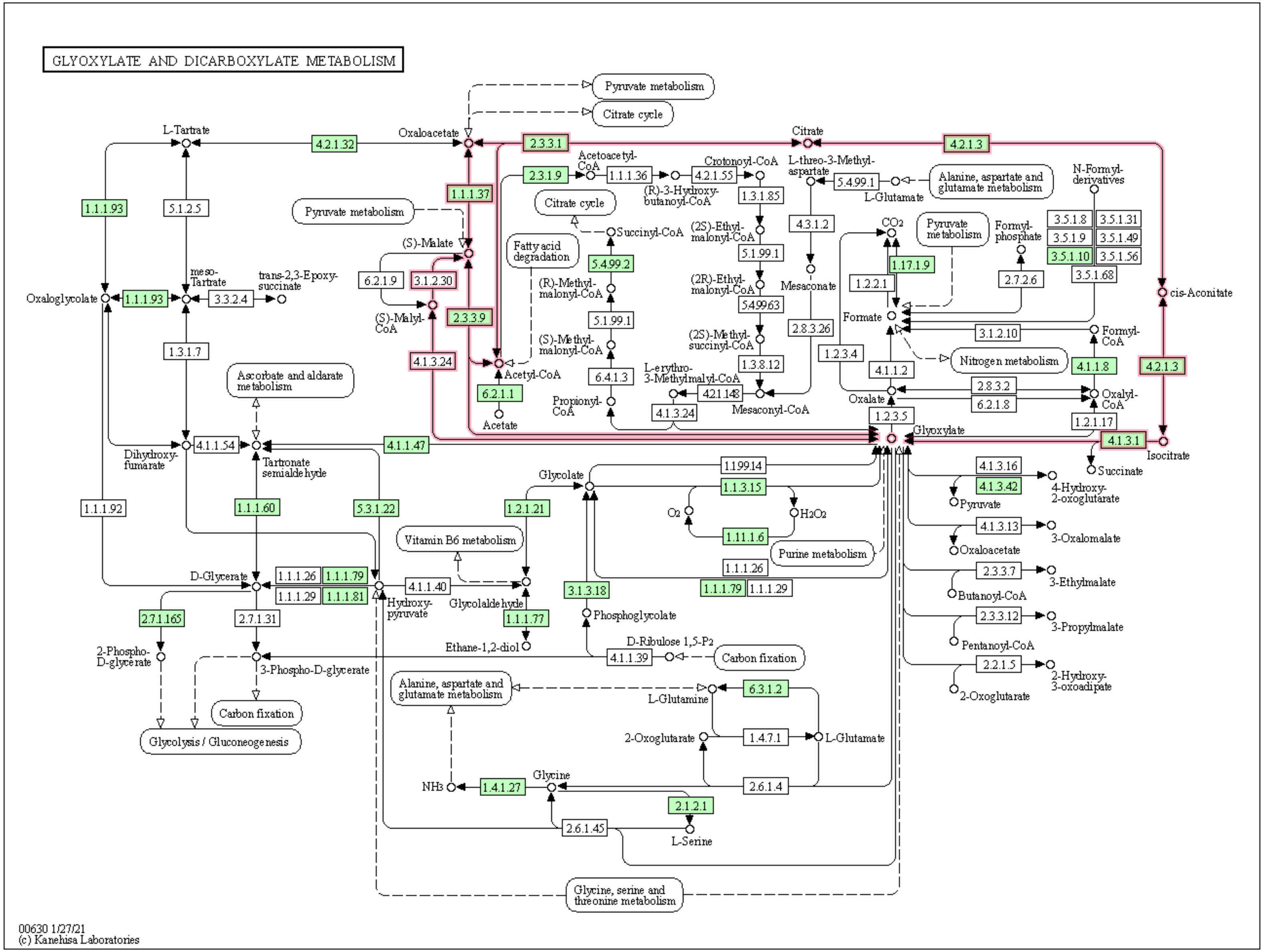
GLYOXYLATE AND DICARBOXYLATE METABOLISM
Pyruvate metabolism
Citrate cycle
L-Tartrate
4.2.1.32
Oxaloacetate
2.3.3.1
Citrate
4.2.1.3
Acetoacetyl-CoA
2.3.1.9
1.1.1.36
4.2.1.55
Crotonoyl-CoA
L-threo-3-Methyl-aspartate
5.4.99.1
L-Glutamate
Alanine, aspartate and glutamate metabolism
N-Formyl-derivatives
(R)-3-Hydroxy-butanoyl-CoA
1.3.1.85
1.1.1.93
5.1.2.5
Pyruvate metabolism
1.1.1.37
Citrate cycle
4.3.1.2
CO2
Pyruvate metabolism
Formyl-phosphate
3.5.1.8
3.5.1.31
3.5.1.9
3.5.1.49
3.5.1.10
3.5.1.56
3.5.1.68
(S)-Malate
Fatty acid degradation
Succinyl-CoA
(2S)-Ethyl-malonyl-CoA
5.1.99.1
5.4.99.2
1.17.1.9
2.7.2.6
meso-Tartrate
trans-2,3-Epoxy-succinate
6.2.1.9
3.1.2.30
(R)-Methyl-malonyl-CoA
(2R)-Ethyl-malonyl-CoA
Mesaconate
1.2.2.1
cis-Aconitate
Oxaloglycolate
1.1.1.93
3.3.2.4
5.4.99.63
(S)-Malyl-CoA
2.3.3.9
5.1.99.1
Formate
2.8.3.26
(2S)-Methyl-succinyl-CoA
3.1.2.10
Formyl-CoA
1.3.1.7
(S)-Methyl-malonyl-CoA
1.2.3.4
4.1.3.24
Acetyl-CoA
1.3.8.12
Nitrogen metabolism
4.1.1.8
4.2.1.3
Ascorbate and aldarate metabolism
6.4.1.3
L-erythro-3-Methylmalyl-CoA
4.1.1.2
2.8.3.2
6.2.1.1
4.2.1.148
Oxalate
Oxalyl-CoA
Propionyl-CoA
4.1.3.24
Mesaconyl-CoA
6.2.1.8
Acetate
1.2.3.5
1.2.1.17
Glyoxylate
Dihydroxy-fumarate
4.1.1.54
Tartronate semialdehyde
4.1.1.47
4.1.3.1
Isocitrate
1.1.99.14
4.1.3.16
Succinate
Glycolate
1.1.3.15
4.1.3.42
4-Hydroxy-2-oxoglutarate
1.1.1.92
1.1.1.60
5.3.1.22
1.2.1.21
O2
H2O2
Pyruvate
4.1.3.13
3-Oxalomalate
Vitamin B6 metabolism
1.11.1.6
Oxaloacetate
Purine metabolism
1.1.1.26
D-Glycerate
1.1.1.26
1.1.1.79
2.3.3.7
3-Ethylmalate
1.1.1.29
1.1.1.81
4.1.1.40
1.1.1.79
1.1.1.29
Butanoyl-CoA
Hydroxy-pyruvate
Glycolaldehyde
3.1.3.18
2.7.1.165
2.7.1.31
1.1.1.77
Phosphoglycolate
2.3.3.12
3-Propylmalate
Pentanoyl-CoA
2-Phospho-D-glycerate
D-Ribulose 1,5-P2
Ethane-1,2-diol
4.1.1.39
Carbon fixation
3-Phospho-D-glycerate
2.2.1.5
2-Hydroxy-3-oxoadipate
Alanine, aspartate and glutamate metabolism
6.3.1.2
2-Oxoglutarate
L-Glutamine
Carbon fixation
Glycolysis / Gluconeogenesis
2-Oxoglutarate
1.4.7.1
L-Glutamate
NH3
1.4.1.27
Glycine
2.6.1.4
2.1.2.1
2.6.1.45
L-Serine
Glycine, serine and threonine metabolism
00630 1/27/21
(c) Kanehisa Laboratories

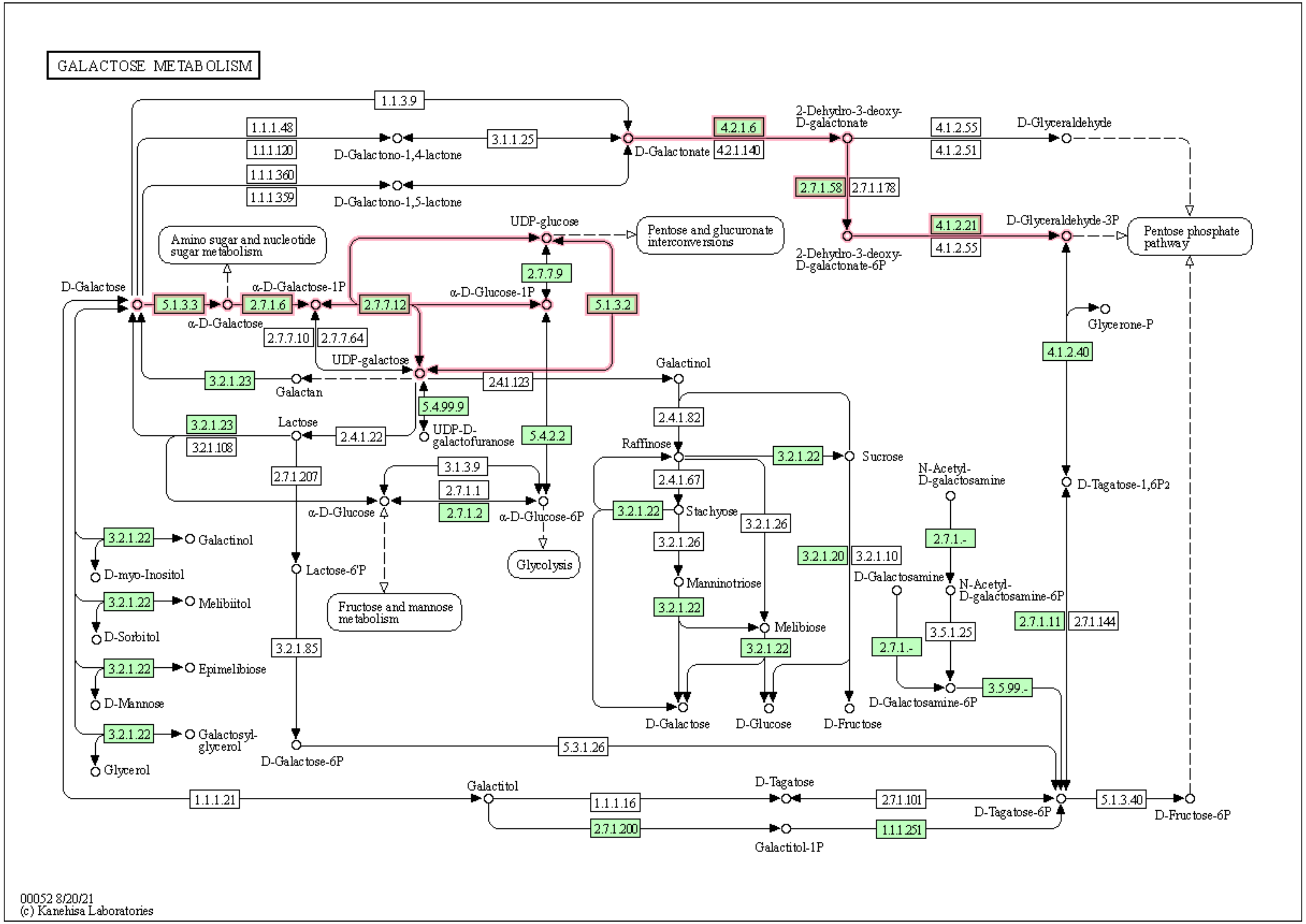
GALACTOSE METABOLISM
1.1.3.9
1.1.1.48
1.1.1.120
3.1.1.25
D-Galactono-1,4-lactone
1.1.1.360
1.1.1.359
D-Galactono-1,5-lactone
4.2.1.6
4.2.1.140
D-Galactonate
2-Dehydro-3-deoxy-D-galactonate
4.1.2.55
4.1.2.51
D-Glyceraldehyde
2.7.1.58
2.7.1.178
2-Dehydro-3-deoxy-D-galactonate-6P
4.1.2.21
4.1.2.55
D-Glyceraldehyde-3P
Pentose phosphate pathway
Amino sugar and nucleotide sugar metabolism
UDP-glucose
Pentose and glucuronate interconversions
2.7.7.9
D-Galactose
5.1.3.3
α-D-Galactose
2.7.1.6
α-D-Galactose-1P
2.7.7.12
α-D-Glucose-1P
5.1.3.2
2.7.7.10
2.7.7.64
UDP-galactose
Glycerone-P
4.1.2.40
3.2.1.23
Galactan
2.4.1.123
Galactinol
5.4.99.9
UDP-D-galactofuranose
5.4.2.2
3.2.1.23
3.2.1.108
Lactose
2.4.1.22
2.4.1.82
Raffinose
3.2.1.22
Sucrose
2.7.1.207
3.1.3.9
2.7.1.1
2.7.1.2
α-D-Glucose
α-D-Glucose-6P
2.4.1.67
3.2.1.22
Stachyose
3.2.1.26
3.2.1.26
N-Acetyl-D-galactosamine
D-Tagatose-1,6P2
Glycolysis
3.2.1.22
Galactinol
D-myo-Inositol
Lactose-6P
Manninotriose
3.2.1.20
3.2.1.10
2.7.1.-
D-Galactosamine
N-Acetyl-D-galactosamine-6P
3.2.1.22
Melibiitol
D-Sorbitol
Fructose and mannose metabolism
3.2.1.22
Melibiose
2.7.1.11
2.7.1.144
3.5.1.25
3.2.1.85
3.2.1.22
2.7.1.-
3.2.1.22
Epimelibiose
D-Mannose
3.5.99.-
D-Galactose
D-Glucose
D-Fructose
D-Galactosamine-6P
3.2.1.22
Galactosyl-glycerol
Glycerol
D-Galactose-6P
5.3.1.26
1.1.1.21
Galactitol
1.1.1.16
D-Tagatose
2.7.1.101
D-Tagatose-6P
5.1.3.40
D-Fructose-6P
2.7.1.200
Galactitol-1P
1.1.1.251
00052 8/20/21
(c) Kanehisa Laboratories

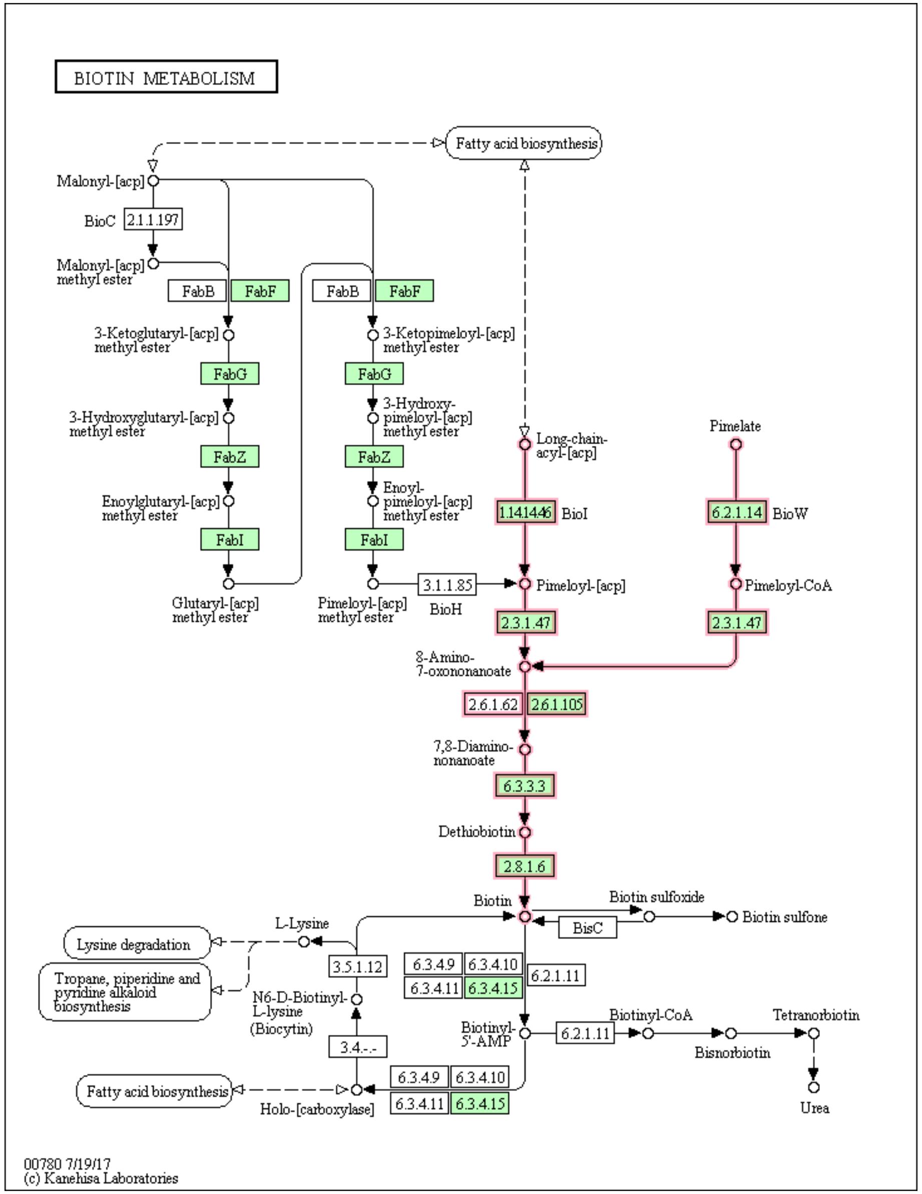
BIOTIN METABOLISM
Fatty acid biosynthesis
Malonyl-[acp]
BioC
2.1.1.197
Malonyl-[acp] methyl ester
FabB
FabF
FabB
FabF
3-Ketoglutaryl-[acp] methyl ester
3-Ketopimeloyl-[acp] methyl ester
FabG
FabG
3-Hydroxyglutaryl-[acp] methyl ester
3-Hydroxy-pimeloyl-[acp] methyl ester
FabZ
FabZ
Enoylglutaryl-[acp] methyl ester
Enoyl-pimeloyl-[acp] methyl ester
FabI
FabI
Glutaryl-[acp] methyl ester
Pimeloyl-[acp] methyl ester
3.1.1.85
BioH
Long-chain-acyl-[acp]
1.14.14.46
BioI
Pimelate
6.2.1.14
BioW
Pimeloyl-[acp]
Pimeloyl-CoA
2.3.1.47
2.3.1.47
8-Amino-7-oxononanoate
2.6.1.62
2.6.1.105
7,8-Diamino-nonanoate
6.3.3.3
Dethiobiotin
2.8.1.6
Biotin
Biotin sulfoxide
Biotin sulfone
BisC
L-Lysine
Lysine degradation
Tropane, piperidine and pyridine alkaloid biosynthesis
3.5.1.12
6.3.4.9
6.3.4.10
6.3.4.11
6.3.4.15
6.2.1.11
N6-D-Biotinyl-L-lysine (Biocytin)
3.4.-.-
Biotinyl-5'-AMP
6.2.1.11
Biotinyl-CoA
Bisnorbiotin
Tetranorbiotin
Urea
Fatty acid biosynthesis
6.3.4.9
6.3.4.10
6.3.4.11
6.3.4.15
Holo-[carboxylase]
00780 7/19/17
(c) Kanehisa Laboratories

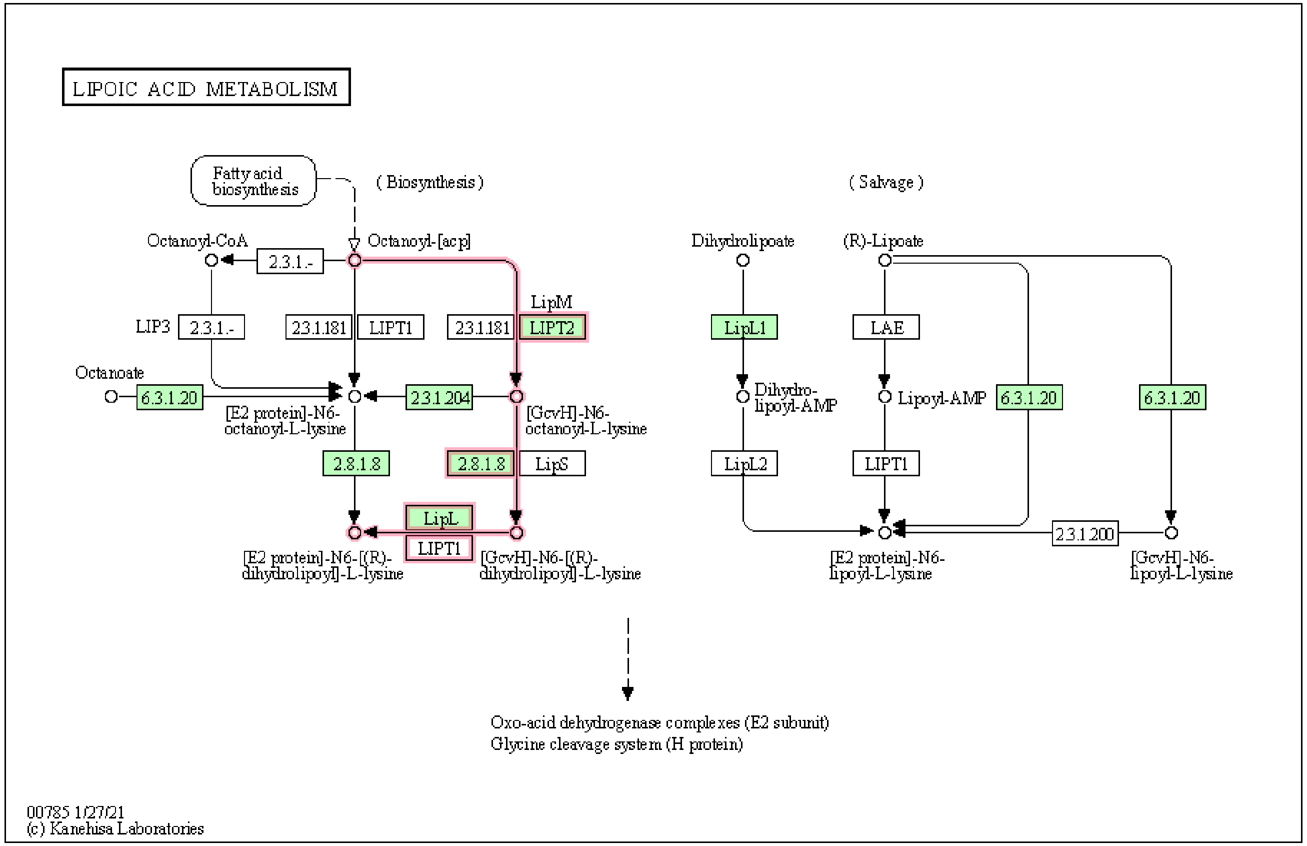
LIPOIC ACID METABOLISM
Fatty acid biosynthesis
(Biosynthesis)
(Salvage)
Octanoyl-CoA
2.3.1.-
Octanoyl-[acp]
LIP3
2.3.1.-
2.3.1.181
LIPT1
2.3.1.181
LIPT2
LipM
Octanoate
6.3.1.20
2.3.1.204
[E2 protein]-N6-octanoyl-L-lysine
[GcvH]-N6-octanoyl-L-lysine
2.8.1.8
2.8.1.8
LipS
LipL
LIPT1
[E2 protein]-N6-[(R)-dihydrolipoyl]-L-lysine
[GcvH]-N6-[(R)-dihydrolipoyl]-L-lysine
Dihydrolipoate
(R)-Lipoate
LipL1
LAE
Dihydro-lipoyl-AMP
Lipoyl-AMP
6.3.1.20
6.3.1.20
LipL2
LIPT1
2.3.1.200
[E2 protein]-N6-lipoyl-L-lysine
[GcvH]-N6-lipoyl-L-lysine
Oxo-acid dehydrogenase complexes (E2 subunit)
Glycine cleavage system (H protein)
00785 1/27/21
(c) Kanehisa Laboratories

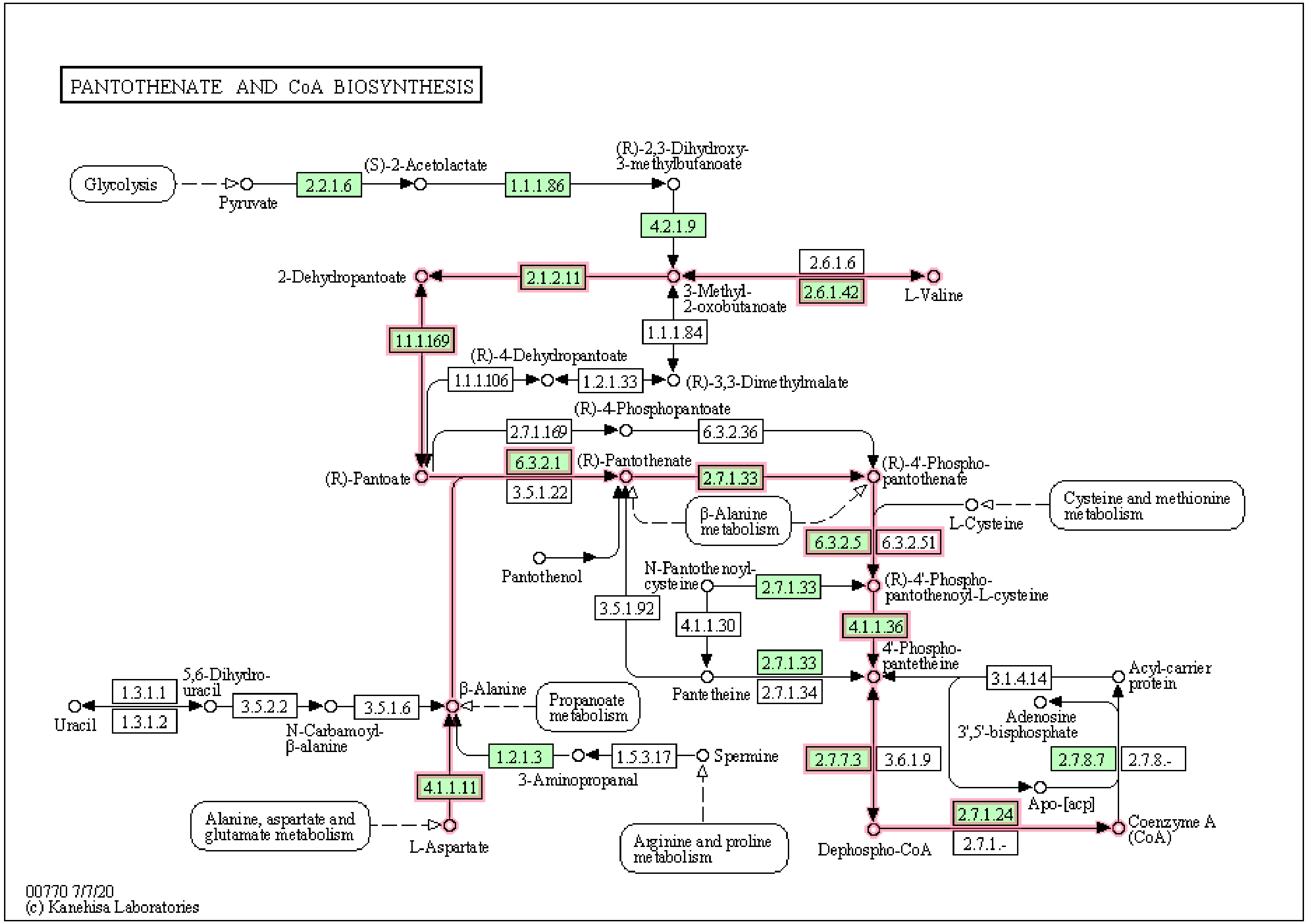
PANTOTHENATE AND CoA BIOSYNTHESIS
Glycolysis
Pyruvate
2.2.1.6
(S)-2-Acetolactate
1.1.1.86
(R)-2,3-Dihydroxy-3-methylbutanoate
4.2.1.9
2-Dehydropantoate
2.1.2.11
3-Methyl-2-oxobutanoate
2.6.1.6
2.6.1.42
L-Valine
1.1.1.169
1.1.1.84
(R)-4-Dehydropantoate
1.1.1.106
1.2.1.33
(R)-3,3-Dimethylmalate
(R)-4-Phosphopantoate
2.7.1.169
6.3.2.36
(R)-Pantoate
6.3.2.1
3.5.1.22
(R)-Pantothenate
2.7.1.33
(R)-4'-Phosphopantothenate
β-Alanine metabolism
Cysteine and methionine metabolism
L-Cysteine
6.3.2.5
6.3.2.51
Pantothenol
N-Pantothenoyl-cysteine
2.7.1.33
(R)-4'-Phosphopantothenoyl-L-cysteine
3.5.1.92
4.1.1.30
4.1.1.36
2.7.1.33
4'-Phosphopantetheine
Pantetheine
2.7.1.34
3.1.4.14
Acyl-carrier protein
Adenosine 3',5'-bisphosphate
Uracil
1.3.1.1
1.3.1.2
5,6-Dihydrouracil
3.5.2.2
N-Carbamoyl-β-alanine
3.5.1.6
β-Alanine
Propanoate metabolism
1.2.1.3
1.5.3.17
Spermine
3-Aminopropanal
4.1.1.11
2.7.7.3
3.6.1.9
2.7.8.7
2.7.8.-
Apo-[acp]
Alanine, aspartate and glutamate metabolism
L-Aspartate
Arginine and proline metabolism
Dephospho-CoA
2.7.1.24
2.7.1.-
Coenzyme A (CoA)
00770 7/7/20
(c) Kanehisa Laboratories

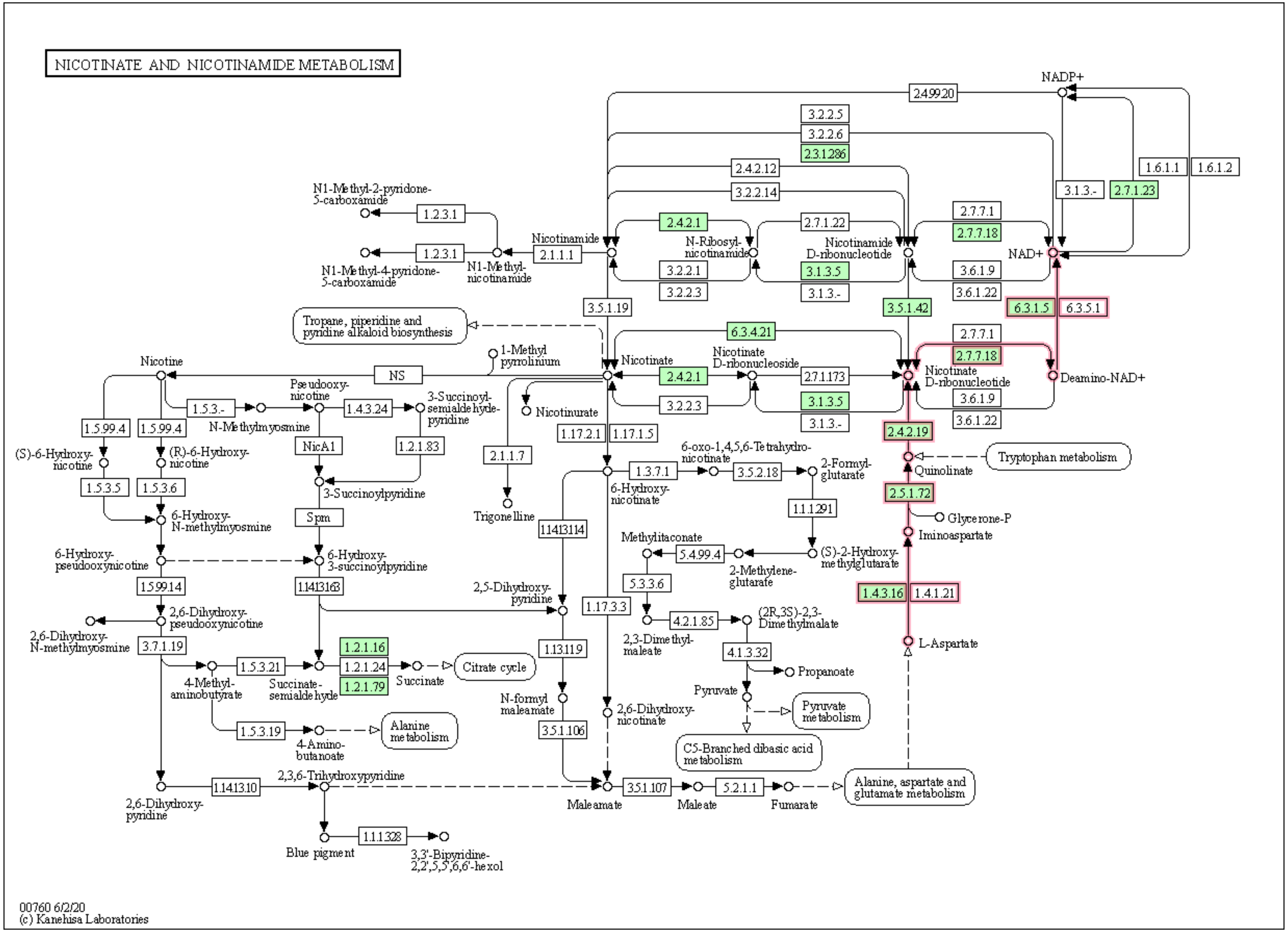
NICOTINATE AND NICOTINAMIDE METABOLISM
NADP+
2.4.99.20
3.2.2.5
3.2.2.6
2.3.1.286
1.6.1.1
1.6.1.2
2.4.2.12
3.1.3.-
2.7.1.23
3.2.2.14
N1-Methyl-2-pyridone-5-carboxamide
1.2.3.1
2.7.7.1
Nicotinamide
2.4.2.1
2.7.1.22
2.7.7.18
N-Ribosyl-nicotinamide
Nicotinamide D-ribonucleotide
NAD+
1.2.3.1
2.1.1.1
N1-Methyl-4-pyridone-5-carboxamide
N1-Methyl-nicotinamide
3.2.2.1
3.1.3.5
3.6.1.9
3.2.2.3
3.1.3.-
3.6.1.22
3.5.1.19
3.5.1.42
6.3.1.5
6.3.5.1
Tropane, piperidine and pyridine alkaloid biosynthesis
6.3.4.21
2.7.7.1
1-Methyl pyrrolinium
2.7.7.18
Nicotine
Nicotinate
Nicotinate D-ribonucleoside
Nicotinate D-ribonucleotide
Deamino-NAD+
NS
2.4.2.1
2.7.1.173
Pseudooxy-nicotine
3-Succinoyl-semialdehyde-pyridine
1.5.3.-
1.4.3.24
3.2.2.3
3.1.3.5
3.6.1.9
Nicotinurate
3.1.3.-
3.6.1.22
1.5.99.4
1.5.99.4
N-Methylmyosmine
1.17.2.1
1.17.1.5
2.4.2.19
NicA1
1.2.1.83
6-oxo-1,4,5,6-Tetrahydro-nicotinate
Tryptophan metabolism
(S)-6-Hydroxy-nicotine
(R)-6-Hydroxy-nicotine
2.1.1.7
1.3.7.1
3.5.2.18
2-Formyl-glutarate
Quinolinate
1.5.3.5
1.5.3.6
3-Succinoylpyridine
6-Hydroxy-nicotinate
2.5.1.72
1.1.1.291
Glycerone-P
6-Hydroxy-N-methylmyosmine
Spm
Trigonelline
1.14.13.114
Iminoaspartate
Methylitaconate
6-Hydroxy-pseudooxynicotine
6-Hydroxy-3-succinoylpyridine
5.4.99.4
(S)-2-Hydroxy-methylglutarate
2-Methylene-glutarate
5.3.3.6
1.4.3.16
1.4.1.21
1.5.99.14
1.14.13.163
2,5-Dihydroxy-pyridine
1.17.3.3
2,6-Dihydroxy-pseudooxynicotine
4.2.1.85
(2R,3S)-2,3-Dimethylmalate
L-Aspartate
2,6-Dihydroxy-N-methylmyosmine
3.7.1.19
1.2.1.16
1.13.11.9
2,3-Dimethyl-maleate
4.1.3.32
1.5.3.21
1.2.1.24
Citrate cycle
Propanoate
4-Methyl-aminobutyrate
Succinate-semialdehyde
1.2.1.79
Succinate
Pyruvate
N-formyl maleamate
2,6-Dihydroxy-nicotinate
Pyruvate metabolism
1.5.3.19
Alanine metabolism
4-Amino-butanoate
3.5.1.106
C5-Branched dibasic acid metabolism
2,3,6-Trihydroxypyridine
1.14.13.10
3.5.1.107
5.2.1.1
Alanine, aspartate and glutamate metabolism
2,6-Dihydroxy-pyridine
Maleamate
Maleate
Fumarate
Blue pigment
1.1.1.328
3,3'-Bipyridine-2,2',5,5',6,6'-hexol
00760 6/2/20
(c) Kanehisa Laboratories

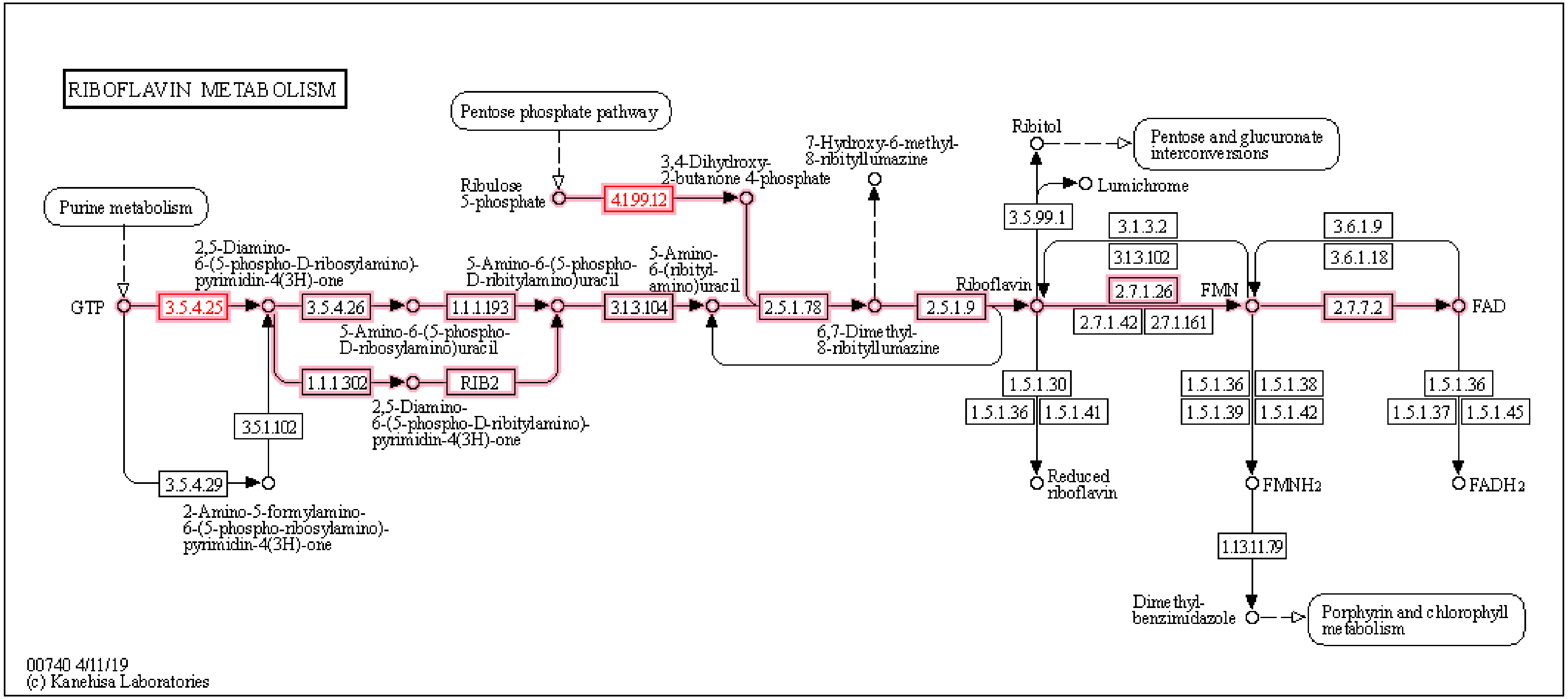
RIBOFLAVIN METABOLISM
Pentose phosphate pathway
Purine metabolism
Ribulose 5-phosphate
4.1.99.12
3,4-Dihydroxy-2-butanone 4-phosphate
7-Hydroxy-6-methyl-8-ribityllumazine
Ribitol
Pentose and glucuronate interconversions
Lumichrome
3.5.99.1
3.1.3.2
3.1.3.102
3.6.1.9
3.6.1.18
GTP
3.5.4.25
2,5-Diamino-6-(5-phospho-D-ribosylamino)-pyrimidin-4(3H)-one
3.5.4.26
5-Amino-6-(5-phospho-D-ribosylamino)uracil
1.1.1.193
5-Amino-6-(5-phospho-D-ribitylamino)uracil
3.1.3.104
5-Amino-6-(ribitylamino)uracil
2.5.1.78
6,7-Dimethyl-8-ribityllumazine
2.5.1.9
Riboflavin
2.7.1.26
2.7.1.42
2.7.1.161
FMN
2.7.7.2
FAD
1.1.1.302
RIB2
2,5-Diamino-6-(5-phospho-D-ribitylamino)-pyrimidin-4(3H)-one
3.5.1.102
3.5.4.29
2-Amino-5-formylamino-6-(5-phospho-ribosylamino)-pyrimidin-4(3H)-one
1.5.1.30
1.5.1.36
1.5.1.41
Reduced riboflavin
1.5.1.36
1.5.1.38
1.5.1.39
1.5.1.42
FMNH2
1.5.1.36
1.5.1.37
1.5.1.45
FADH2
1.13.11.79
Dimethyl-benzimidazole
Porphyrin and chlorophyll metabolism
00740 4/11/19
(c) Kanehisa Laboratories

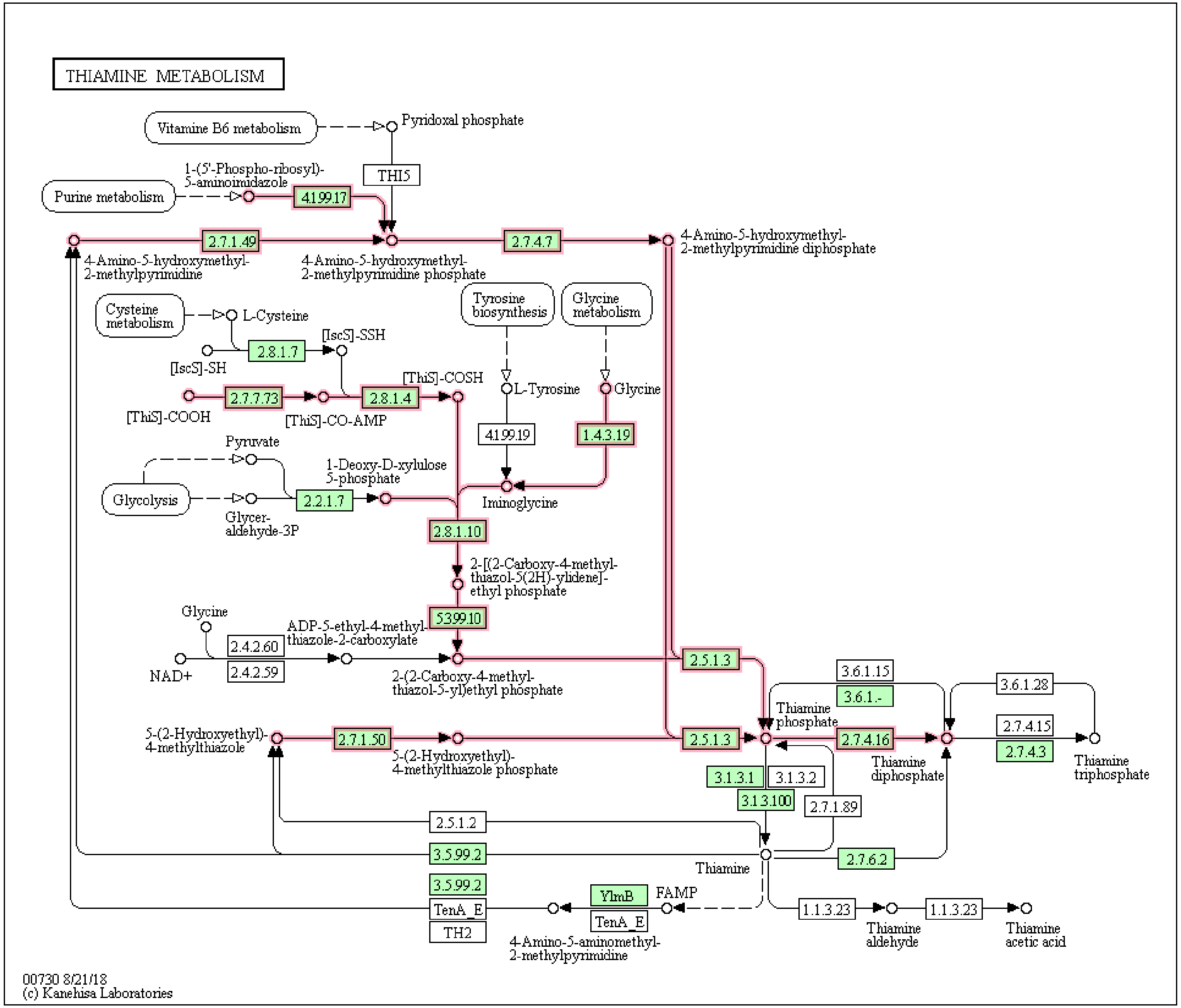
THIAMINE METABOLISM
Vitamine B6 metabolism
Pyridoxal phosphate
THI5
Purine metabolism
1-(5'-Phospho-ribosyl)-5-aminoimidazole
4.1.99.17
2.7.1.49
4-Amino-5-hydroxymethyl-2-methylpyrimidine
4-Amino-5-hydroxymethyl-2-methylpyrimidine phosphate
2.7.4.7
4-Amino-5-hydroxymethyl-2-methylpyrimidine diphosphate
Cysteine metabolism
L-Cysteine
[IscS]-SSH
2.8.1.7
[IscS]-SH
Tyrosine biosynthesis
Glycine metabolism
[ThiS]-COSH
2.7.7.73
2.8.1.4
[ThiS]-COOH
[ThiS]-CO-AMP
L-Tyrosine
Glycine
4.1.99.19
1.4.3.19
Pyruvate
1-Deoxy-D-xylulose 5-phosphate
Glycolysis
2.2.1.7
Glyceraldehyde-3P
Iminoglycine
2.8.1.10
2-[(2-Carboxy-4-methyl-thiazol-5(2H)-ylidene]-ethyl phosphate
5.3.99.10
Glycine
ADP-5-ethyl-4-methyl-thiazole-2-carboxylate
2.4.2.60
NAD+
2.4.2.59
2-(2-Carboxy-4-methyl-thiazol-5-yl)ethyl phosphate
2.5.1.3
3.6.1.15
3.6.1.-
3.6.1.28
Thiamine phosphate
5-(2-Hydroxyethyl)-4-methylthiazole
2.7.1.50
5-(2-Hydroxyethyl)-4-methylthiazole phosphate
2.5.1.3
2.7.4.16
2.7.4.15
2.7.4.3
Thiamine diphosphate
Thiamine triphosphate
3.1.3.1
3.1.3.2
3.1.3.100
2.7.1.89
2.5.1.2
3.5.99.2
Thiamine
2.7.6.2
3.5.99.2
YlmB
FAMP
TenA_E
TH2
TenA_E
4-Amino-5-aminomethyl-2-methylpyrimidine
1.1.3.23
Thiamine aldehyde
1.1.3.23
Thiamine acetic acid
00730 8/21/18
(c) Kanehisa Laboratories

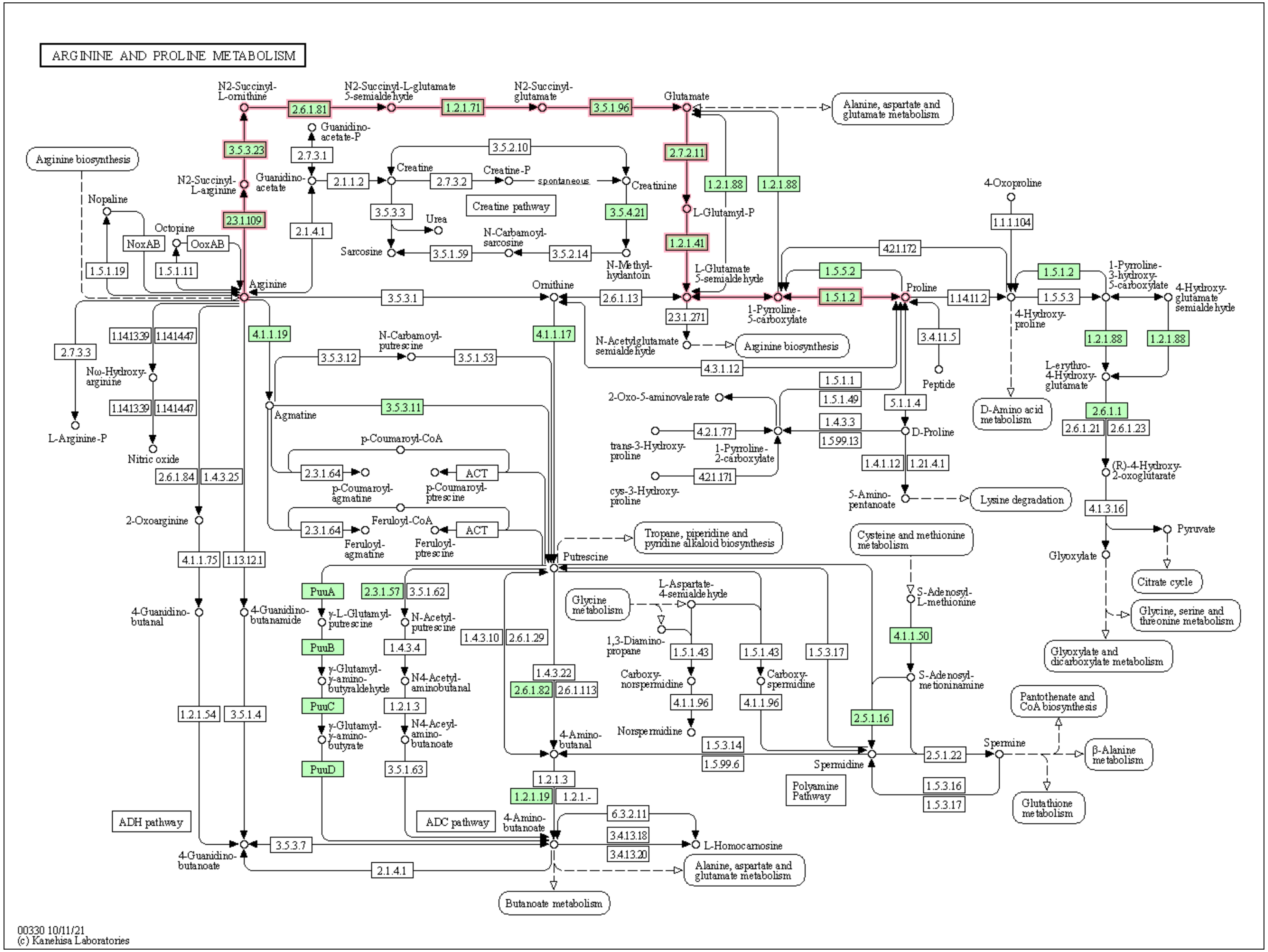
ARGININE AND PROLINE METABOLISM
N2-Succinyl-L-ornithine
2.6.1.81
N2-Succinyl-L-glutamate 5-semialdehyde
1.2.1.71
N2-Succinyl-glutamate
3.5.1.96
Glutamate
Alanine, aspartate and glutamate metabolism
Guanidino-acetate-P
3.5.3.23
2.7.3.1
3.5.2.10
Arginine biosynthesis
Creatine
Creatine-P
N2-Succinyl-L-arginine
Guanidino-acetate
2.1.1.2
2.7.3.2
spontaneous
Creatinine
2.7.2.11
1.2.1.88
1.2.1.88
4-Oxoproline
Nopaline
3.5.3.3
Creatine pathway
3.5.4.21
L-Glutamyl-P
2.3.1.109
Urea
1.1.1.104
Octopine
2.1.4.1
N-Carbamoyl-sarcosine
NoxAB
OoxAB
Sarcosine
3.5.1.59
3.5.2.14
1.2.1.41
4.2.1.172
1.5.1.19
1.5.1.11
N-Methyl-hydantoin
L-Glutamate 5-semialdehyde
1.5.5.2
1.5.1.2
1-Pyrroline-3-hydroxy-5-carboxylate
Arginine
Ornithine
Proline
4-Hydroxy-glutamate semialdehyde
3.5.3.1
2.6.1.13
1.5.1.2
1.14.11.2
1.5.5.3
1-Pyrroline-5-carboxylate
4-Hydroxy-proline
2.3.1.271
4.1.1.19
4.1.1.17
1.14.13.39
1.14.14.47
N-Carbamoyl-putrescine
3.4.11.5
1.2.1.88
1.2.1.88
2.7.3.3
N-Acetylglutamate semialdehyde
Arginine biosynthesis
3.5.3.12
3.5.1.53
Nω-Hydroxy-arginine
4.3.1.12
Peptide
L-erythro-4-Hydroxy-glutamate
1.5.1.1
1.5.1.49
2-Oxo-5-aminovalerate
5.1.1.4
D-Amino acid metabolism
Agmatine
3.5.3.11
1.14.13.39
1.14.14.47
2.6.1.1
1.4.3.3
L-Arginine-P
4.2.1.77
D-Proline
2.6.1.21
2.6.1.23
1.5.99.13
p-Coumaroyl-CoA
trans-3-Hydroxy-proline
1-Pyrroline-2-carboxylate
Nitric oxide
1.4.1.12
1.21.4.1
(R)-4-Hydroxy-2-oxoglutarate
2.3.1.64
ACT
2.6.1.84
1.4.3.25
4.2.1.171
p-Coumaroyl-agmatine
p-Coumaroyl-ptrescine
cys-3-Hydroxy-proline
5-Amino-pentanoate
Lysine degradation
4.1.3.16
2-Oxoarginine
Feruloyl-CoA
2.3.1.64
ACT
Tropane, piperidine and pyridine alkaloid biosynthesis
Cysteine and methionine metabolism
Pyruvate
Feruloyl-agmatine
Feruloyl-ptrescine
4.1.1.75
1.13.12.1
Putrescine
Glyoxylate
Citrate cycle
PuuA
2.3.1.57
3.5.1.62
L-Aspartate-4-semialdehyde
S-Adenosyl-L-methionine
4-Guanidino-butanal
4-Guanidino-butanamide
γ-L-Glutamyl-putrescine
N-Acetyl-putrescine
Glycine metabolism
Glycine, serine and threonine metabolism
1.4.3.10
2.6.1.29
1,3-Diamino-propane
4.1.1.50
PuuB
1.4.3.4
1.5.1.43
1.5.1.43
1.5.3.17
Glyoxylate and dicarboxylate metabolism
1.4.3.22
γ-Glutamyl-γ-amino-butyraldehyde
N4-Acetyl-aminobutanal
Carboxy-norspermidine
Carboxy-spermidine
S-Adenosyl-methioninamine
2.6.1.82
2.6.1.113
Pantothenate and CoA biosynthesis
PuuC
1.2.1.3
4.1.1.96
4.1.1.96
1.2.1.54
3.5.1.4
2.5.1.16
γ-Glutamyl-γ-amino-butyrate
N4-Aceyl-amino-butanoate
4-Amino-butanal
Norspermidine
1.5.3.14
Spermine
2.5.1.22
β-Alanine metabolism
1.5.99.6
Spermidine
PuuD
3.5.1.63
1.2.1.3
Polyamine Pathway
1.5.3.16
1.2.1.19
1.2.1.-
1.5.3.17
Glutathione metabolism
ADH pathway
ADC pathway
4-Amino-butanoate
6.3.2.11
3.4.13.18
L-Homocarnosine
3.5.3.7
3.4.13.20
4-Guanidino-butanoate
2.1.4.1
Alanine, aspartate and glutamate metabolism
Butanoate metabolism
00330 10/11/21
(c) Kanehisa Laboratories

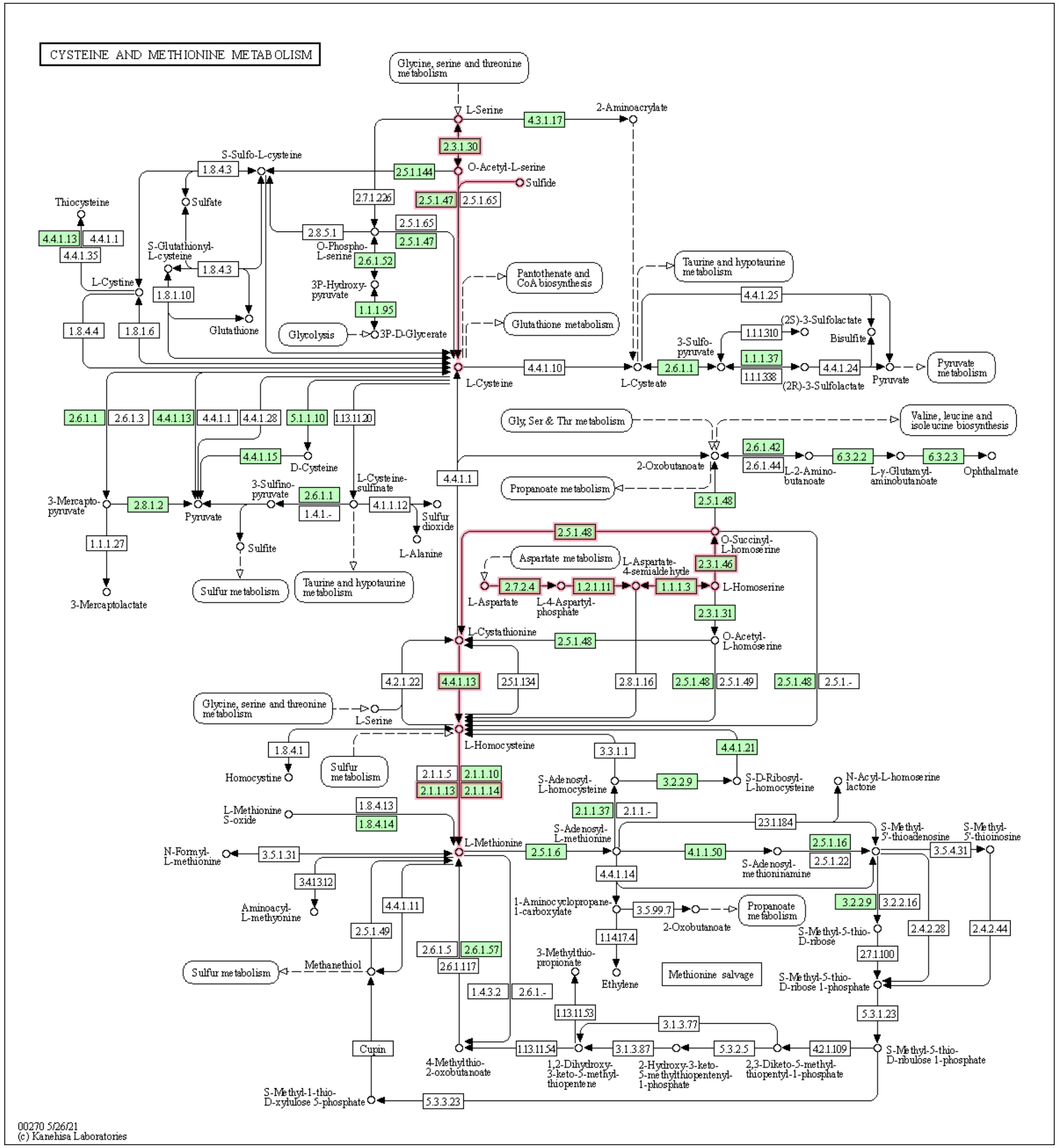
CYSTEINE AND METHIONINE METABOLISM
Glycine, serine and threonine metabolism
L-Serine
4.3.1.17
2-Aminoacrylate
2.3.1.30
O-Acetyl-L-serine
Sulfide
2.5.1.144
S-Sulfo-L-cysteine
1.8.4.3
Sulfate
Thiocysteine
4.4.1.13
4.4.1.1
4.4.1.35
2.7.1.226
2.5.1.47
2.5.1.65
2.8.5.1
2.5.1.65
2.5.1.47
O-Phospho-L-serine
S-Glutathionyl-L-cysteine
1.8.4.3
2.6.1.52
L-Cystine
3P-Hydroxy-pyruvate
1.8.1.10
1.1.1.95
Pantothenate and CoA biosynthesis
Taurine and hypotaurine metabolism
4.4.1.25
Glutathione
Glycolysis
3P-D-Glycerate
Glutathione metabolism
1.8.4.4
1.8.1.6
(2S)-3-Sulfolactate
1.1.1.310
Bisulfite
3-Sulfo-pyruvate
L-Cysteine
4.4.1.10
L-Cysteate
2.6.1.1
1.1.1.37
1.1.1.338
4.4.1.24
Pyruvate
Pyruvate metabolism
(2R)-3-Sulfolactate
2.6.1.1
2.6.1.3
4.4.1.13
4.4.1.1
4.4.1.28
5.1.1.10
1.13.11.20
Gly, Ser & Thr metabolism
Valine, leucine and isoleucine biosynthesis
2.6.1.42
2.6.1.44
4.4.1.15
D-Cysteine
2-Oxobutanoate
L-2-Amino-butanoate
6.3.2.2
L-γ-Glutamyl-aminobutanoate
6.3.2.3
Ophthalmate
4.4.1.1
3-Sulfino-pyruvate
L-Cysteine-sulfinate
Propanoate metabolism
3-Mercapto-pyruvate
2.8.1.2
Pyruvate
2.6.1.1
1.4.1.-
4.1.1.12
Sulfur dioxide
2.5.1.48
Sulfite
L-Alanine
1.1.1.27
2.5.1.48
O-Succinyl-L-homoserine
Aspartate metabolism
L-Aspartate-4-semialdehyde
2.3.1.46
Sulfur metabolism
Taurine and hypotaurine metabolism
2.7.2.4
1.2.1.11
1.1.1.3
L-Homoserine
3-Mercaptolactate
L-Aspartate
L-4-Aspartyl-phosphate
2.3.1.31
L-Cystathionine
2.5.1.48
O-Acetyl-L-homoserine
4.2.1.22
4.4.1.13
2.5.1.134
2.8.1.16
2.5.1.48
2.5.1.49
2.5.1.48
2.5.1.-
Glycine, serine and threonine metabolism
L-Serine
L-Homocysteine
1.8.4.1
3.3.1.1
4.4.1.21
Homocystine
Sulfur metabolism
S-Adenosyl-L-homocysteine
3.2.2.9
S-D-Ribosyl-L-homocysteine
N-Acyl-L-homoserine lactone
2.1.1.5
2.1.1.10
2.1.1.13
2.1.1.14
1.8.4.13
2.1.1.37
2.1.1.-
L-Methionine S-oxide
1.8.4.14
2.3.1.184
S-Adenosyl-L-methionine
S-Methyl-5'-thioadenosine
S-Methyl-5'-thioinosine
N-Formyl-L-methionine
3.5.1.31
L-Methionine
2.5.1.6
4.1.1.50
S-Adenosyl-methioninamine
2.5.1.16
2.5.1.22
3.5.4.31
3.4.13.12
4.4.1.14
Aminoacyl-L-methionine
4.4.1.11
1-Aminocyclopropane-1-carboxylate
3.5.99.7
2-Oxobutanoate
Propanoate metabolism
3.2.2.9
3.2.2.16
2.5.1.49
S-Methyl-5-thio-D-ribose
2.4.2.28
2.4.2.44
1.14.17.4
2.6.1.5
2.6.1.57
3-Methylthio-propionate
2.7.1.100
2.6.1.117
Ethylene
Methionine salvage
Sulfur metabolism
Methanethiol
S-Methyl-5-thio-D-ribose 1-phosphate
1.4.3.2
2.6.1.-
1.13.11.53
5.3.1.23
3.1.3.77
Cupin
1.13.11.54
3.1.3.87
5.3.2.5
4.2.1.109
S-Methyl-5-thio-D-ribulose 1-phosphate
4-Methylthio-2-oxobutanoate
1,2-Dihydroxy-3-keto-5-methyl-thiopentene
2-Hydroxy-3-keto-5-methylthiopentenyl-1-phosphate
2,3-Diketo-5-methyl-thiopentyl-1-phosphate
S-Methyl-1-thio-D-xylulose 5-phosphate
5.3.3.23
00270 5/26/21
(c) Kanehisa Laboratories

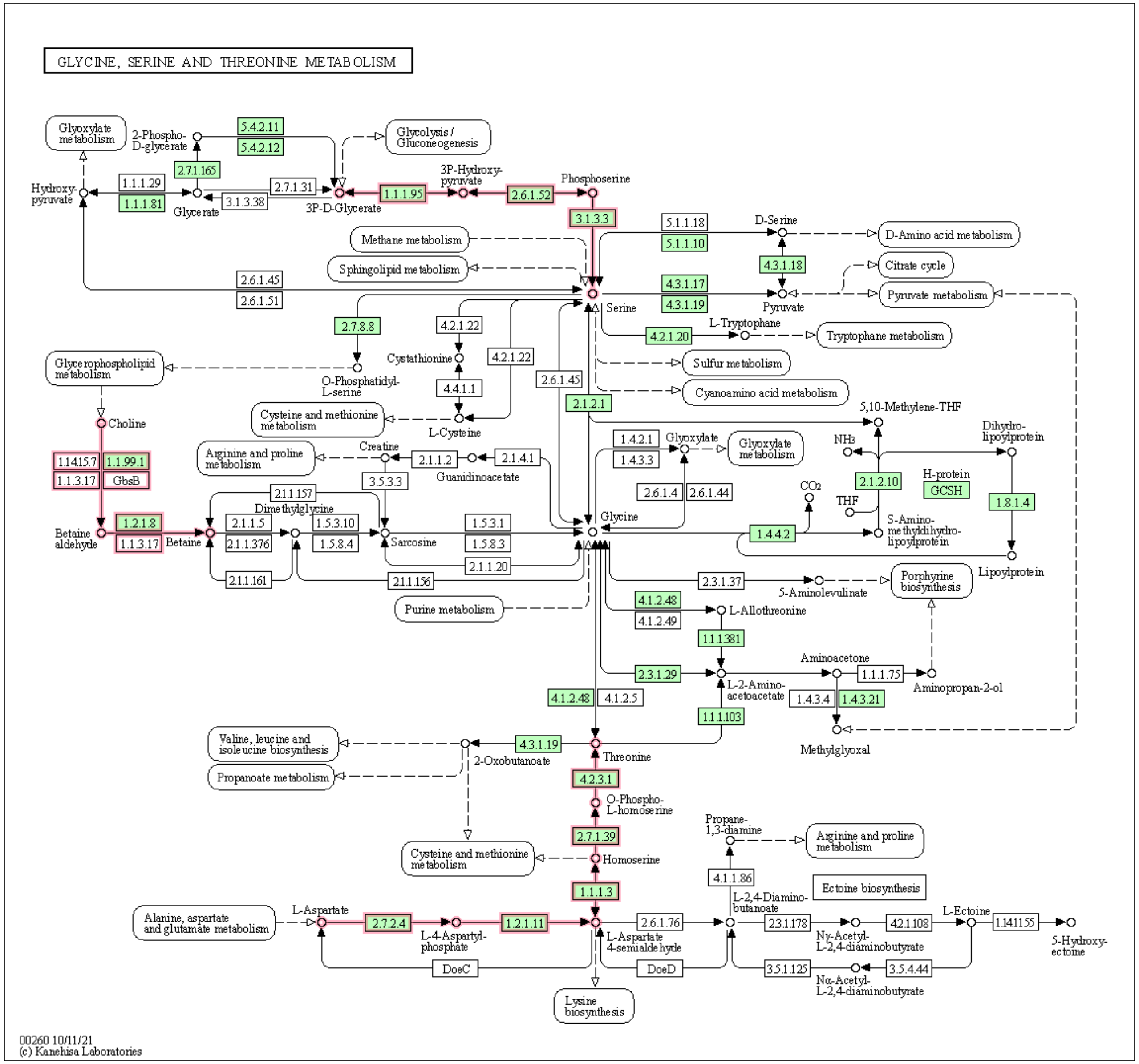
GLYCINE, SERINE AND THREONINE METABOLISM
Glyoxylate metabolism
2-Phospho-D-glycerate
5.4.2.11
5.4.2.12
Glycolysis / Gluconeogenesis
2.7.1.165
Hydroxy-pyruvate
1.1.1.29
1.1.1.81
Glycerate
3.1.3.38
2.7.1.31
3P-D-Glycerate
1.1.1.95
3P-Hydroxy-pyruvate
2.6.1.52
Phosphoserine
3.1.3.3
5.1.1.18
5.1.1.10
D-Serine
D-Amino acid metabolism
4.3.1.18
Citrate cycle
Methane metabolism
Sphingolipid metabolism
2.6.1.45
2.6.1.51
4.3.1.17
4.3.1.19
Pyruvate
Pyruvate metabolism
Serine
2.7.8.8
4.2.1.22
4.2.1.22
Cystathionine
4.2.1.20
L-Tryptophan
Tryptophan metabolism
Glycerophospholipid metabolism
O-Phosphatidyl-L-serine
4.4.1.1
2.6.1.45
Sulfur metabolism
Cyanoamino acid metabolism
Cysteine and methionine metabolism
L-Cysteine
2.1.2.1
5,10-Methylene-THF
Choline
1.1.4.15.7
1.1.99.1
1.1.3.17
GbsB
Arginine and proline metabolism
Creatine
2.1.1.2
2.1.4.1
Guanidinoacetate
3.5.3.3
1.4.2.1
1.4.3.3
Glyoxylate
Glyoxylate metabolism
NH3
Dihydro-lipoylprotein
2.1.2.10
H-protein
GCSH
2.6.1.4
2.6.1.44
CO2
THF
1.8.1.4
2.1.1.157
Dimethylglycine
Betaine aldehyde
1.2.1.8
1.1.3.17
Betaine
2.1.1.5
2.1.1.376
1.5.3.10
1.5.8.4
Sarcosine
1.5.3.1
1.5.8.3
Glycine
1.4.4.2
S-Amino-methyldihydro-lipoylprotein
Lipoylprotein
2.1.1.20
2.1.1.161
2.1.1.156
2.3.1.37
5-Aminolevulinate
Porphyrine biosynthesis
Purine metabolism
4.1.2.48
4.1.2.49
L-Allothreonine
1.1.1.381
Aminoacetone
2.3.1.29
L-2-Amino-acetoacetate
1.1.1.75
Aminopropan-2-ol
4.1.2.48
4.1.2.5
1.4.3.4
1.4.3.21
1.1.1.103
Methylglyoxal
Valine, leucine and isoleucine biosynthesis
4.3.1.19
2-Oxobutanoate
Threonine
Propanoate metabolism
4.2.3.1
O-Phospho-L-homoserine
Propane-1,3-diamine
Arginine and proline metabolism
2.7.1.39
Cysteine and methionine metabolism
Homoserine
4.1.1.86
Ectoine biosynthesis
1.1.1.3
L-2,4-Diamino-butanoate
Alanine, aspartate and glutamate metabolism
L-Aspartate
2.7.2.4
L-4-Aspartyl-phosphate
1.2.1.11
L-Aspartate 4-semialdehyde
2.6.1.76
2.3.1.178
Nγ-Acetyl-L-2,4-diaminobutyrate
4.2.1.108
L-Ectoine
1.14.11.55
5-Hydroxy-ectoine
DoeC
DoeD
3.5.1.125
3.5.4.44
Nα-Acetyl-L-2,4-diaminobutyrate
Lysine biosynthesis
00260 10/11/21
(c) Kanehisa Laboratories

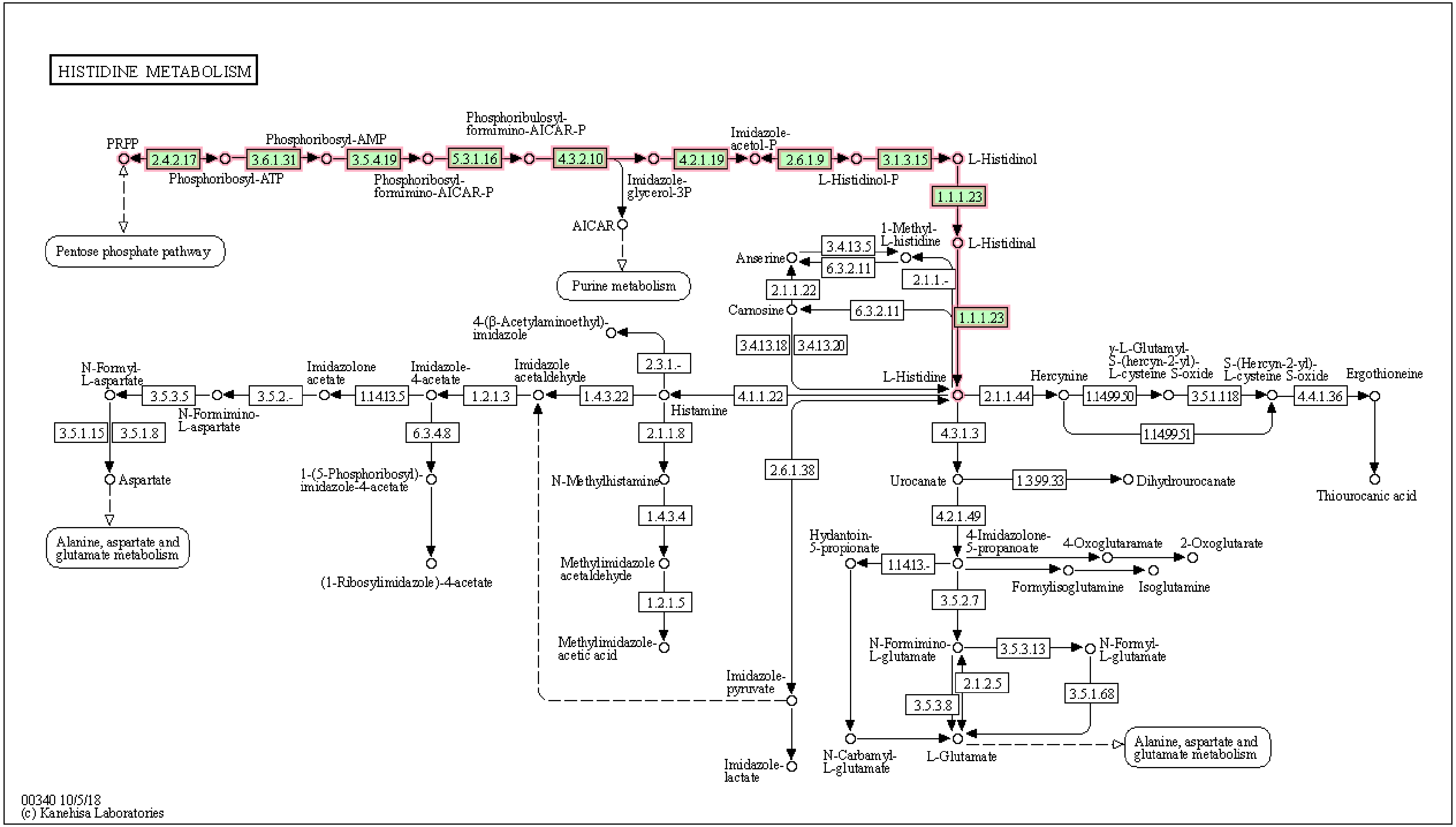
HISTIDINE METABOLISM
PRPP
2.4.2.17
Phosphoribosyl-ATP
3.6.1.31
Phosphoribosyl-AMP
3.5.4.19
Phosphoribosyl-formimino-AICAR-P
5.3.1.16
Phosphoribulosyl-formimino-AICAR-P
4.3.2.10
Imidazole-glycerol-3P
AICAR
Purine metabolism
4.2.1.19
Imidazole-acetol-P
2.6.1.9
L-Histidinol-P
3.1.3.15
L-Histidinol
1.1.1.23
L-Histidinal
1.1.1.23
Pentose phosphate pathway
1-Methyl-L-histidine
3.4.13.5
6.3.2.11
Anserine
2.1.1.-
2.1.1.22
Carnosine
6.3.2.11
3.4.13.18
3.4.13.20
L-Histidine
4-(β-Acetylaminoethyl)-imidazole
2.3.1.-
4.1.1.22
Histamine
1.4.3.22
Imidazole acetaldehyde
1.2.1.3
Imidazole-4-acetate
1.14.13.5
Imidazolone acetate
3.5.2.-
N-Formimino-L-aspartate
3.5.3.5
N-Formyl-L-aspartate
3.5.1.15
3.5.1.8
Aspartate
Alanine, aspartate and glutamate metabolism
6.3.4.8
1-(5-Phosphoribosyl)-imidazole-4-acetate
(1-Ribosylimidazole)-4-acetate
2.1.1.8
N-Methylhistamine
1.4.3.4
Methylimidazole acetaldehyde
1.2.1.5
Methylimidazole-acetic acid
2.6.1.38
Imidazole-pyruvate
Imidazole-lactate
2.1.1.44
Hercynine
1.14.99.50
γ-L-Glutamyl-S-(hercyn-2-yl)-L-cysteine S-oxide
3.5.1.118
S-(Hercyn-2-yl)-L-cysteine S-oxide
1.14.99.51
4.4.1.36
Ergothioneine
Thiourocanic acid
4.3.1.3
Urocanate
1.3.99.33
Dihydrourocanate
4.2.1.49
4-Imidazolone-5-propanoate
4-Oxoglutaramate
2-Oxoglutarate
Formylisoglutamine
Isoglutamine
1.14.13.-
Hydantoin-5-propionate
3.5.2.7
N-Formimino-L-glutamate
3.5.3.13
N-Formyl-L-glutamate
2.1.2.5
3.5.3.8
3.5.1.68
N-Carbamyl-L-glutamate
L-Glutamate
Alanine, aspartate and glutamate metabolism
00340 10/5/18
(c) Kanehisa Laboratories

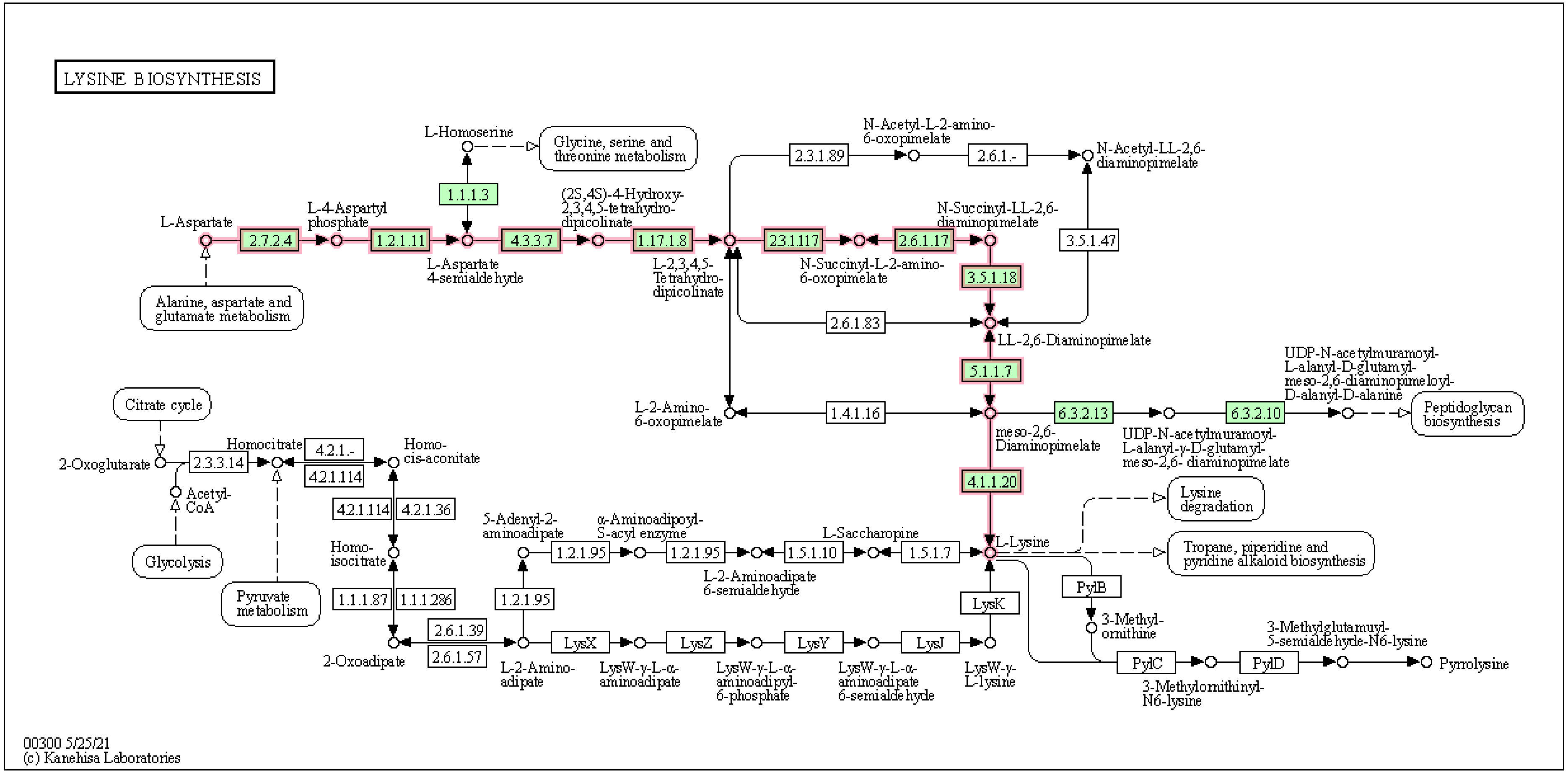
LYSINE BIOSYNTHESIS
L-Homoserine
Glycine, serine and threonine metabolism
1.1.1.3
L-Aspartate
2.7.2.4
L-4-Aspartyl phosphate
1.2.1.11
L-Aspartate 4-semialdehyde
4.3.3.7
(2S,4S)-4-Hydroxy-2,3,4,5-tetrahydro-dipicolinate
1.17.1.8
L-2,3,4,5-Tetrahydro-dipicolinate
2.3.1.117
N-Succinyl-L-2-amino-6-oxopimelate
2.6.1.17
N-Succinyl-LL-2,6-diaminopimelate
3.5.1.18
2.3.1.89
N-Acetyl-L-2-amino-6-oxopimelate
2.6.1.-
N-Acetyl-LL-2,6-diaminopimelate
3.5.1.47
2.6.1.83
LL-2,6-Diaminopimelate
5.1.1.7
Alanine, aspartate and glutamate metabolism
L-2-Amino-6-oxopimelate
1.4.1.16
meso-2,6-Diaminopimelate
6.3.2.13
UDP-N-acetylmuramoyl-L-alanyl-γ-D-glutamyl-meso-2,6- diaminopimelate
6.3.2.10
UDP-N-acetylmuramoyl-L-alanyl-D-glutamyl-meso-2,6-diaminopimeloyl-D-alanyl-D-alanine
Peptidoglycan biosynthesis
4.1.1.20
Lysine degradation
L-Lysine
Tropane, piperidine and pyridine alkaloid biosynthesis
Citrate cycle
2-Oxoglutarate
2.3.3.14
Homocitrate
4.2.1.-
4.2.1.114
Homo-cis-aconitate
Acetyl-CoA
4.2.1.114
4.2.1.36
Glycolysis
Pyruvate metabolism
Homo-isocitrate
1.1.1.87
1.1.1.286
2-Oxoadipate
2.6.1.39
2.6.1.57
5-Adenyl-2-aminoadipate
1.2.1.95
α-Aminoadipoyl-S-acyl enzyme
1.2.1.95
L-2-Aminoadipate 6-semialdehyde
1.5.1.10
L-Saccharopine
1.5.1.7
1.2.1.95
L-2-Amino-adipate
LysX
LysW-γ-L-α-aminoadipate
LysZ
LysW-γ-L-α-aminoadipyl-6-phosphate
LysY
LysW-γ-L-α-aminoadipate 6-semialdehyde
LysJ
LysW-γ-L-lysine
LysK
PylB
3-Methyl-ornithine
PylC
3-Methylornithinyl-N6-lysine
PylD
3-Methylglutamuyl-5-semialdehyde-N6-lysine
Pyrrolysine
00300 5/25/21
(c) Kanehisa Laboratories

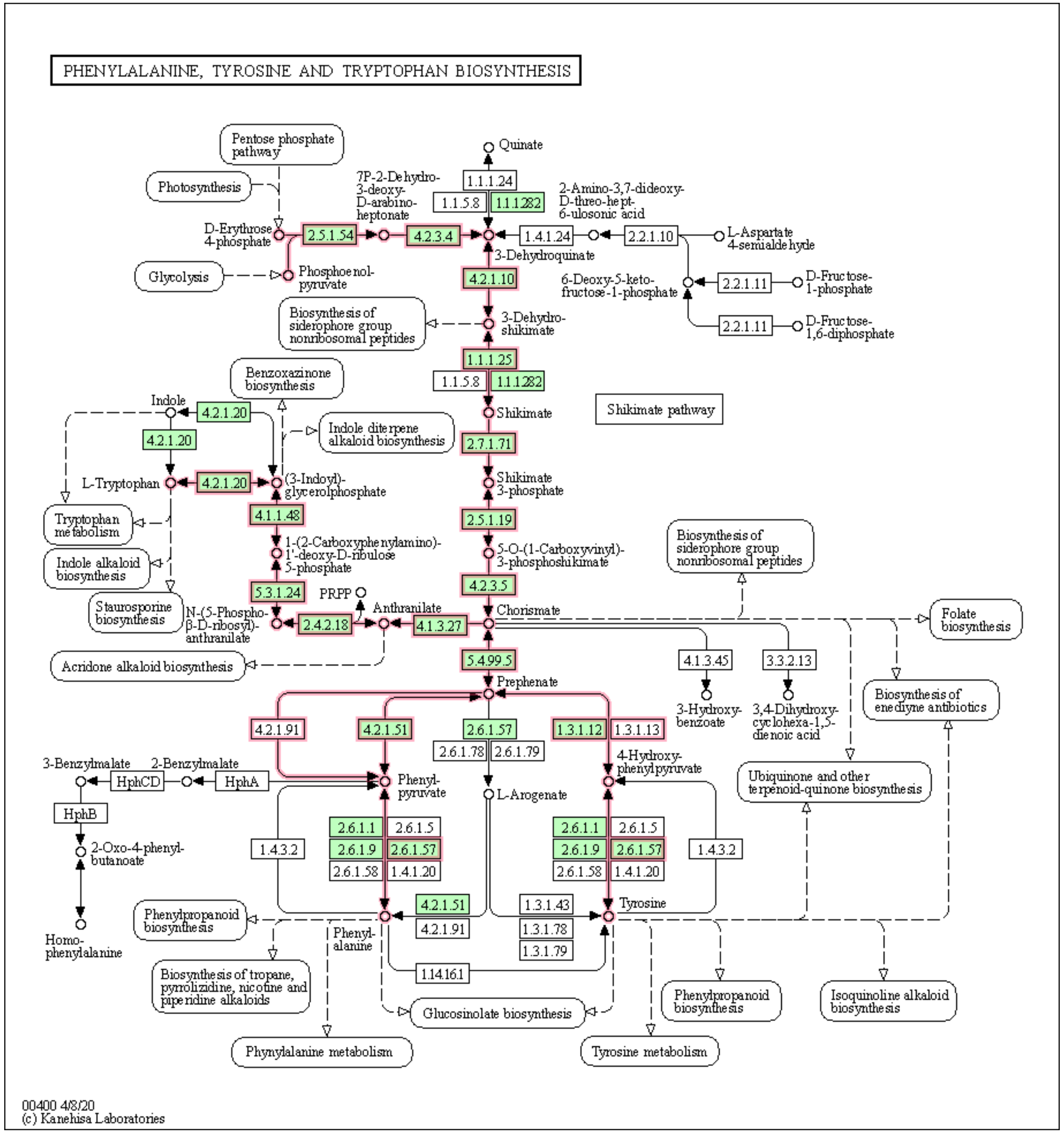
PHENYLALANINE, TYROSINE AND TRYPTOPHAN BIOSYNTHESIS
Pentose phosphate pathway
Photosynthesis
Glycolysis
D-Erythrose 4-phosphate
Phosphoenol-pyruvate
2.5.1.54
7P-2-Dehydro-3-deoxy-D-arabino-heptonate
4.2.3.4
Quinate
1.1.1.24
1.1.5.8
1.1.1.282
2-Amino-3,7-dideoxy-D-threo-hept-6-ulosonic acid
1.4.1.24
2.2.1.10
L-Aspartate 4-semialdehyde
3-Dehydroquinate
4.2.1.10
6-Deoxy-5-keto-fructose-1-phosphate
2.2.1.11
D-Fructose-1-phosphate
2.2.1.11
D-Fructose-1,6-diphosphate
Biosynthesis of siderophore group nonribosomal peptides
3-Dehydro-shikimate
1.1.1.25
1.1.5.8
1.1.1.282
Shikimate
Shikimate pathway
Benzoxazinone biosynthesis
Indole
4.2.1.20
4.2.1.20
Indole diterpene alkaloid biosynthesis
2.7.1.71
L-Tryptophan
4.2.1.20
(3-Indoyl)-glycerolphosphate
Shikimate 3-phosphate
4.1.1.48
Tryptophan metabolism
2.5.1.19
1-(2-Carboxyphenylamino)-1'-deoxy-D-ribulose 5-phosphate
5-O-(1-Carboxyvinyl)-3-phosphoshikimate
Indole alkaloid biosynthesis
Biosynthesis of siderophore group nonribosomal peptides
5.3.1.24
PRPP
4.2.3.5
Staurosporine biosynthesis
N-(5-Phospho-β-D-ribosyl)-anthranilate
2.4.2.18
Anthranilate
4.1.3.27
Chorismate
Folate biosynthesis
Acridone alkaloid biosynthesis
5.4.99.5
4.1.3.45
3.3.2.13
Prephenate
3-Hydroxy-benzoate
3,4-Dihydroxy-cyclohexa-1,5-dienoic acid
Biosynthesis of enediyne antibiotics
4.2.1.91
4.2.1.51
2.6.1.57
2.6.1.78
2.6.1.79
1.3.1.12
1.3.1.13
3-Benzylmalate
2-Benzylmalate
HphCD
HphA
Phenyl-pyruvate
L-Arogenate
4-Hydroxy-phenylpyruvate
Ubiquinone and other terpenoid-quinone biosynthesis
HphB
2-Oxo-4-phenyl-butanoate
1.4.3.2
2.6.1.1
2.6.1.5
2.6.1.9
2.6.1.57
2.6.1.58
1.4.1.20
2.6.1.1
2.6.1.5
2.6.1.9
2.6.1.57
2.6.1.58
1.4.1.20
1.4.3.2
4.2.1.51
4.2.1.91
1.3.1.43
1.3.1.78
1.3.1.79
Tyrosine
Homo-phenylalanine
Phenylpropanoid biosynthesis
Phenyl-alanine
1.14.16.1
Biosynthesis of tropane, pyrrolizidine, nicotine and piperidine alkaloids
Glucosinolate biosynthesis
Phenylpropanoid biosynthesis
Isoquinoline alkaloid biosynthesis
Phynylalanine metabolism
Tyrosine metabolism
00400 4/8/20
(c) Kanehisa Laboratories

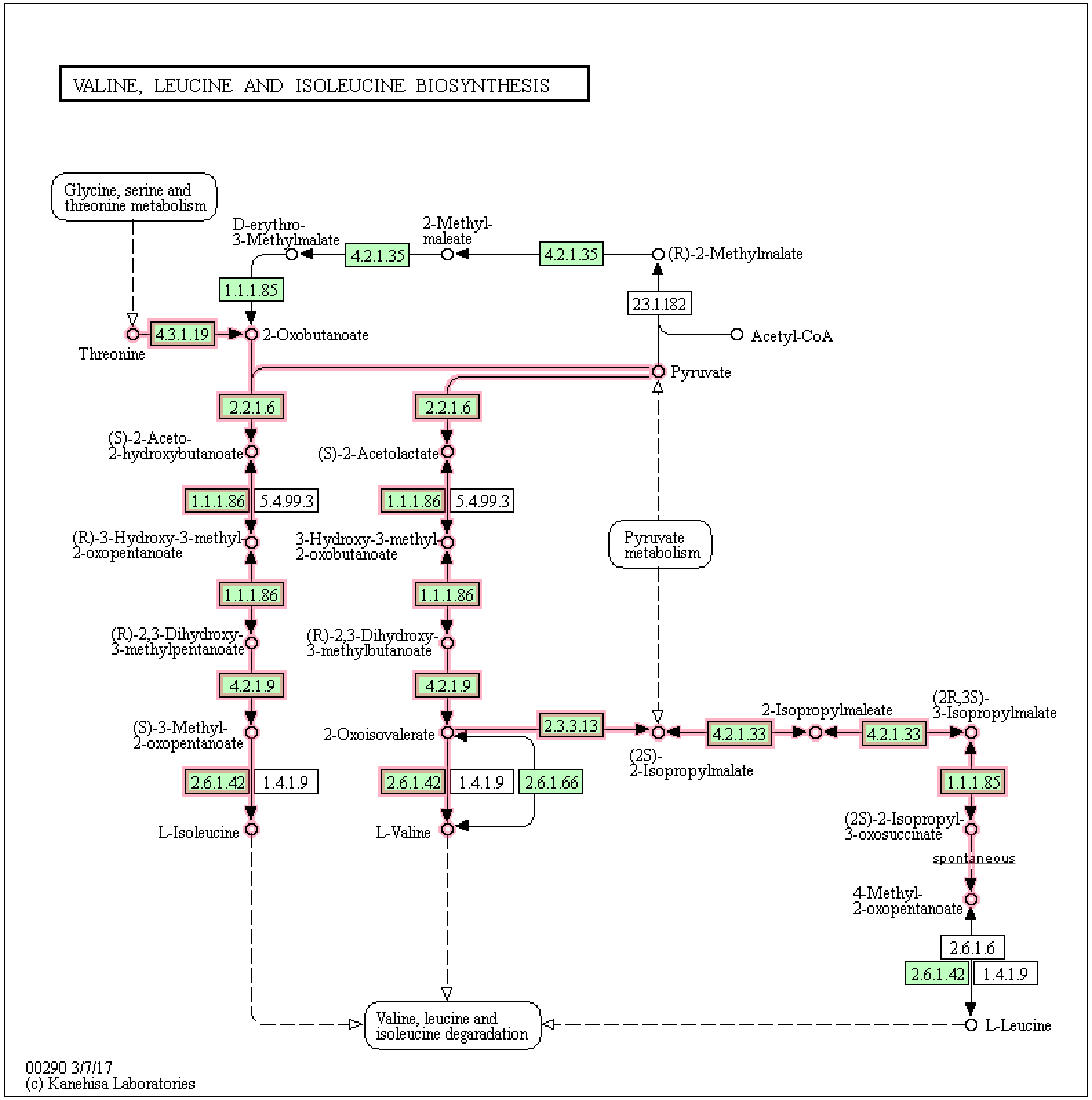
VALINE, LEUCINE AND ISOLEUCINE BIOSYNTHESIS
Glycine, serine and threonine metabolism
D-erythro-3-Methylmalate
2-Methyl-maleate
4.2.1.35
4.2.1.35
(R)-2-Methylmalate
1.1.1.85
2.3.1.182
Acetyl-CoA
4.3.1.19
Threonine
2-Oxobutanoate
Pyruvate
2.2.1.6
2.2.1.6
(S)-2-Aceto-2-hydroxybutanoate
(S)-2-Acetolactate
1.1.1.86
5.4.99.3
1.1.1.86
5.4.99.3
(R)-3-Hydroxy-3-methyl-2-oxopentanoate
3-Hydroxy-3-methyl-2-oxobutanoate
Pyruvate metabolism
1.1.1.86
1.1.1.86
(R)-2,3-Dihydroxy-3-methylpentanoate
(R)-2,3-Dihydroxy-3-methylbutanoate
4.2.1.9
4.2.1.9
(S)-3-Methyl-2-oxopentanoate
2-Oxoisovalerate
2.3.3.13
(2S)-2-Isopropylmalate
4.2.1.33
2-Isopropylmaleate
4.2.1.33
(2R,3S)-3-Isopropylmalate
2.6.1.42
1.4.1.9
2.6.1.42
1.4.1.9
2.6.1.66
1.1.1.85
L-Isoleucine
L-Valine
(2S)-2-Isopropyl-3-oxosuccinate
spontaneous
4-Methyl-2-oxopentanoate
2.6.1.6
2.6.1.42
1.4.1.9
Valine, leucine and isoleucine degaradation
L-Leucine
00290 3/7/17
(c) Kanehisa Laboratories

Supplementary Figure S10. Gene Ontology (GO) profiling of dominant microbial metabolisms with higher frequency (a) and lower frequency (b) activities.

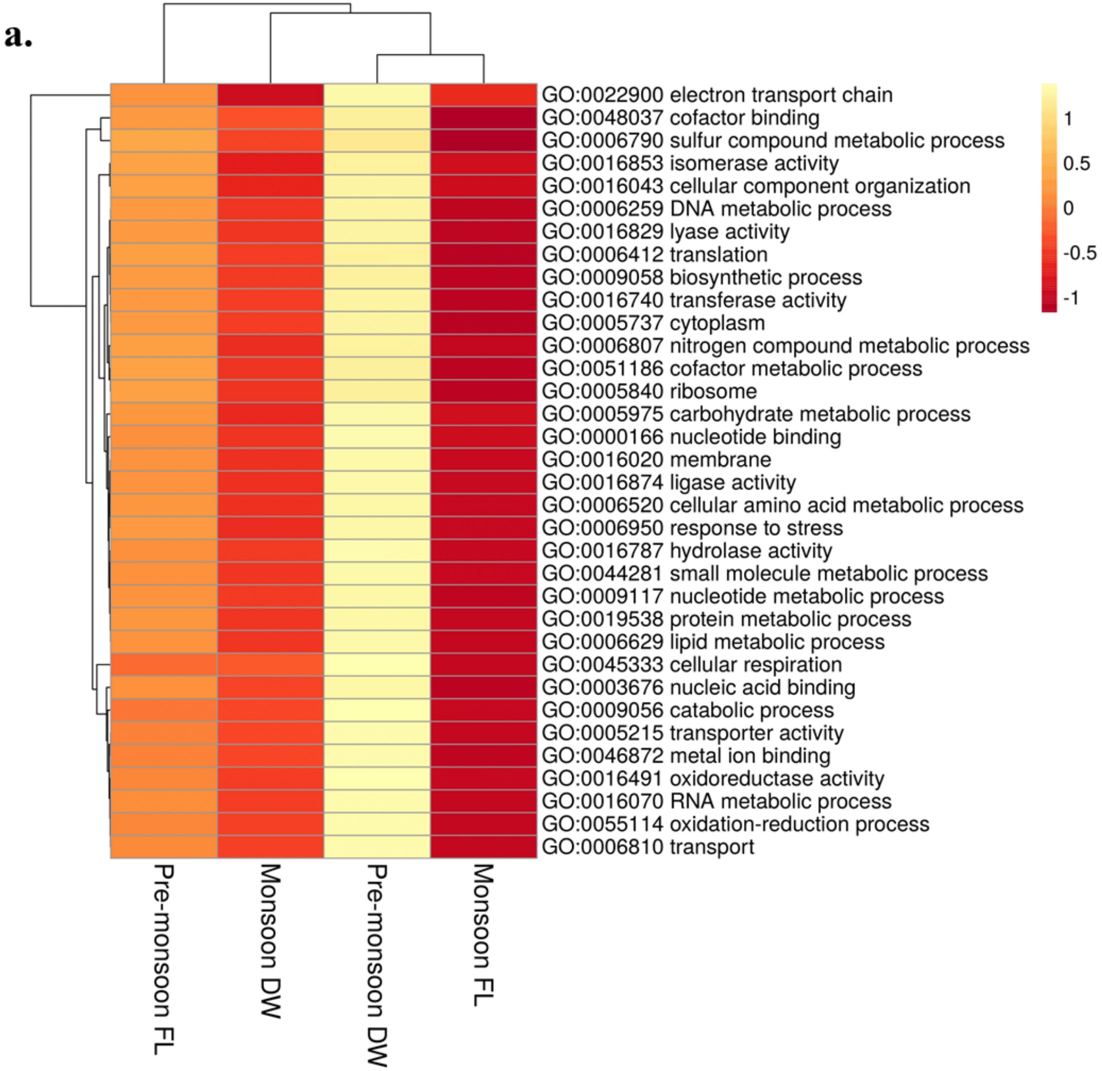

b.

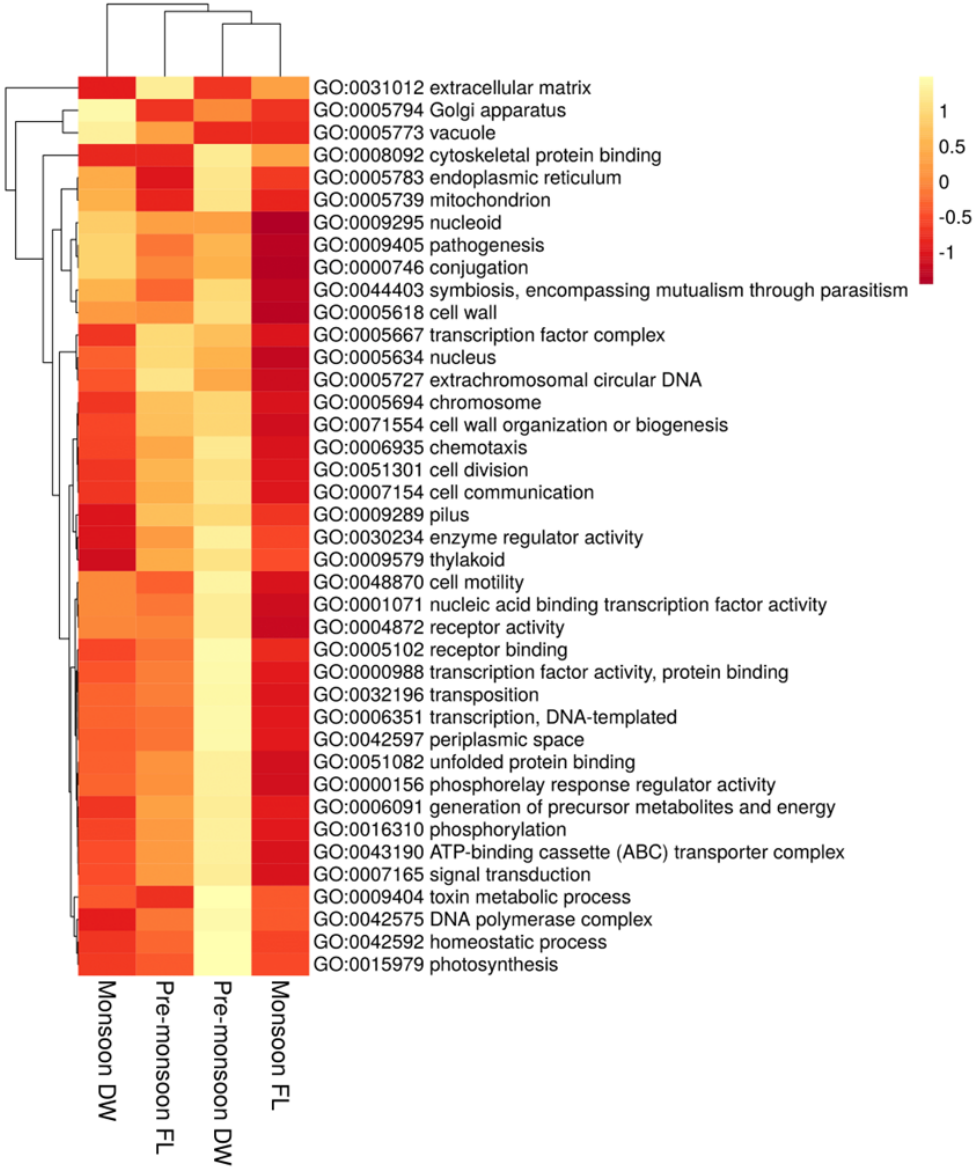
GO:0031012 extracellular matrix
GO:0005794 Golgi apparatus
GO:0005773 vacuole
GO:0008092 cytoskeletal protein binding
GO:0005783 endoplasmic reticulum
GO:0005739 mitochondrion
GO:0009295 nucleoid
GO:0009405 pathogenesis
GO:0000746 conjugation
GO:0044403 symbiosis, encompassing mutualism through parasitism
GO:0005618 cell wall
GO:0005667 transcription factor complex
GO:0005634 nucleus
GO:0005727 extrachromosomal circular DNA
GO:0005694 chromosome
GO:0071554 cell wall organization or biogenesis
GO:0006935 chemotaxis
GO:0051301 cell division
GO:0007154 cell communication
GO:0009289 pilus
GO:0030234 enzyme regulator activity
GO:0009579 thylakoid
GO:0048870 cell motility
GO:0001071 nucleic acid binding transcription factor activity
GO:0004872 receptor activity
GO:0005102 receptor binding
GO:0000988 transcription factor activity, protein binding
GO:0032196 transposition
GO:0006351 transcription, DNA-templated
GO:0042597 periplasmic space
GO:0051082 unfolded protein binding
GO:0000156 phosphorelay response regulator activity
GO:0006091 generation of precursor metabolites and energy
GO:0016310 phosphorylation
GO:0043190 ATP-binding cassette (ABC) transporter complex
GO:0007165 signal transduction
GO:0009404 toxin metabolic process
GO:0042575 DNA polymerase complex
GO:0042592 homeostatic process
GO:0015979 photosynthesis
1
0.5
0
-0.5
-1
Monsoon DW
Pre-monsoon FL
Pre-monsoon DW
Monsoon FL

Supplementary Figure S11. Arsenic responsive gene-dependent dominant microbial network analysis in pre-monsoonal dry-wet/flooded (a,b) and monsoonal dry-wet/flooded (c,d) phases respectively.

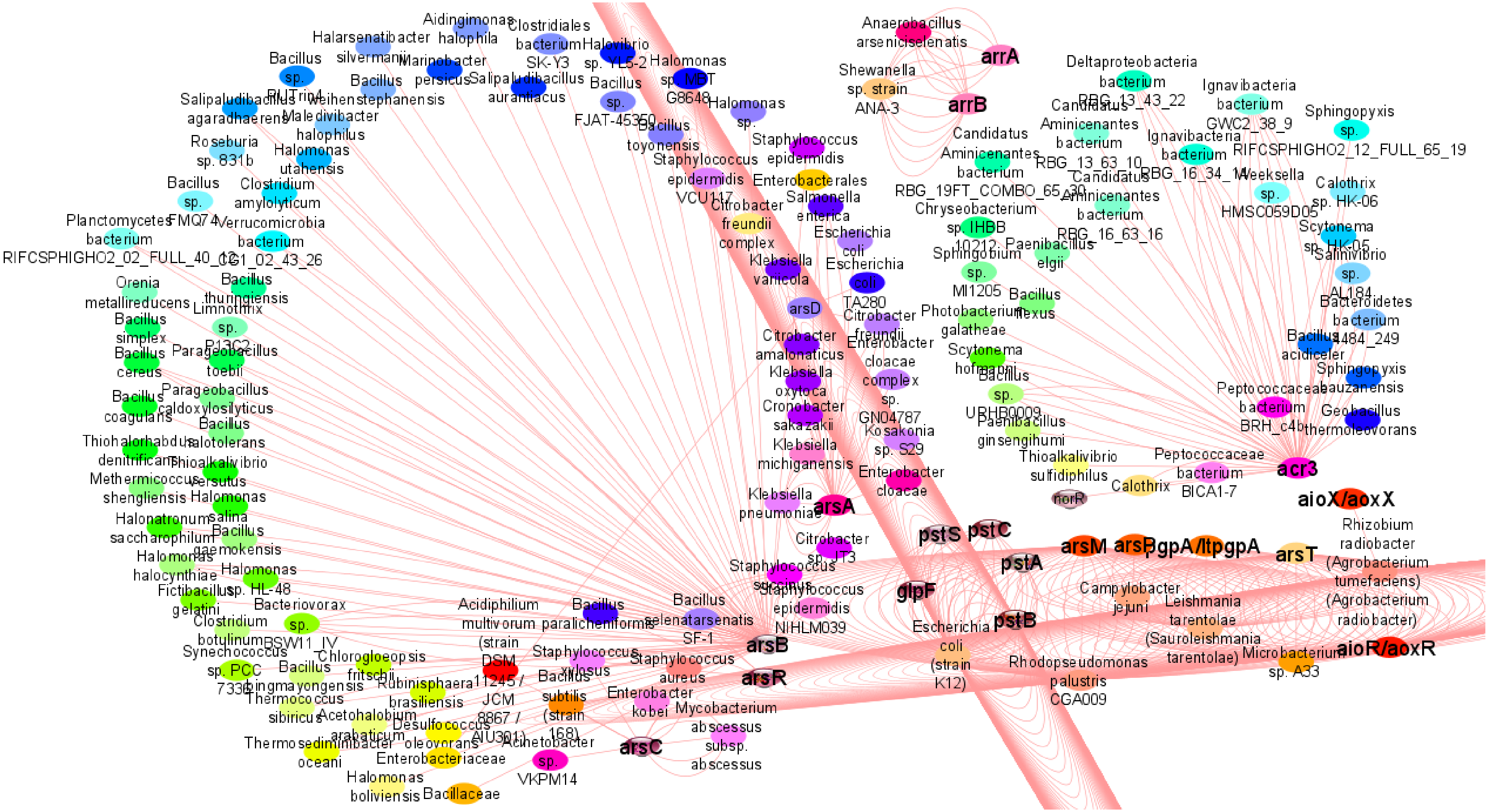

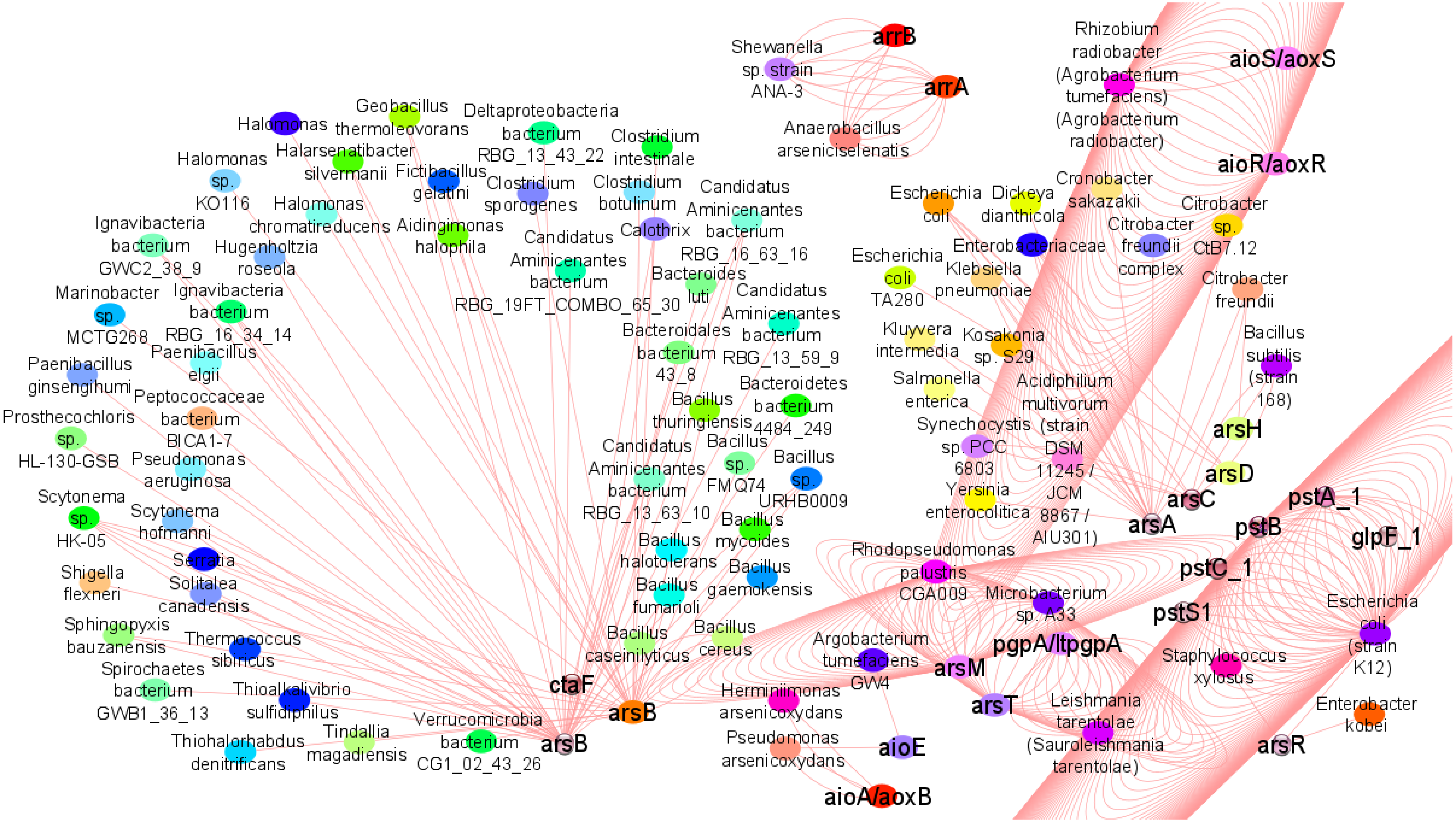
arrB
Shewanella sp. strain ANA-3
arrA
Anaerobacillus arseniciselenatis
Rhizobium radiobacter (Agrobacterium tumefaciens) (Agrobacterium radiobacter)
aioS/aoxS
aioR/aoxR
Geobacillus thermoleovorans
Deltaproteobacteria bacterium RBG_13_43_22
Halomonas
Halarsenatibacter silvermanii
Clostridium intestinale
Halomonas sp. KO116
Fictibacillus gelatini
Clostridium sporogenes
Clostridium botulinum
Candidatus Aminicenantes bacterium RBG_16_63_16
Halomonas chromatireducens
Aidingimonas halophila
Calothrix
Candidatus Aminicenantes bacterium RBG_19FT_COMBO_65_30
Ignavibacteria bacterium GWC2_38_9
Hugenholtzia roseola
Bacteroides luti
Candidatus Aminicenantes bacterium RBG_13_59_9
Marinobacter sp. MCTG268
Ignavibacteria bacterium RBG_16_34_14
Bacteroidales bacterium 43_8
Paenibacillus elgii
Paenibacillus ginsengihumi
Peptococcaceae bacterium BICA1-7
Bacteroidetes bacterium 4484_249
Bacillus thuringiensis
Prosthecochloris sp. HL-130-GSB
Pseudomonas aeruginosa
Candidatus Aminicenantes bacterium RBG_13_63_10
Bacillus sp. FMQ74
Bacillus sp. URHB0009
Scytonema sp. HK-05
Scytonema hofmanni
Bacillus mycoides
Serratia
Bacillus halotolerans
Bacillus gaemokensis
Shigella flexneri
Solitalea canadensis
Bacillus fumarioli
Sphingopyxis bauzanensis
Thermococcus sibiricus
Bacillus caseinilyticus
Bacillus cereus
Spirochaetes bacterium GWB1_36_13
Thioalkalivibrio sulfidiphilus
ctaF
arsB
Verrucomicrobia bacterium CG1_02_43_26
Tindallia magadiensis
Thiohalorhabdus denitrificans
arsB
Escherichia coli
Dickeya dianthicola
Cronobacter sakazakii
Citrobacter sp. CtB7.12
Citrobacter freundii complex
Enterobacteriaceae
Escherichia coli TA280
Klebsiella pneumoniae
Citrobacter freundii
Kluyvera intermedia
Kosakonia sp. S29
Bacillus subtilis (strain 168)
Salmonella enterica
Acidiphilium multivorum (strain DSM 11245 / JCM 8867 / AIU301)
Synechocystis sp. PCC 6803
Yersinia enterocolitica
arsH
arsD
arsC
arsA
pstA_1
pstB
glpF_1
Rhodopseudomonas palustris CGA009
pstC_1
Microbacterium sp. A33
pstS1
Escherichia coli (strain K12)
Argobacterium tumefaciens GW4
pgpA/ltpgpA
arsM
Staphylococcus xylosus
Herminiimonas arsenicoxydans
arsT
Leishmania tarentolae (Sauroleishmania tarentolae)
Enterobacter kobei
Pseudomonas arsenicoxydans
aioE
arsR
aioA/aoxB

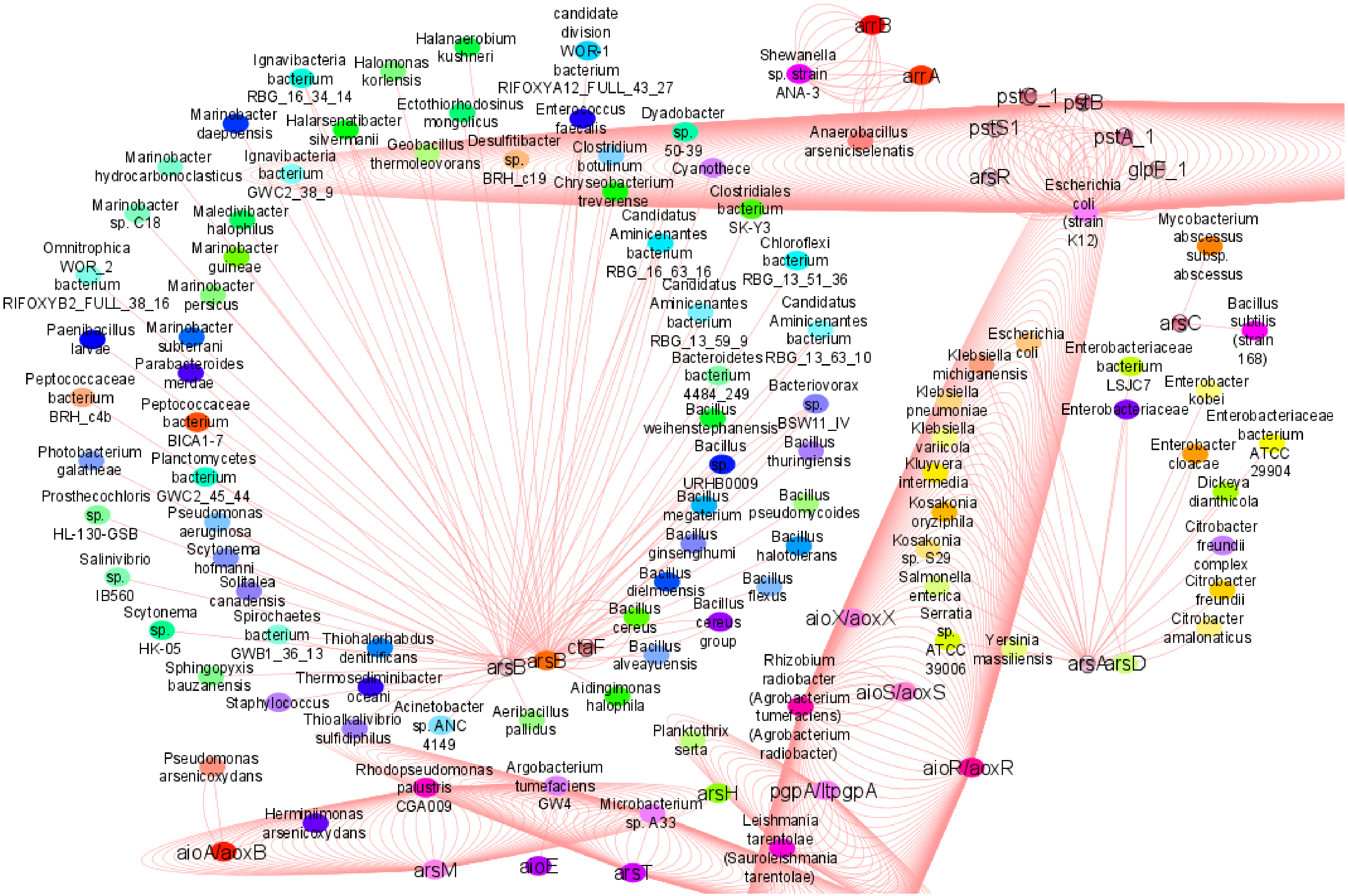
candidate division WOR-1 bacterium RIFOXYA12_FULL_43_27
Halanaerobium kushneri
Ignavibacteria bacterium RBG_16_34_14
Halomonas korlensis
Shewanella sp. strain ANA-3
arrB
arrA
pstC_1
pstB
pstS1
pstA_1
glpF_1
arsR
Escherichia coli (strain K12)
Marinobacter daepoensis
Halarsenatibacter silvermanii
Ectothiorhodosinus mongolicus
Enterococcus faecalis
Dyadobacter sp. 50-39
Anaerobacillus arseniciselenatis
Marinobacter hydrocarbonoclasticus
Ignavibacteria bacterium GWC2_38_9
Geobacillus thermoleovorans
Desulfitibacter sp. BRH_c19
Clostridium botulinum
Cyanothece
Chryseobacterium treverense
Clostridiales bacterium SK-Y3
Marinobacter sp. C18
Maledivibacter halophilus
Candidatus Aminicenantes bacterium RBG_16_63_16
Chloroflexi bacterium RBG_13_51_36
Mycobacterium abscessus subsp. abscessus
Omnitrophica WOR_2 bacterium RIFOXYB2_FULL_38_16
Marinobacter guineae
Marinobacter persicus
Candidatus Aminicenantes bacterium RBG_13_59_9
Candidatus Aminicenantes bacterium RBG_13_63_10
arsC
Bacillus subtilis (strain 168)
Paenibacillus larvae
Marinobacter subterrani
Parabacteroides merdae
Bacteroidetes bacterium 4484_249
Escherichia coli
Klebsiella michiganensis
Enterobacteriaceae bacterium LSJC7
Peptococcaceae bacterium BRH_c4b
Peptococcaceae bacterium BICA1-7
Bacteriovorax sp. BSW11_IV
Bacillus weihenstephanensis
Klebsiella pneumoniae
Enterobacter kobei
Enterobacteriaceae
Enterobacteriaceae bacterium ATCC 29904
Photobacterium galatheae
Planctomycetes bacterium GWC2_45_44
Bacillus sp. URHB0009
Bacillus thuringiensis
Klebsiella variicola
Kluyvera intermedia
Enterobacter cloacae
Prosthecochloris sp. HL-130-GSB
Pseudomonas aeruginosa
Bacillus megaterium
Bacillus pseudomycoides
Kosakonia oryziphila
Dickeya dianthicola
Scytonema hofmanni
Bacillus ginsengihumi
Bacillus halotolerans
Kosakonia sp. S29
Citrobacter freundii complex
Salinivibrio sp. IB560
Solitalea canadensis
Bacillus dielmoensis
Bacillus flexus
Salmonella enterica
Citrobacter freundii
Scytonema sp. HK-05
Spirochaetes bacterium GWB1_36_13
Bacillus cereus
Bacillus cereus group
aioX/aoxX
Serratia sp. ATCC 39006
Citrobacter amalonaticus
Thiohalorhabdus denitrificans
arsB
arsB
ctaF
Bacillus alveayuensis
Yersinia massiliensis
arsA
arsD
Sphingopyxis bauzanensis
Thermosediminibacter oceani
Rhizobium radiobacter (Agrobacterium tumefaciens) (Agrobacterium radiobacter)
aioS/aoxS
Staphylococcus
Acinetobacter sp. ANC 4149
Aidingimonas halophila
Thioalkalivibrio sulfidiphilus
Aeribacillus pallidus
Planktothrix serta
aioR/aoxR
Pseudomonas arsenicoxydans
Rhodopseudomonas palustris CGA009
Argobacterium tumefaciens GW4
arsH
pgpA/ltpgpA
Herminiimonas arsenicoxydans
Microbacterium sp. A33
Leishmania tarentolae (Sauroleishmania tarentolae)
aioA/aoxB
arsM
aioE
arsT

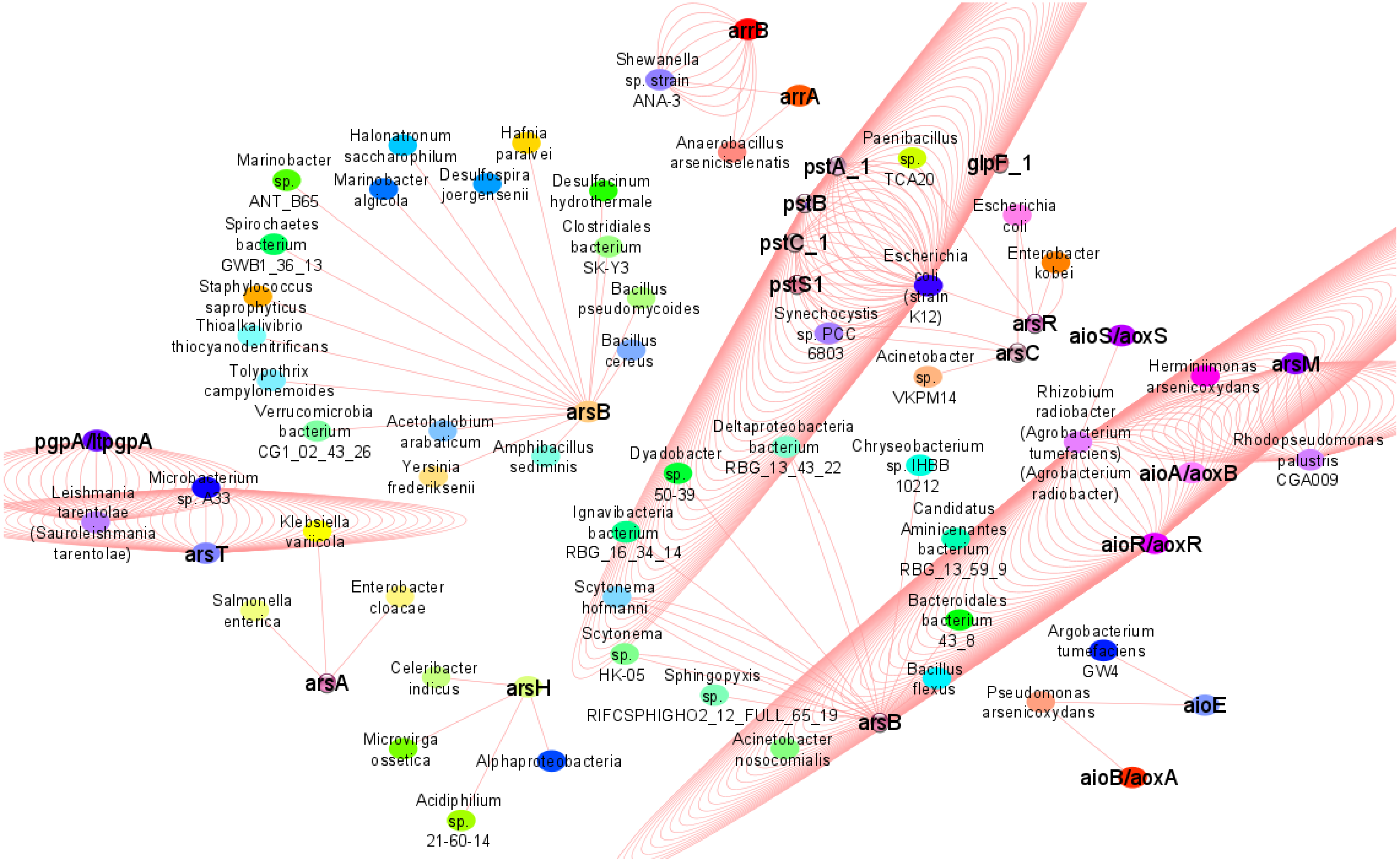

Soil microbial communities actively express different arsenic-responsive and related genes that also influence their diversity, inter-connectivity and networking pattern as presented in Figure 5a-d. Pre-monsoonal and monsoonal soil microbes under dry-wet and flooded conditions are presented here. Data are representative of mean read counts from 24 sampling sites.

Supplementary Figure S12. Network relationship of As-responsive and related genes under pre-monsoonal dry-wet and flooded soils (a-b) and monsoonal dry-wet and flooded soils (c-d). The genes are named within the figure.

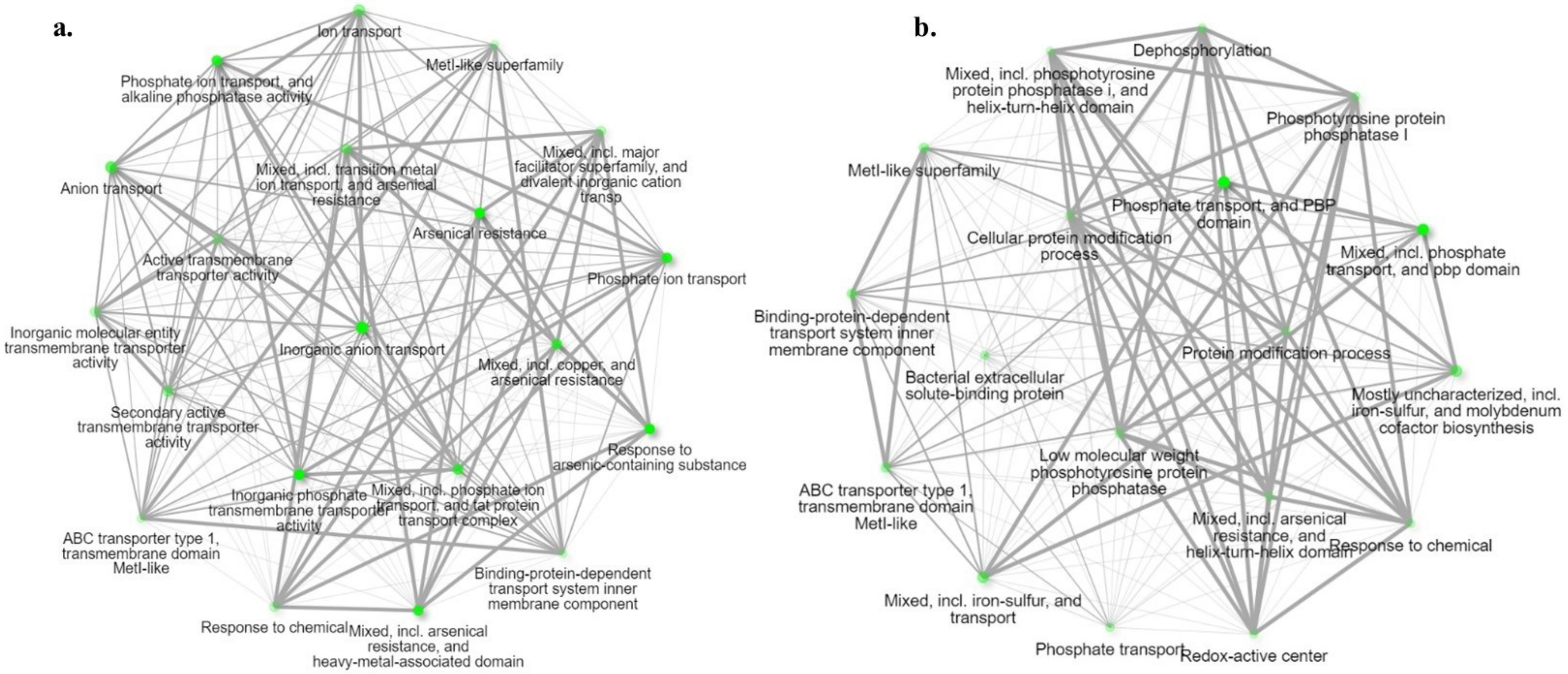

arrB, aioA, arrA, arsR, arsB, arsC, arsA, arsR, arsD, arsH, aioE, arsT, arrB, pstS, pstC, pstB, pstA, pgpA, arsP, arsM, aioX, aioS, aioR, aioA, aoxX, aoxS, aoxR, aoxB, ltpgpA, aoxB

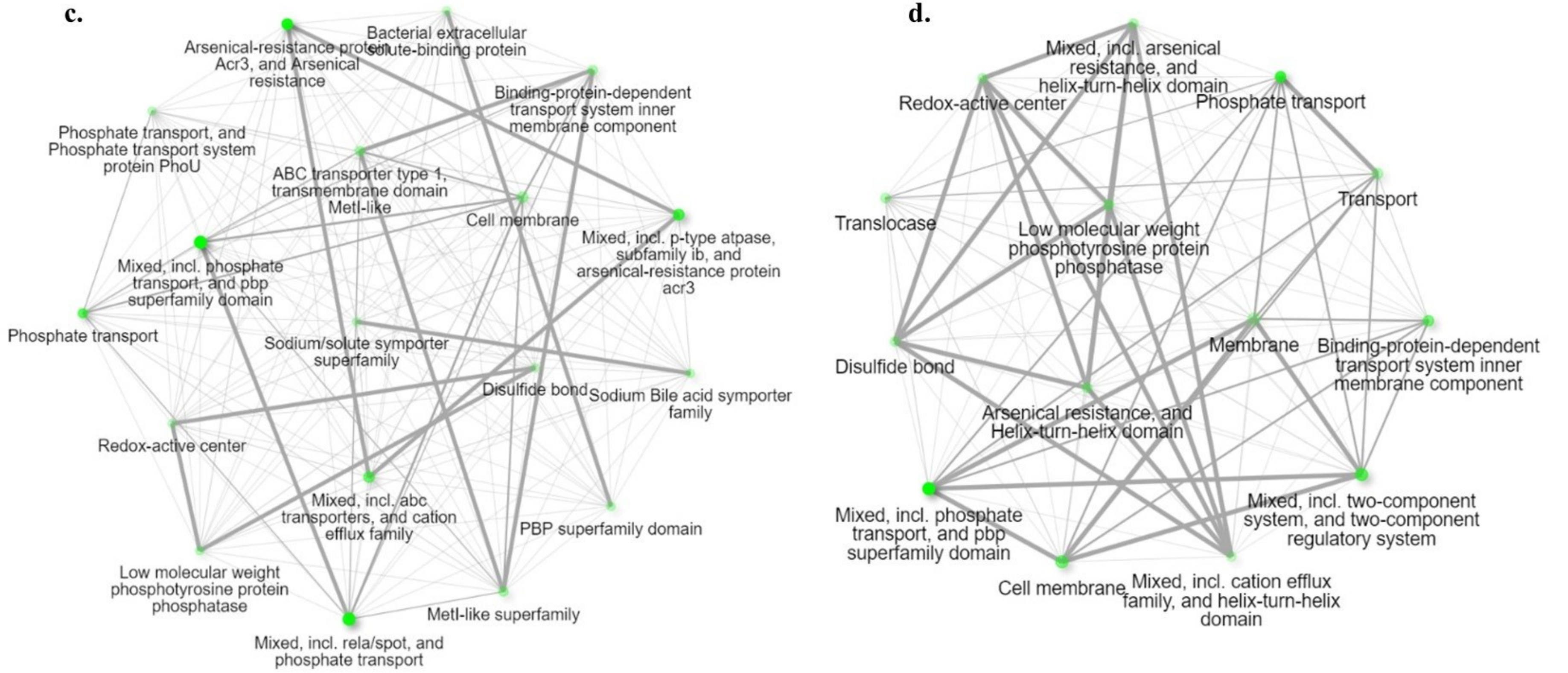

arrB, aioA, arrA, arsR, arsB, arsC, arsA, arsR, arsD, arsH, aioE, arsT, arrB, pstS, pstC, pstB, pstA, pgpA, arsP, arsM, aioX, aioS, aioR, aioA, aoxX, aoxS, aoxR, aoxB, ltpgpA, aoxB

Supplementary Table S1. Standard reference material values as analyzed for quality assurance.

SRM Name	As (mg kg^{-1})	SiO_2(%)
MESS3 Obtained data	102.4	57.13
Certified data	107	57.76
RD	4.492187	1.09072
NIST 2711a Obtained data	22.47	66.72
Certified data	21.2	67.17
RD	-5.65198	0.669942
JSD3 Obtained data	2.37	60.05
Certified data	2.42	60.78
RD	2.109705	1.201053
SDC1 Obtained data	25	65.61
Certified data	25.7	65.8
RD	2.8	0.288754

NIST1568c	As (mg kg^{-1})
Obtained data	0.348
Certified data	0.359
RD	3.064

Supplementary Table S2. Soil texture analysis by ASTM sieve method of all 24 sites within a radius of 1km from the Ganga bed.

Gangetic divisions	**Sites**	**Sand%**	**Silt%**	**Clay%**
Upper Ganga (Uttarakhand)	Site 1	24.00±1.6	26.00±1.9	50.00±2.3
	Site 2	23.00±1.8	25.00±2.6	52.00±1.5
	Site 3	26.00±1.6	26.00±2.3	48.00±1.6
	Site 4	24.00±1.9	27.00±1.5	49.00±1.9
Upper-middle Ganga (Uttar Pradesh)	Site 5	22.00±2.1	23.00±1.6	55.00±2.3
	Site 6	23.00±2.5	24.00±1.2	53.00±2.1
	Site 7	25.00±1.7	28.00±1.3	47.00±2.2
	Site 8	24.00±2.3	26.00±2.4	50.00±1.5
Middle Ganga (Uttar Pradesh)	Site 9	21.00±2.1	24.00±2.6	55.00±2.6
	Site 10	22.00±1.5	27.00±2.3	51.00±1.7
	Site 11	21.00±2.8	26.00±2.7	53.00±2.1
	Site 12	23.00±1.9	23.00±1.9	54.00±2.4
Middle Ganga (Bihar)	Site 13	24.00±2.6	21.00±1.8	55.00±1.9
	Site 14	21.00±2.4	28.00±1.2	51.00±1.6
	Site 15	21.00±1.7	24.00±2.5	55.00±2.5
	Site 16	20.00±2.3	25.00±2.3	55.00±2.4
Middle-lower Ganga (West Bengal)	Site 17	19.00±1.8	29.00±2.2	52.00±2.3
	Site 18	16.00±2.5	25.00±1.8	59.00±1.8
	Site 19	19.00±1.1	28.00±1.4	53.00±1.2
	Site 20	18.00±1.9	27.00±1.6	55.00±2.9
Lower Ganga (West Bengal)	Site 21	17.00±1.7	26.00±2.1	57.00±2.4
	Site 22	19.00±2.3	24.00±1.8	57.00±2.5
	Site 23	18.00±2.2	28.00±1.6	54.00±1.8
	Site 24	17.00±2.8	25.00±2.1	58.00±2.4

Supplementary Table S3. Alpha and Beta diversity indices of soil microbiome under different field setups and seasonal changes.

Gangetic Division 1 (Uttarakhand)				**Gangetic Division 2 (Uttar Pradesh)**				**Gangetic Division 3 (Uttar Pradesh)**			
Field samples	**Alpha diversity indices**			**Field samples**	**Alpha diversity indices**			**Field samples**	**Alpha diversity indices**		
Pre-monsoon	**Shannon**	**Simpson**	**Chao1**	**Pre-monsoon**	**Shannon**	**Simpson**	**Chao1**	**Pre-monsoon**	**Shannon**	**Simpson**	**Chao1**
Flooded	8.76	0.859	1733.2	Flooded	8.81	0.846	1866.48	Flooded	8.69	0.911	1908.32
Dry-wet	8.97	0.882	1809.5	Dry-wet	8.91	0.883	1903.75	Dry-wet	8.95	0.946	2044.65
Monsoon	**Shannon**	**Simpson**	**Chao1**	**Monsoon**	**Shannon**	**Simpson**	**Chao1**	**Monsoon**	**Shannon**	**Simpson**	**Chao1**
Flooded	8.29	0.841	1869.3	Flooded	8.77	0.861	1832.65	Flooded	8.56	0.871	1907.66
Dry-wet	8.43	0.867	1921.6	Dry-wet	8.49	0.841	1839.44	Dry-wet	8.77	0.884	1921.46
Gangetic Division 4 (Bihar)				**Gangetic Division 5 (West Bengal)**				**Gangetic Division 6 (West Bengal)**			
Field samples	**Alpha diversity indices**			**Field samples**	**Alpha diversity indices**			**Field samples**	**Alpha diversity indices**		
Pre-monsoon	**Shannon**	**Simpson**	**Chao1**	**Pre-monsoon**	**Shannon**	**Simpson**	**Chao1**	**Pre-monsoon**	**Shannon**	**Simpson**	**Chao1**
Flooded	9.13	0.911	2013.7	Flooded	9.25	0.921	2088.26	Flooded	9.37	0.923	2163.58
Dry-wet	9.62	0.949	2347.6	Dry-wet	9.44	0.953	2609.74	Dry-wet	9.71	0.9618	2691.35
Monsoon	**Shannon**	**Simpson**	**Chao1**	**Monsoon**	**Shannon**	**Simpson**	**Chao1**	**Monsoon**	**Shannon**	**Simpson**	**Chao1**
Flooded	8.41	0.807	1962.4	Flooded	8.52	0.869	1967.14	Flooded	8.62	0.859	1987.55
Dry-wet	8.92	0.883	2044.7	Dry-wet	8.73	0.899	2119.58	Dry-wet	8.79	0.896	2207.54

Note: Standard deviations were within 0.03-0.05 margin for the Shannon index, 0.007-0.009 margin for the Simpson index and 24.98-46.77 margin for the Chao1 index.

Supplementary Table S4. The volume of water (in L) which can be saved in AWD practice compared to the flooded.

Water-saving data related to the AWD practice								
Study divisions	Study sites	Pre-monsoonal DW	Pre-monsoonal FL	Monsoonal DW	Monsoonal FL	Average water consumption (DW)	Average water consumption (FL)	Per hectare water save through AWD
Upper Ganga	Site 1	24800	111600	16550	99100	20675	105350	1058438
	Site 2	25250	113400	17000	100900	21125	107150	1075313
	Site 3	25900	116550	17650	104050	21775	110300	1106563
	Site 4	23800	107100	15550	94600	19675	100850	1014688
Upper Middle Ganga	Site 5	27350	122850	19100	110350	23225	116600	1167188
	Site 6	27450	123300	19200	110800	23325	117050	1171563
	Site 7	28100	126450	19850	114950	23975	120700	1209063
	Site 8	29600	133200	21350	121700	25475	127450	1274688
Middle Ganga	Site 9	28750	129150	20800	117650	24775	123400	1232813
	Site 10	29500	132750	21550	121250	25525	127000	1268438
	Site 11	31400	141300	23450	129800	27425	135550	1351563
	Site 12	31650	142200	23700	124700	27675	133450	1322188
Middle Ganga	Site 13	32700	147150	24750	129650	28725	138400	1370938
	Site 14	32900	148050	24950	130550	28925	139300	1379688
	Site 15	36400	163800	28450	144300	32425	154050	1520313
	Site 16	33150	148950	25200	131450	29175	140200	1387813
Middle Lower Ganga	Site 17	34500	120750	24350	109250	29425	115000	1069688
	Site 18	36200	126700	26050	115200	31125	120950	1122813
	Site 19	35100	122850	24950	111350	30025	117100	1088438
	Site 20	31850	111300	21700	102800	26775	107050	1003438
Lower Ganga	Site 21	36750	128450	26600	119950	31675	124200	1156563
	Site 22	35900	125650	25750	117150	30825	121400	1132188
	Site 23	34350	120050	24200	111550	29275	115800	1081563
	Site 24	38600	135100	28450	122600	33525	128850	1191563

Note: Data are mean values with a SD of 1.24-2.08% range of the mean.

Supplementary Table S5. Profit calculation based on the rice productivity per hectare (H) in dry-wet (DW) and flooded (FL) fields. Average data for India has been collected from the Ministry of Agriculture database. Yields are in kg, profits are in INR.

Cost-benefit calculations and profit gained from yield data								
Study divisions	Study sites	Average Yield (DW)	Average Yield (FL)	Average yield India	Difference in Yield per H	Average Price yield India	Difference in price Yield per H	Average price DW
Upper Ganga	Site 1	5126.5	4899.5	2809	2317.5	57584.5	47508.75	105093.3
	Site 2	5225	4888.5	2809	2416	57584.5	49528	107112.5
	Site 3	5346	5047	2809	2537	57584.5	52008.5	109593
	Site 4	5616.5	5006.5	2809	2807.5	57584.5	57553.75	115138.3
Upper Middle Ganga	Site 5	5747	5155.5	2809	2938	57584.5	60229	117813.5
	Site 6	5776	4945	2809	2967	57584.5	60823.5	118408
	Site 7	5371.5	5144.5	2809	2562.5	57584.5	52531.25	110115.8
	Site 8	5526	5189.5	2809	2717	57584.5	55698.5	113283
Middle Ganga	Site 9	5523	5224	2809	2714	57584.5	55637	113221.5
	Site 10	5825.5	5215.5	2809	3016.5	57584.5	61838.25	119422.8
	Site 11	5920	5328.5	2809	3111	57584.5	63775.5	121360
	Site 12	6087	5256	2809	3278	57584.5	67199	124783.5
Middle Ganga	Site 13	5616.5	5389.5	2809	2807.5	57584.5	57553.75	115138.3
	Site 14	5827	5490.5	2809	3018	57584.5	61869	119453.5
	Site 15	5700	5401	2809	2891	57584.5	59265.5	116850
	Site 16	6034.5	5424.5	2809	3225.5	57584.5	66122.75	123707.3
Middle Lower Ganga	Site 17	6093	5501.5	2809	3284	57584.5	67322	124906.5
	Site 18	6398	5567	2809	3589	57584.5	73574.5	131159
	Site 19	5881	5058	2809	3072	57584.5	62976	120560.5
	Site 20	6073.5	5328	2809	3264.5	57584.5	66922.25	124506.8
Lower Ganga	Site 21	5865.5	5368	2809	3056.5	57584.5	62658.25	120242.8
	Site 22	5929	5387	2809	3120	57584.5	63960	121544.5
	Site 23	5946	5271	2809	3137	57584.5	64308.5	121893
	Site 24	6122.5	5378	2809	3313.5	57584.5	67926.75	125511.3

Note: Data are mean values with a SD of 1.62-2.11% range of the mean.

Supplementary Table S6. Profit calculations (in INR) based on the average income per hectare from dry-wet and flooded fields.

Cost-benefit calculations and average profit from monitory data							
Study divisions	Study sites	Pre-monsoonal DW	Pre-monsoonal FL	Monsoonal DW	Monsoonal FL	Average Profit (DW)	Average Profit (FL)
Upper Ganga	Site 1	67500.28	47347.43	58511.5	49892.33	63005.89	48619.88
	Site 2	68918.9	47766.86	59525.75	49210.86	64222.32	48488.86
	Site 3	70530.96	49272.98	60889.73	50852.6	65710.35	50062.79
	Site 4	76373.07	54852.74	61915.64	49613.55	69144.36	52233.14
Upper Middle Ganga	Site 5	92611.54	56316.74	72073.27	51255.29	82342.4	53786.01
	Site 6	88380.93	57938.73	76744.3	49707.18	82562.62	53822.96
	Site 7	81617.92	54894.87	71895.71	57499.06	76756.82	56196.96
	Site 8	84090.74	55948.11	73848.81	57385.8	78969.77	56666.96
Middle Ganga	Site 9	84105.64	66998.21	73753.2	57782.19	78929.42	62390.2
	Site 10	91330.44	67888.01	69872.16	56785.56	80601.3	62336.78
	Site 11	95188.64	69178.85	68986.1	58178.58	82087.37	63678.71
	Site 12	93013.75	72838.31	75061.94	57929.38	84037.84	65383.84
Middle Ganga	Site 13	102439.6	68389.31	69732.92	65595.78	86086.24	66992.54
	Site 14	106412.6	70344.36	83667.86	66162.75	95040.23	68253.55
	Site 15	104211.3	64913.14	81747.67	65065.79	92979.49	64989.47
	Site 16	113463.8	66123.73	83975.68	64375.56	98719.75	65249.65
Middle Lower Ganga	Site 17	117454.7	66911.2	82421.93	65447.87	99938.33	66179.53
	Site 18	117311.6	71965.09	91480.58	66773.58	104396.1	69369.33
	Site 19	118105.6	61246.13	79571.51	65361.09	98838.57	63303.61
	Site 20	123418	74354.73	81183.15	62935.86	102300.6	68645.3
Lower Ganga	Site 21	121706.9	71998.64	76676.01	66507.07	99191.45	69252.85
	Site 22	128053.9	71422.15	74053.68	67626.41	101053.8	69524.28
	Site 23	125328.1	71447.21	76389.19	64508.26	100858.6	67977.74
	Site 24	129585.9	73139.09	78287.66	65560.97	103936.8	69350.03

Note: Data are mean values with a SD of 1.49-2.26% range of the mean.